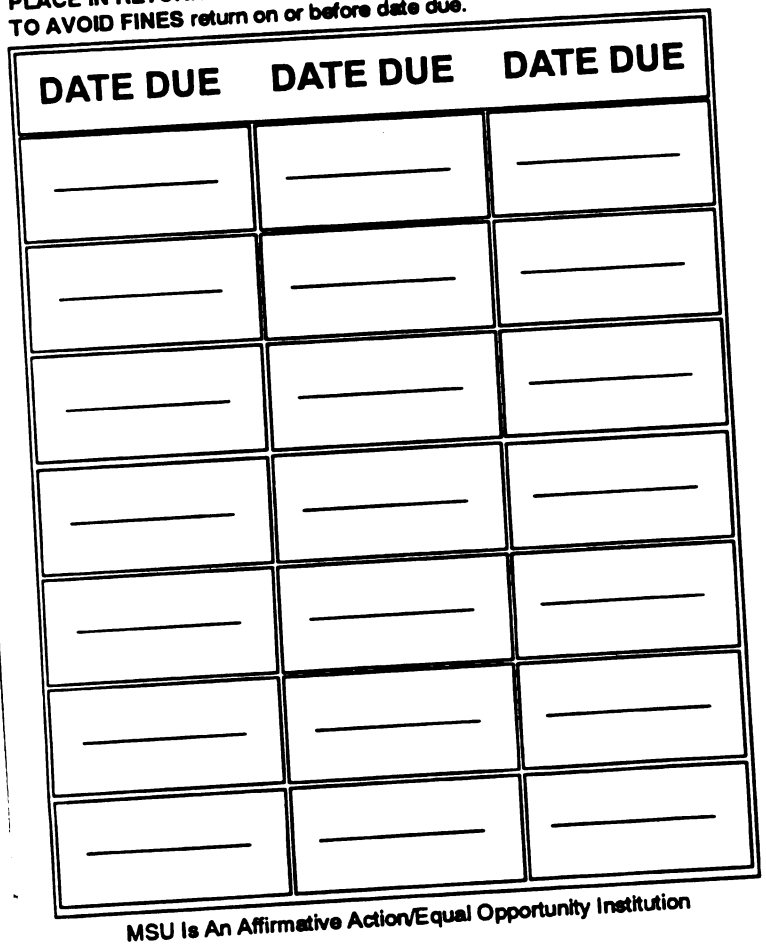

SOFTENING MECHANISMS AND MICROSTRUCTURAL INSTABILITIES OF NICKEL DURING HIGH TEMPERATURE LOW CYCLE FATIGUE

By

Shuhrong Chen

A DISSERTATION

Submitted to

Michigan State University

in partial fulfillment of the requirements

for the degree of

DOCTOR OF PHILOSOPHY

Department of Metallurgy, Mechanics and Materials Science

1989

ABSTRACT

SOFTENING MECHANISMS AND MICROSTRUCTURAL INSTABILITIES
OF NICKEL DURING HIGH TEMPERATURE LOW CYCLE FATIGUE

By

Shuhrong Chen

The microstructural development and its effect on mechanical properties was investigated during high temperature low cycle fatigue in Ni. Even at small strain amplitudes (ϵ<0.004) substantial microstructural changes were observed due to grain growth, grain boundary positioning with respect to the applied stress and dynamic recrystallization. Dynamic recrystallization during cyclic deformation even at strain amplitude as large as 2% was only observed in polycrystals. Large differences in the dislocation arrangement was observed between grain interior and grain boundary regions. The introduced changes are particularly important for control or retention of grain size during high temperature applications and in the context of intergranular fatigue crack propagation associated with grain boundary sliding. The microstructural development is reflected in the mechanical behavior of the material and correspondingly will affect the performance of parts during high temperature service. By appropriate selection of deformation temperature, strain amplitude and cycle frequency the evolution of the microstructure can be substantially influenced, in particular under controlled over-straining.

ACKNOWLEDGEMENTS

First and foremost, I would like to thank my advisor, Professor G. Gottstein, for his patient guidance and beneficial discussions in making this project a success. Also, I would like to express my deepest gratitude to my family for their full support in these years.

The financial support of the U.S. Department of Energy, Office of Basic Science, under grant number DE-FG02-85ER45205 is gratefully acknowledged.

TABLE OF CONTENTS

LIST OF TABLES

LIST OF FIGURES

I INTRODUCTION

Materials for high temperature applications have become progressively in demand for high technology products: turbine blades for jet engines or structural components in high temperature reactors are prominent examples. The excellent mechanical properties of advanced materials are generally achieved by optimizing the microstructure during the processing to the final product. A change of this microstructure or even a breakdown, therefore, will cause serious consequences for the part in service and may introduce premature failure.

One well known high temperature phenomenon is the recrystallization of the material during deformation, also referred to as dynamic recrystallization (DRX). DRX has been reported in a variety of fcc metals and alloys in which the degree of dynamic recovery is restricted [1], such as Cu [2,3]; CuAl [4]; CuZn [5]; Ag [6]; Ni [7,8]; Ni-Fe [8]; Ni superalloys [9]; stainless steel [10], etc.. These experimental reports were based on the tests conducted in monotonic loading conditions, namely in tension, compression, or torsion. In a recent paper, DRX was found at the grain boundaries during low cycle fatigue (LCF) in bicrystals of Ni with special grain boundaries [11]. The occurrence of DRX during cyclic deformation in polycrystals has recently been reported [12]. The results on DRX were the minor observations in these studies. So far no systematical research has been done on DRX during LCF.

Most parts under high temperature service conditions, however, are subjected to cyclic loading conditions due to vibrations or temperature fluctuations. A major difference between cyclic and monotonic loading is that the strain amplitude under cyclic conditions is commonly small compared to the critical strain to set off DRX in monotonic tests. However, the critical conditions for DRX to occur are determined by the microstructure, namely by the development of a cell-or subgrain structure [3,7,13]. The existence of dynamic recrystallization during high temperature low cycle fatigue is not immediately obvious. It is expected because the microstructural development during high temperature low cycle fatigue is similar in character (although different in scale) to the structure evolution during monotonic loading at high temperatures, namely the build-up of a cell structure that dynamically transforms (recovers) to a subgrain structure [14,15]. Moteff and collaborators [16-18] have studied the microstructural evolution of AISI 304 stainless steel at different fractions of the fatigue life. Their results show that at 0.5 T_m (T_m- melting temperature) already in the first two cycles the dislocations tend to arrange in a cell structure which becomes progressively pronounced with increasing number of cycles, and finally will be converted to a subgrain structure with sharply defined boundaries. In a study on the nucleation of DRX in single crystals during monotonic deformation [7] it was found that DRX is triggered by dynamic recovery as a consequence of fluctuations in the recovery rate. This was attributed to the local appearance of mobile subboundary segments in an internally highly stressed environment. The microstructural studies of Bhat and Laird [14,15] and Nahm et al. [16] show exactly this arrangement of dislocations in fatigued specimens, so

that critical conditions for DRX should also exist in cyclic deformation mode, although stress and instantaneous strain level remain comparably small in cyclic loading.

Also, extensive grain boundary migration was observed during high temperature LCF. Quantitative studies on this phenomenon have been reported on Pb [19-21] and Al [22,23]. Since the nucleation of DRX in polycrystals is likely to occur by bulging of existing grain boundaries [24,25], the grain boundary migration during LCF may be instrumental in the nucleation of DRX.

In ductile materials, fatigue crack propagation is accompanied by a plastic deformation zone. In the case of metals, plastic deformation usually takes place by slip which involves the generation and multiplication of dislocations and their movement through the lattice. According to the model proposed by Rice and Thomson [26], dislocations can be emitted from crack tips and thereby shield the concentrated stress field before the stress intensity factor reaches the critical fracture stress. This highly plastic deformation may recover at high temperature and set off DRX during crack propagation and reduce stress concentrations and thus, decelerate or arrest crack propagation.

In the present study these problems were addressed by investigating the microstructural development during LCF.

II LITERATURE SURVEY

2.1 Grain Boundary Migration During LCF

It is clear from the data available to date that the movement of grain boundaries is an important microstructural process in high temperature fatigue. The paper published by Snowden in 1961 [19] indicated that the effect of the alternating strain in bending fatigue test of pure lead was the appearance of slip traces and grain boundary migration. The rate of migration increased with increasing strain amplitude and was highest in the early part of the life. One or two hundred microns displacement of the boundary was found to be common. He observed that some boundaries including coherent twin boundaries, did not move. One more important feature of the migration was that boundaries tended to migrate to positions at ±45° to the specimen axis. This type of boundary migration resulted in the formation of an orthogonal grain structure. He explained this phenomenon on the basis that, in general, different amounts of deformation were built up on each side of the boundaries so that the migration is produced by unequal numbers of dislocations on opposite sides of the boundaries. A possible reason for the diminished rate of migration after larger numbers of cycles, suggested by Snowden, was that the boundaries moved to align themselves in the directions of maximum shear stress. The enhanced grain boundary sliding at orientations in the shear direction, i.e., at ±45° to the specimen axis, would take care of the deformation necessary to respond the straining imposed by cyclic fatigue.

Quantitative studies on grain boundary migration and grain boundary sliding have been reported on Pb [20,21], Al [22,23,27], Pb-Sn solid solution alloy [28,29] and Al-Mg solid solution alloy [30]. The results will be briefly reviewed. Langdon et al. [20,21] conducted experiments on high purity lead (99.9995%) at room temperature ($0.5T_m$) using reverse bending and torsion fatigue. On contrary to Snowden, the strain amplitude was increased to more than 0.2% and the structural development was observed from the very first cycle. The results showed that a large number of the grain boundaries revealed very extensive migration. As a result of this migration, a series of essentially parallel markings at many of the boundaries could be easily observed under optical microscope. By detailed inspection that there was a well defined one-to-one correspondence between the number of grain boundary markings and the total number of whole cycles imposed on the specimen which Snowden didn't report due to his observation was taken after $\simeq 10^4$ cycles with a very small strain amplitude such that the markings were too dense to be distinguished. The exceptional clarity of each separate migration marking suggested that grain boundary sliding may also occur cyclically at the interface, giving a small displacement of material perpendicular to the specimen surface at each marking. Evidence for cyclic grain boundary sliding was confirmed by using two-beam interferometry. The cyclic markings are repetitive through each fatigue cycle, and the sharp discontinuities in the fringes confirm that sliding occur at the grain boundaries as an alternating process during cyclic deformation. Further investigation by optical microscopy using Nomarski interference contrast showed the presence of a fine structure within the migration markings. An additional observation noted only when examining the longer grain

boundaries in specimens containing a very coarse grain size, was the formation of a zig-zag pattern of migration markings. The individual boundary segments of the zig-zag pattern were generally fairly close to 45° with respect to the stress axis. A model was proposed by Langdon et al. to explain the occurrence of markings on the surface due to alternation of grain boundary migration and sliding. They assumed that the migration is stress-induced in response to the cyclic loading which is different from the explanation Snowden made (strain induced grain boundary migration). The measurements of grain boundary sliding was done by using a two-beam interference microscope with a resolution of $\pm 0.06\ \mu m$. The average sliding offset perpendicular to the surface was measured after testing for various numbers of cycles. The value of the average offset perpendicular to the surface, $\bar{v}$ (in the order of $10^{-1}\mu m$), increases rapidly over the initial stage, and thereafter the rate of the increase is reduced and ultimately the value of $\bar{v}$ essentially stabilizes.

The saturation in $\bar{v}$ is likely to correspond to the attainment of the diamond grain configuration after large numbers of cyclic deformation. The measurements of grain boundary migration was performed by Yavari et al. [23] using Al fatigued at 300°C ($0.61T_m$). The average distance of grain boundary migration $\bar{m}$ for polycrystalline Al with strain amplitude less than $\approx \pm 0.4\%$ was found to obey the empirical relationship

$$\bar{m} = A f^{-0.35} N^{0.5} \Delta\epsilon^{0.66} \exp(-62.0/RT)$$

where f : frequency

N : number of loading cycles

$\Delta\epsilon$: strain amplitude

R : gas constant in kJ/mol•k

T : absolute temperature

A : $\simeq 3.2\times10^{7}\ \mu m s^{0.35}$

Also, the occurrence of cyclic migration leads to the disappearance of grains and thus is a mechanism of grain coarsening.

A change of the grain morphology due to grain boundary migration during cyclic deformation at 650°C at a low strain rate ($\dot{\epsilon}$= $4\times10^{-4}\ s^{-1}$) was also reported on OFHC Cu [31]. But this change in grain shape was found to be strain rate dependent and at high strain rates , no such change in grain morphology occurred. That impurities or precipitates slow down or inhibit grain boundary migration explains why type 304 stainless steel does not exhibit any change in grain structure at 760°C at the lower strain rate [31].

2.2 DRX In Monotonic Tests

DRX has been investigated extensively in monotonic loading. As is known from previous investigations, the onset of DRX in single crystals is indicated by a sharp drop in the flow stress (Fig.2-1) [6,32]. It has already been shown previously [33], the shear stress (τ_R) rather than shear strain (γ_R) is the critical quantity governing the initiation of DRX. In single crystals, DRX is controlled by nucleation rather than by growth of recrystallized grains. In the same paper, they also showed that DRX is not only triggered but is also totally controlled by the

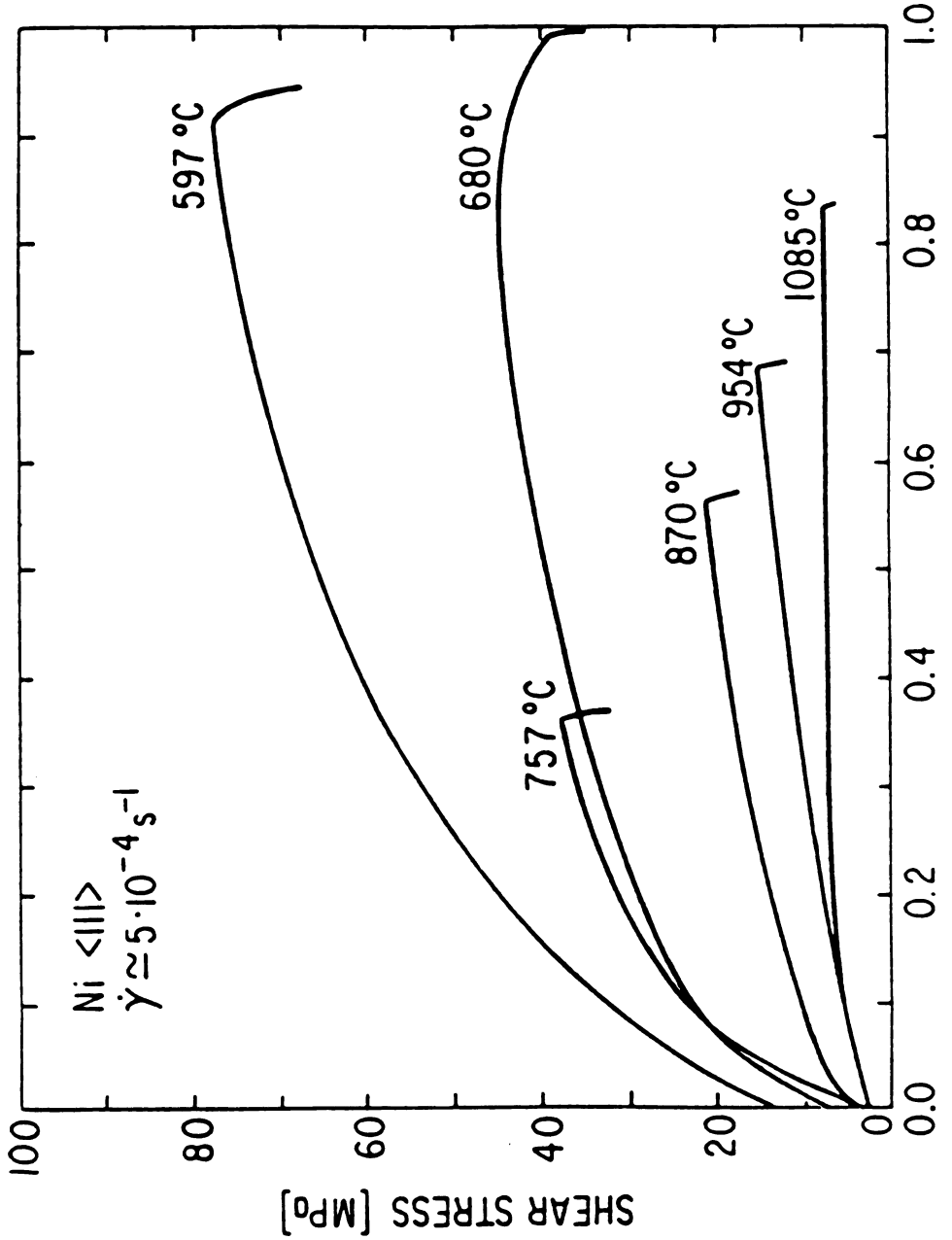

Fig. 2-1. True resolved shear stress vs. true resolved shear strain for <111> Ni single crystals [6]. (Courtesy of Gottstein).

deformation process. The growth of a nucleus is stopped by a strain rate increase, and, once stopped, it is not activated again in a subsequent recrystallization event. For a constant deformation path, i.e., same material, orientation, strain rate and temperature, DRX is set off reproducibly at a definite value of flow stress (τ_R). From the experiments on Cu and Ni Gottstein and Kocks [7] came up with a conclusion that dynamic recovery rather than a competing process, is a precondition to occurrence of DRX. Dynamic recovery of dislocations leads to rearrangement of cell walls on a local scale which give rise to mobile subboundary segments [34] in an elastically stressed environment and thus can trigger DRX. Gottstein et al. [7] also found that two temperature regimes can be distinguished with a rather sharp transition at 0.75 T_m. The recrystallized structure was composed of discontinuously grown subgrains at very high temperature ($T>0.75T_m$, vhT), or complete families of annealing twins at medium high temperature ($0.4<T/T_m<0.75$, mhT).

For nucleation mechanisms Karduck et al. [3] suggested

(1) DRX is nucleated at vhT most likely by discontinuous subgrain growth originating from kink bands owing to their special subgrain size and shape (Fig. 2-2 [35]).

(2) The nucleation of DRX at mhT is suggested to occur by emission of twins from subgrain boundaries. Twin formation is probably assisted by internal stresses and favourable dislocation arrangements in the subboundaries (Fig. 2-3).

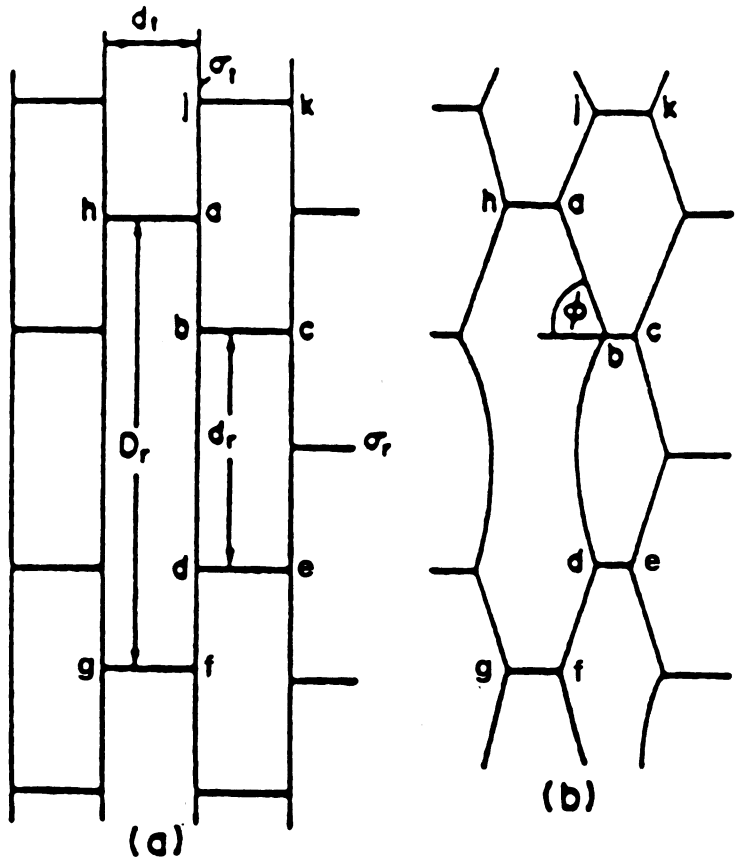

Fig. 2-2. Subgrain coarsening owing to subboundary relaxation, schematically according to Dillamore et al. [35], (a) unrelaxed; (b)relaxed [3]. (Courtesy of Gottstein).

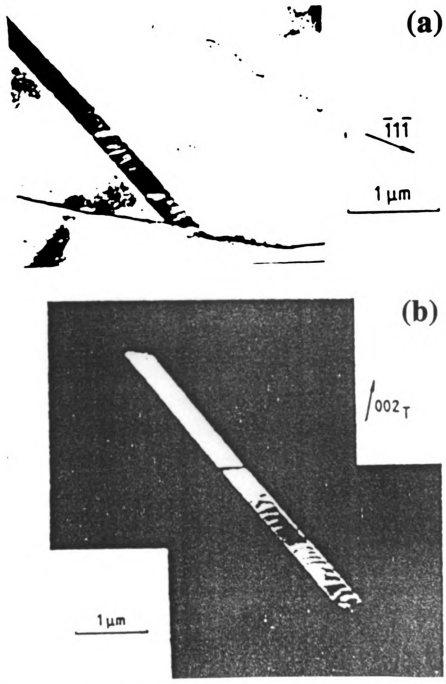

Fig. 2-3. TEM micrograph of a twin lamella emanating from a subgrain boundary by consecutive emission of partial dislocations for a specimen deformed to the start of DRX at T=707°C, $\dot{\gamma}=4\times10^{-3}s^{-1}$, $\tau_R=14.2$MPa. (a) bright field image $\vec{g}=(1\bar{1}1)_M$; (b) dark field image with $(002)_T$ [3]. (Courtesy of Gottstein).

For polycrystalline materials, as known, the grain boundaries influence the development of the dislocation structure as well as the recrystallization behavior. Hence, additional effects can occur in polycrystals so that the results on single crystals may not be sufficient to understand all recrystallization phenomena in polycrystalline aggregates. The initiation of DRX in polycrystals is also indicated by the drop of true stress as seen in Fig. 2-4 [36]. The strain rate has a strong influence on DRX. At the higher strain rates, the flow curve exhibits the typical shape for DRX, but at low strain rates, the flow curve is periodic due to recurrent cycles of recrystallization. Sakai and Jonas [37] mentioned that there are two basic differences between single and polycrystal observations. The first is the initiation stress (τ_R, σ_R) in a typical single crystal oriented for multiple slip can be high as two or more times that in a polycrystal of the same conditions. The second difference is that nucleation in polycrystals is mostly restricted to the original grain boundaries, which it occurs in the grain interiors in single crystals. They explained the difference of the critical stress (τ_R, σ_R) by homogeneous nucleation for single crystals and heterogeneous nucleation for polycrystals.

The effect of grain boundaries on dynamic recrystallization behavior of copper isoaxial bicrystals with <001> tilt boundaries was investigated by Takada et al. [38]. They found that the recrystallized grains form on the already present tilt boundary. This indicates that the boundary is the preferred nucleation site for dynamic recrystallization. It was also found in that study that the tilt boundaries migrate before the onset of dynamic recrystallization.

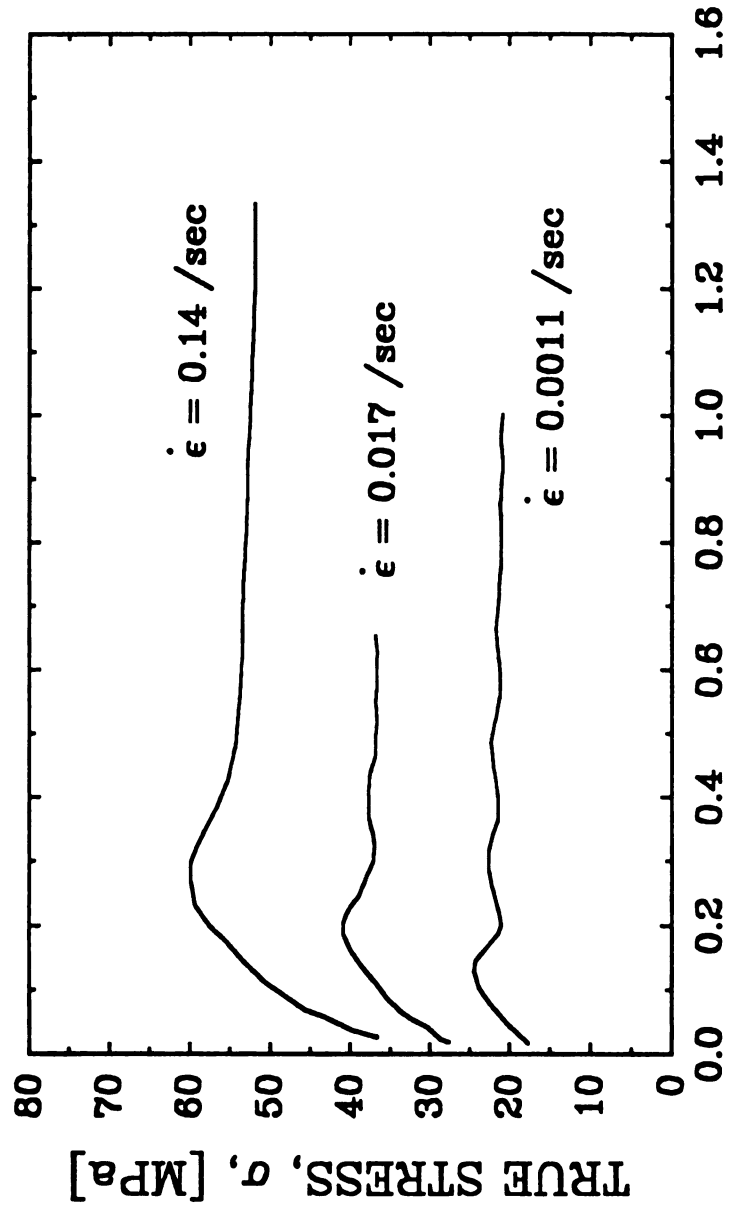

Fig. 2-4. Flow curves of a plain 0.25% C steel in the austenite state (fcc) at 1100°C (0.76 T_m), illustrating the strong influence of strain rate, drawing after Rossard [36].

In polycrystalline materials, static recrystallization is known to nucleate at original boundaries by the buldging mechanism in moderately deformed materials, by nucleation in regions of strong orientation gradients such as deformation bands in heavily deformed materials, and by the single subgrain growth mechanism [39]. Similar mechanism are also expected to operate during dynamic recrystallization. The bulging mechanism for the nucleation of DRX were discussed by Ito et al. [25] and Roberts et al. [40].

2.3 DRX During High Temperature Low Cycle Fatigue

The elevated temperature LCF effect on the mechanical behavior of structural materials has attracted particular attention in recent years. Most investigations [41-44] focused on macroscopic parameters such as stress, strain and cycles to failure, rather than on details of the microstructural evolution. Microstructural developments during LCF have been extensively studied during deformation at ambient temperature [45-47], but very few investigators have addressed the microstructural aspect of LCF at elevated temperatures.

Not much information is available on DRX during HTLCF. In the same paper cited in section 2.1 [19], DRX was observed in Pb which straddled the original orthogonal grain boundary after 8×10^{6} cycles with $\pm0.092\%$ strain amplitude. At a higher strain amplitude, similar structural instability near grain boundaries was detected earlier ($\simeq10^{5}$ cycles). But in more recent papers [20,21], no occurrence of DRX under similar

test conditions was reported. One reason might be the small number of cycles imposed on the specimen ($<10^3$ cycles). During the duration of the current project, a few papers on DRX during LCF were published [11,12,48]. Lim and Raj [11] conducted tests on pure Ni bicrystals with special orientation relationships between these two grains. They found that symmetrically strained bicrystals behave differently from those which are deformed nonsymmetrically. The edge component of the residual dislocations left in the boundary by reaction of lattice dislocations was found important for slip induced cavitation, migration and dynamic recrystallization. Symmetrical reactions which leave a low energy array of edge dislocations in the boundary are most likely to suffer dynamic recrystallization. Lim and Raj explained this as follows: the arrangement of the dislocations leads to the compensation of stress fields, and therefore, to the accommodation of a higher density of dislocations in the grain boundary. Since the onset of dynamic recrystallization is likely to occur when the density of grain boundary dislocations exceeds a critical value, it is conceivable that a low energy dislocation array is a necessary condition for the nucleation of fresh grains. Raman and Reiley investigated DRX on a Pb-Sn solid solution alloy [12,48]. They observed that the nuclei were most often found at or near existing grain boundaries, but in some cases were observed in the grain interior adjacent to a high density of slip bands, and the newly formed grains also participated in cyclic migration and eventually developed boundary markings.

No systematical research has been reported yet on DRX during LCF and its effect on material properties.

2.4 Crack Propagation During High Temperature Low Cycle Fatigue

Extensive grain boundary migration occurs during HTLCF. Grain boundary sliding will be enhanced when a grain boundary migrates such as to align under 45° with respect to the stress axis. Grain boundary sliding will cause cavity formation [49]. An investigation on an Al-Mg solid solution alloy [50] has demonstrated that numerous microcavities are formed at the various migratory positions of the boundaries. The coalescence of these cavities will eventually lead to intergranular fracture under HTLCF.

According to the crack tip shielding model proposed by Rice and Thomson [26], an atomically sharp crack will have been blunted by one atomic plane after the production and emission of a dislocation from the crack tip due to the external stress field as concentrated by the presence of the crack. In ductile materials more dislocations will be emitted from the crack tip and form the plastic deformation zone. The plastic zone size was calculated by applying fracture mechanics concepts [51]. A recrystallization technique can be used to reveal the plastic zone size of specimens fatigued at room temperature [52-54]. The zone was clearly identified as the statically recrystallized area when the proper annealing temperature and time was selected. The stored energy associated with the dislocations might be sufficient to set off DRX during crack propagation. It has been found that most of the deformation work is converted into heat, which causes the temperature to rise in the vicinity of a propagating fatigue crack. Birol conducted tension-tension fatigue tests on Fe-2.6wt%Si at room temperature [55].

He observed that DRX occurred during the latter stages of fatigue crack propagation. The same phenomenon is likely to also occur during high temperature fatigue crack propagation.

III EXPERIMENTAL PROCEDURE

3.1 Testing Materials

Very pure Ni polycrystals having the nominal compositions given in Table 3-1 were used. Also Cu single crystals (99.999% pure) and two Al polycrystals with the composition given in Table 3-2 were tested.

Table 3-1 Composition of Ni studied

Element :	Ag	Al	Cu	Fe	K	Li	Mg	Mo	Na	Pb
Wt ppm :	<10	<10	<10	<10	<10	<10	<10	<10	<10	<10

Element :	Si	Sn	Ti	V	Zr	O	N	C	Ni
Wt ppm :	<10	<10	<10	<10	<10	14	1	*	Bal.

* no information was given by the vendor (Material Research Corporation). The concentration may be higher than 10 ppm but less than 130 ppm as typical in commercial Ni (grade 270).

Table 3-2 Composition of Al studied

Element :	Ca	Cu	Fe	K	Mg	Na	Si	Ce
Wt ppm :	.22	.25	.32	.22	3.5	<1.0	1.4	.29

Element :	C	Cl	H	N	O	P	Al
Wt ppm :	15	1.1	<1.0	<1.0	<5.0	.29	Bal.

According to the vendor (Material Research Corporation), Ni and Al polycrystals are cold extruded into 9.525 mm diameter rods. Two charges of Ni rods had been received two years apart which resulted in different

microstructures after annealing. This will explain in the heat treatment section.

3.2 Specimen Preparation

3.2.1 Mechanical Testing Specimens

(1) Ni polycrystal specimens were machined from 9.525 mm diameter rods. The cold extruded material was sufficiently stiff for machining without destroying the axial alignment. The specimen shape and dimensions are shown in Fig. 3-1. Specimens with the shape as Fig. 3-1(a) were used in the previous testing system (Instron equipped with a reduced atmosphere furnace). Specimens with the shape as shown in Figs. 3-1(b)-(d) were used in the current testing system (MTS equipped with a high vacuum high temperature furnace). Because of the limitation of the raw material, threaded specimens as shown in Figs. 3-1(c)-(d) were used in order to increase the cross sectional area, which corresponded to an increase in stiffness and were suitable for a high strain amplitude test. A few hour-glass shape specimens were used to observe the effect of a strain amplitude resulted from area gradient along the stress axis.

(2) Two Cu single crystal specimens were machined down the center section, using an electric discharge machine. This method confines the introduced cold work to a thin surface layer which can be removed chemically. The orientation of the stress axis was determined by the

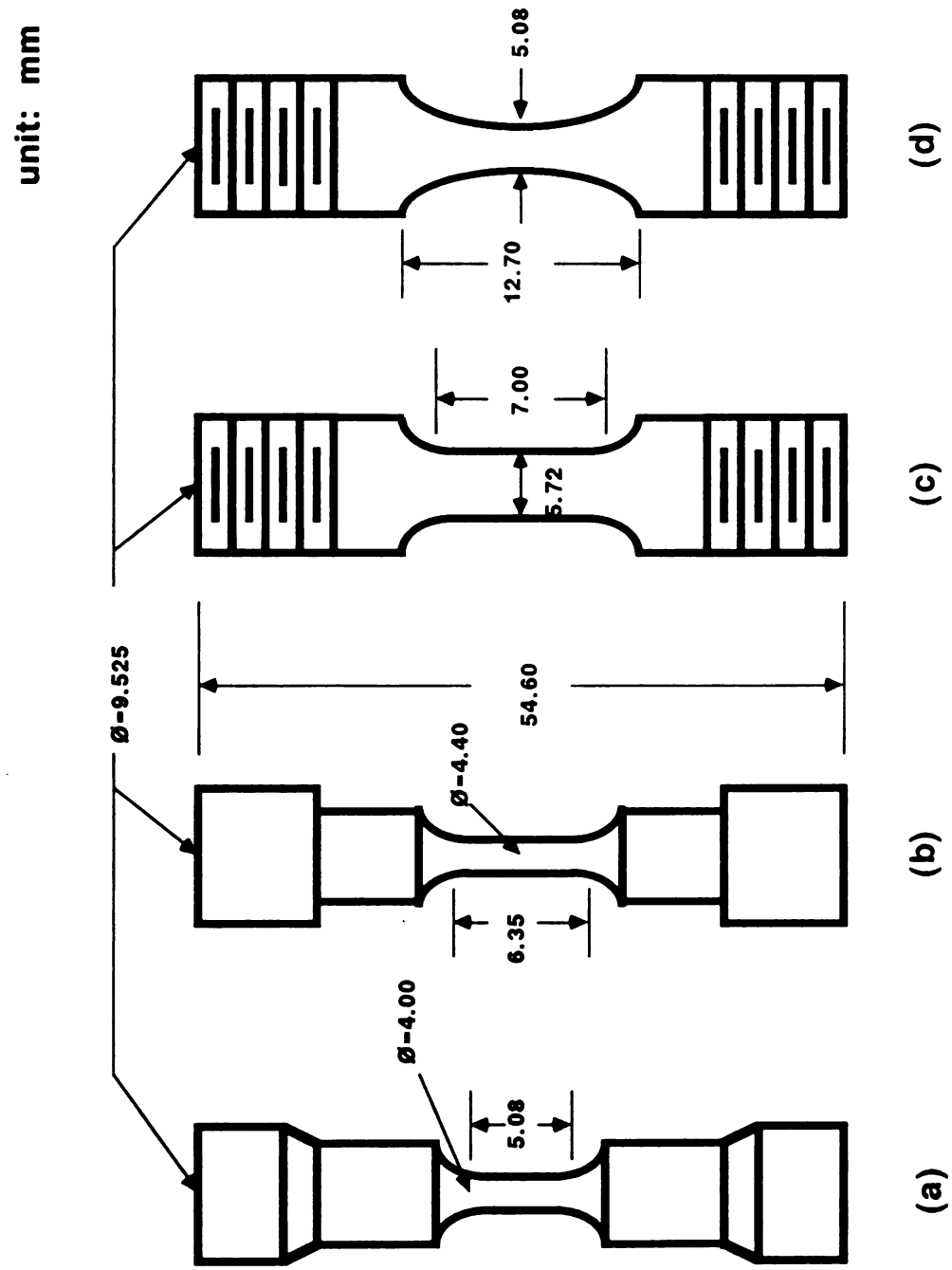

Fig. 3-1. Geometry and dimensions of testing samples.

back-reflection Laue method. Specimen shape and orientation are shown in Figs. 3-2.

(3) Al polycrystal specimens were machined from 9.525 mm diameter rods to the same shape as described for Ni.(see Fig. 3-1)

(4) For crack propagation tests, a single-edge or double-edge or circumferential notch was introduced to the specimen as shown in Fig. 3-3.

(5) Heat Treatment

All specimens were annealed in a vacuum furnace at a pressure of approximately 10^{-3} Pa. The Ni specimens were chemically polished in the following solution at 70°C for 30 s to remove any surface irregularities,

glacial acetic acid	64 ml
nitric acid	34 ml
hydrofluoric acid	1 ml.

Two batches of Ni material were received two years apart. The specimens machined from the first batch were annealed at 900°C for 5 hours. This heat treatment resulted in a grain size of 0.3 mm. (Fig. 3-4). The specimens machined from the second batch of Ni material were heat treated in the same condition, but a different microstructure was observed as shown in Fig. 3-5. This difference can be attributed to different fabrication methods. The second batch of Ni rods probably were obtained from extruded raw material at medium to high temperature

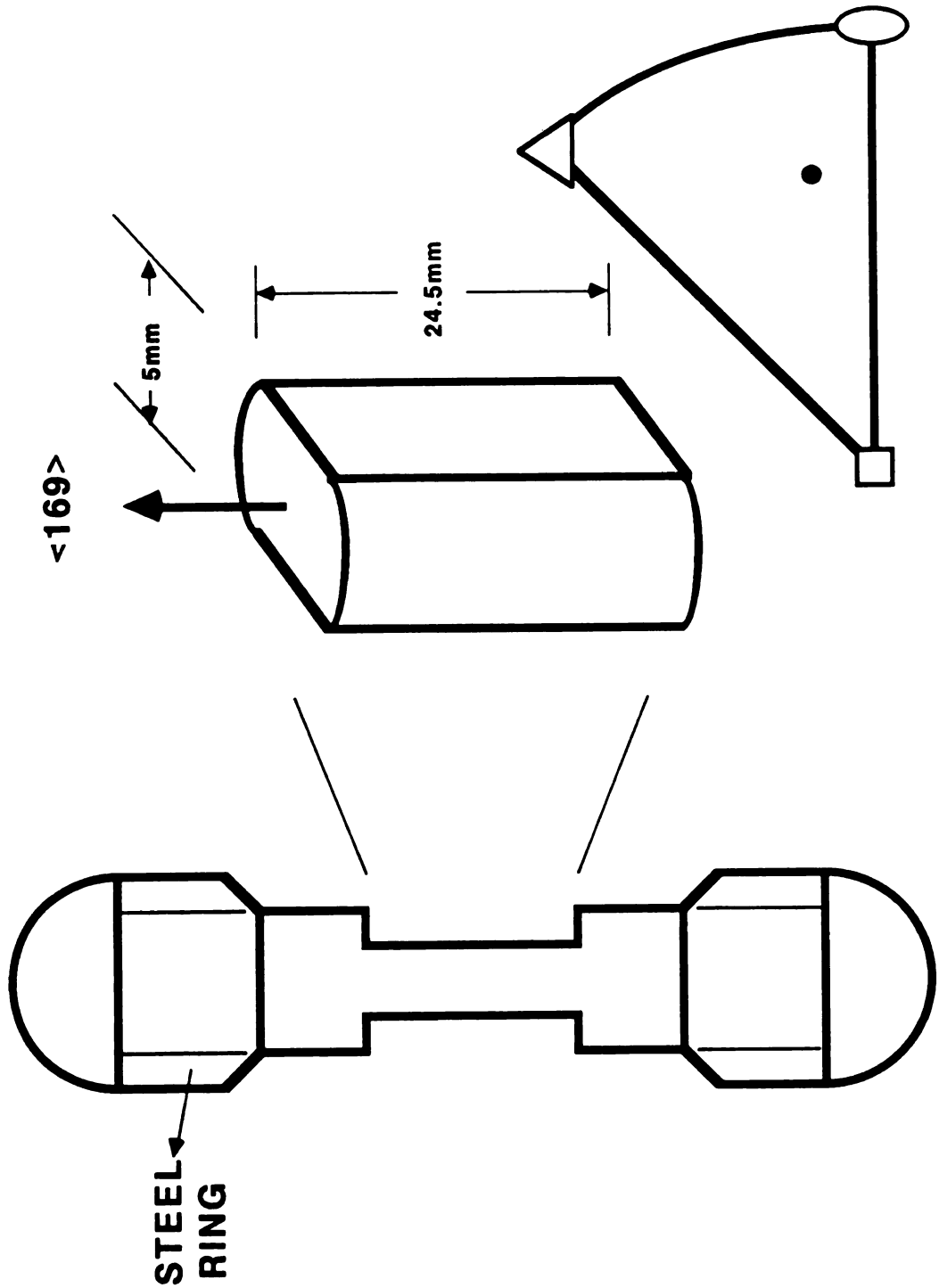

Fig. 3-2. Gauge sectional geometry and orientation of the Cu single crystal.

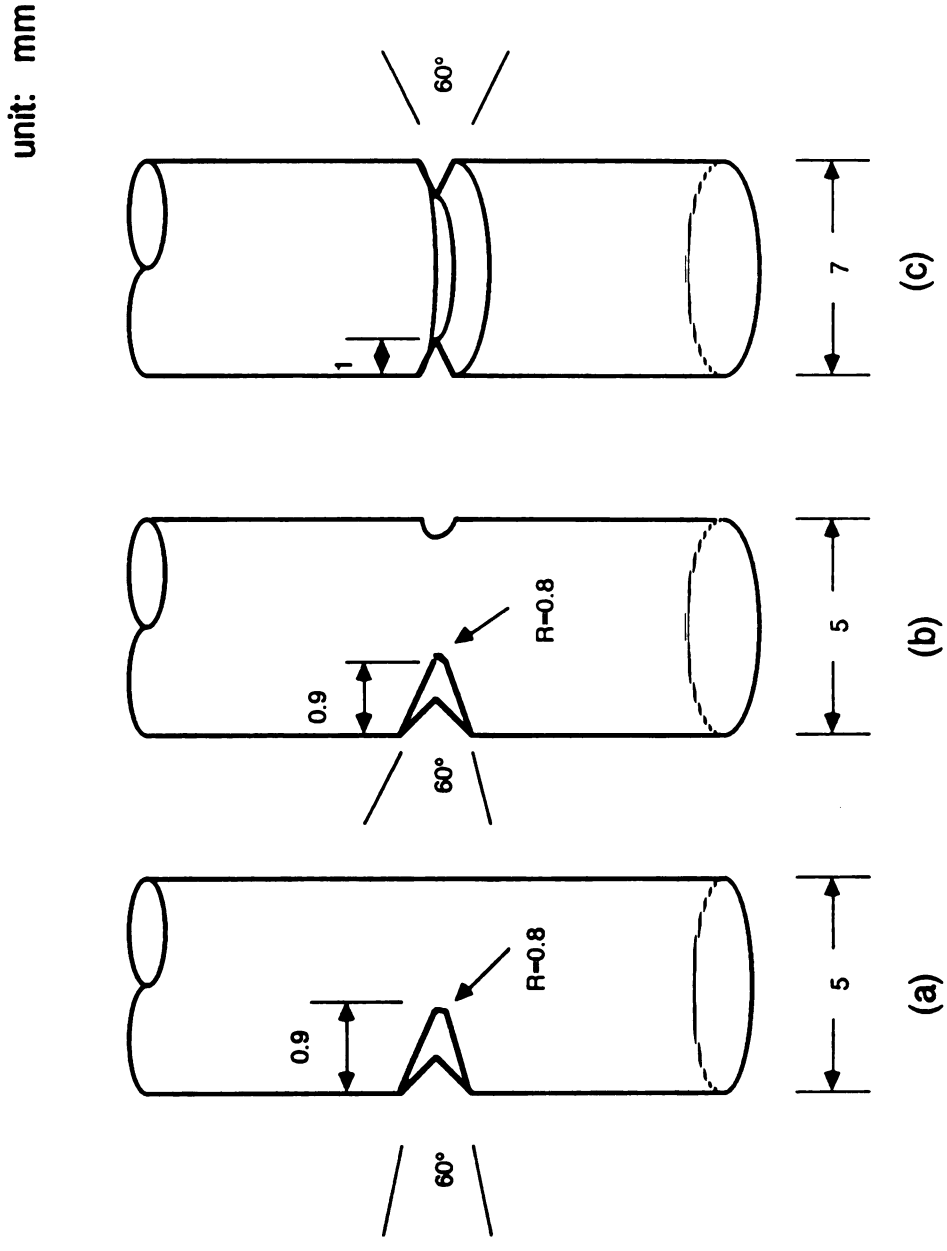

Fig. 3-3. Geometry and dimensions of notches pre-machined for crack propagation tests. (a) single-edge; (b) double-edge and (c) circumferential notches.

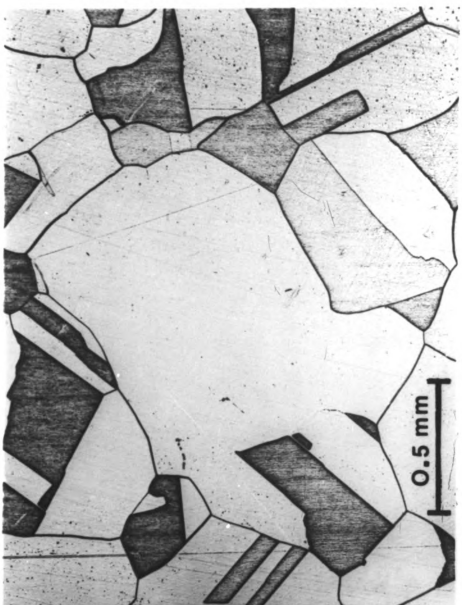

Fig. 3-4. The microstructure of Ni (first batch of material) after annealing at 900°C for 5 hours.

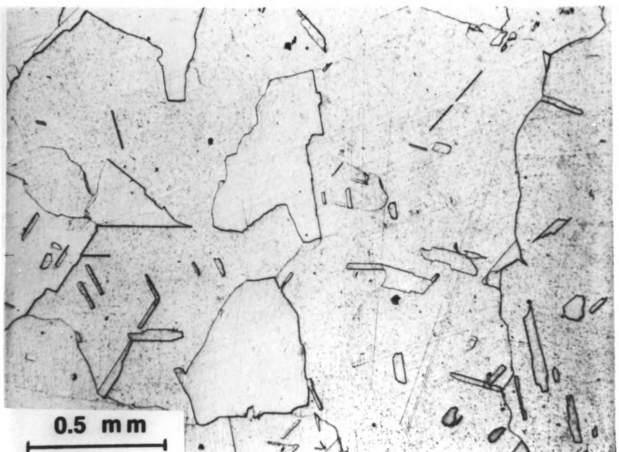

Fig. 3-5. The microstructure of Ni (second batch of material) after annealing at 900°C for 5 hours.

where texture development is apparent and the microstructure was indicated by the large grains containing many small twins. Therefore, a few Ni rods with 305 mm original length were annealed at 900°C for 3 hours. These soft rods were elongated at room temperature with an initial strain rate of $2 \times 10^{-4} s^{-1}$ to 10% of engineering strain (Fig. 3-6). The specimens then were machined from these deformed Ni rods as specified in 3.2.1. Subsequently the specimens were annealed at 850°C for various length of time. The microstuctures are shown in Fig. 3-7. The annealing condition was chosen as 850°C for 20 mins.

The Al specimens were annealed at 310°C for 5 hours (Fig. 3-8). The Cu single crystal specimens were chemically polished to remove 0.1 mm from the surface to avoid any potential sites for recrystallization during annealing, using the following solution

phosphoric acid	33 ml
glacial acetic acid	33 ml
nitric acid	33 ml

Subsequently, it was annealed at 800°C for 12 hours.

3.2.2 Optical Microscopy Specimens

Some of the optical micrographs were taken directly from the planar side surface of the specimen (Fig. 3-9), when the test was interrupted after some cycles. The others were taken after the end of the tests. Specimens were cut from test samples with a very low speed diamond wheel cutting machine (Buehler Isomet) along a plane either perpendicular or

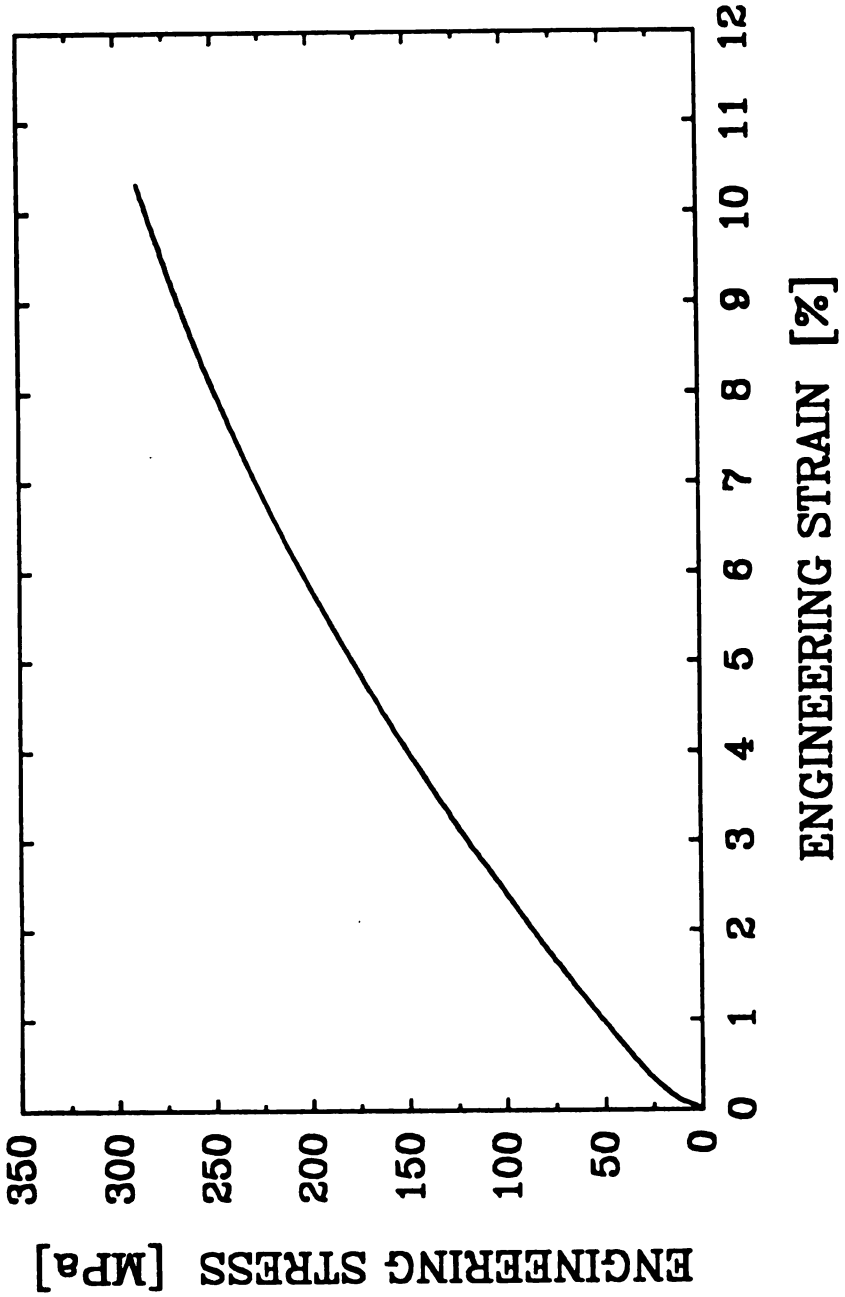

Fig. 3-6. Engineering stress-strain curve of a Ni bar, which was annealed at 900°C for 3 hours, elongated at room temperature with an initial strain rate of $2 \times 10^{-4}\ s^{-1}$.

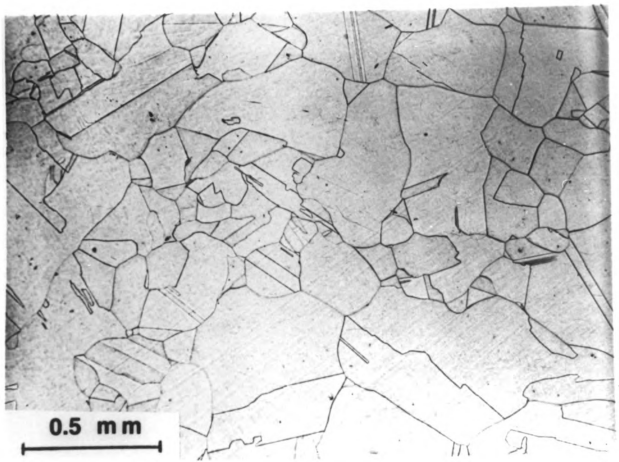

(a)

Fig. 3-7. The microstructure of the elongated Ni after annealing at 850°C for (a) 20 min.; (b) 1 hour.

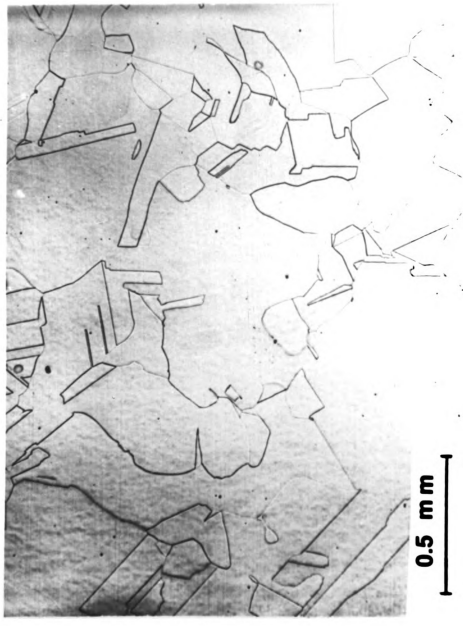

(b)

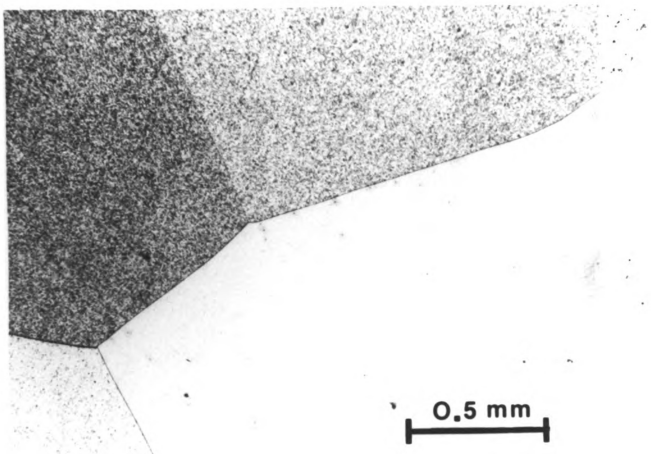

Fig. 3-8. The microstructure of Al after annealing at 310°C for 5 hours.

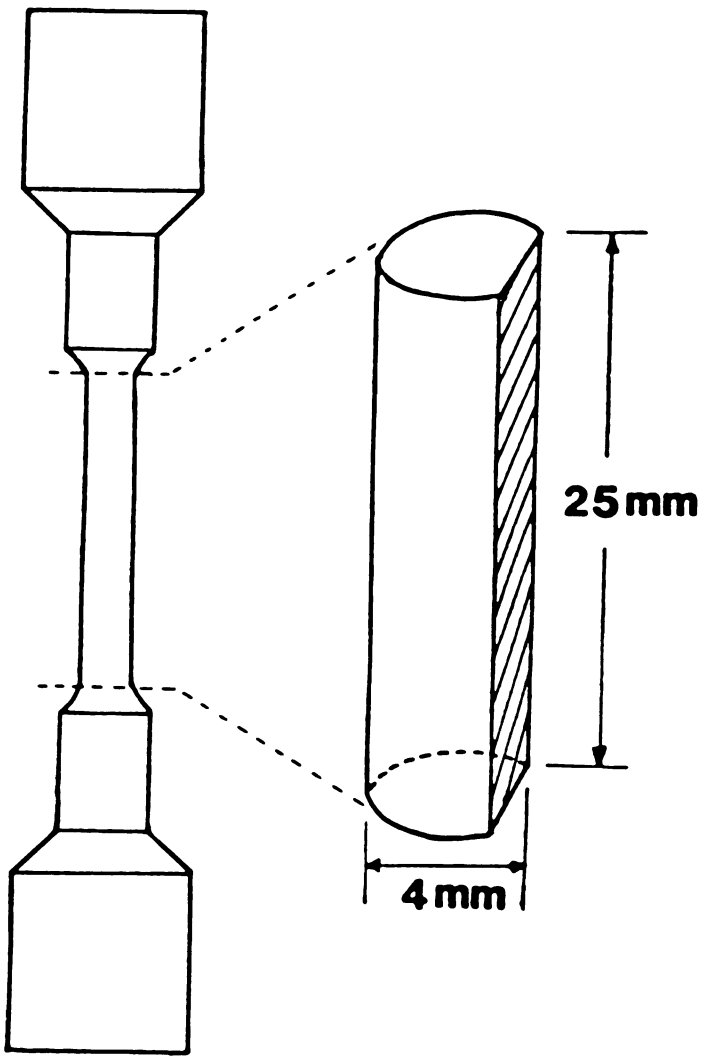

Fig. 3-9. Geometry and dimension of a Ni specimen with pre-machined planar side surface.

parallel to the stress axis. Subsequently they were mounted in cold setting resin before mechanical polishing. All specimens were first polished on abrasive grit paper and then on a cloth by using aluminum oxide to get a mirror-like surface.

The etchants were

nitric acid	67 ml	
glacial acetic acid	33 ml	
hydrochloric acid	1 ml	for Ni
hydrofluoric acid	46.2 ml	
water	46.2 ml	
hydrochloric acid	7.6 ml	for Al, and
ammonium hydroxide ≃ 58%	50 ml	
water	50 ml	
hydrogen peroxide ≃ 30%	25 ml	for Cu.

All optical micrographs were taken with a Neophot 21 Microscope.

3.2.3 Transmission Electron Microscopy Specimens

Slices of approximately 0.3-0.4 mm thickness were sectioned from testing samples, using an Isomet low speed saw with diamond wheel such that the foil plane normal is parallel to the direction of loading.

These slices were thinned down to 0.1 mm by careful mechanical polishing.

The final jet polishing was done in a Tenupol jet polishing device. Electrolytes used were A8(*) for Ni, A7(*) for Al and D2(*) for Cu. The optimal jet polishing conditions are given in Table 3-3.

Table 3-3 Jet polishing conditions for Ni, Al and Cu

	Electrolyte		Temp (°C)	Voltage (V)	Current (A)
Ni	A8		13	70	0.18
	acetic acid	950 ml			
	perchloric acid	50 ml			
Al	A7		-5 - -10	12	0.12
	perchloric acid	100 ml			
	glecerol	200 ml			
	methanol	700 ml			
Cu	D2		15	8	0.11
	distilled water	500 ml			
	phosphoric acid	250 ml			
	ethanol	250 ml			
	Vogel's Sparbeize	2 ml			
	propanol	50 ml			
	urea	5 g			

* A7, A8 and D2 are registered trade marks of Struers Scientific Instruments, Inc..

All specimens were examined in a Hitachi H-800 electron microscope with double tilt stage. The applied voltage was 200 kV.

3.2.4 Scanning Electron Microscopy Specimens

Some specimens were fatigued until fracture. The fracture surface was ultrasonically cleaned with acetone before examining. A JEOL 35C

SEM was adopted to observe the fracture surface. The applied voltage was 25 kV.

3.3 Mechanical Testing

Two types of machines and setups were used during the process of the program.

3.3.1 Instron Testing Machine

By July 1988, the tests were conducted on a floor model electro-mechanical Instron testing machine with a 500 kg tension-compression reversible load cell.

Pull rods and button head grips were designed and machined out of AISI 310 heat resistant stainless steel.

To avoid oxidation of the specimen during testing a cylindrical protective chamber was designed as shown in Fig. 3-10. A stainless steel ring with a clearance of 0.75 mm to the pull rod was welded at the top of the tube, while the lower ring which fitted on the lower pull rod was made of Invar and the dimensions were chosen such that at temperatures in excess of 200°C a tight fit with the lower pull rod was obtained due to the difference in thermal expansion between Invar ring and lower pull rod.

With this chamber design a protective atmosphere of 90% N_2 + 10% H_2 was maintained during the test inside the chamber to minimize oxidation. A flow rate of 12 liters/hour at 5 psi of this gas mixture was found sufficient to avoid oxidation. Higher flow rates were avoided since the

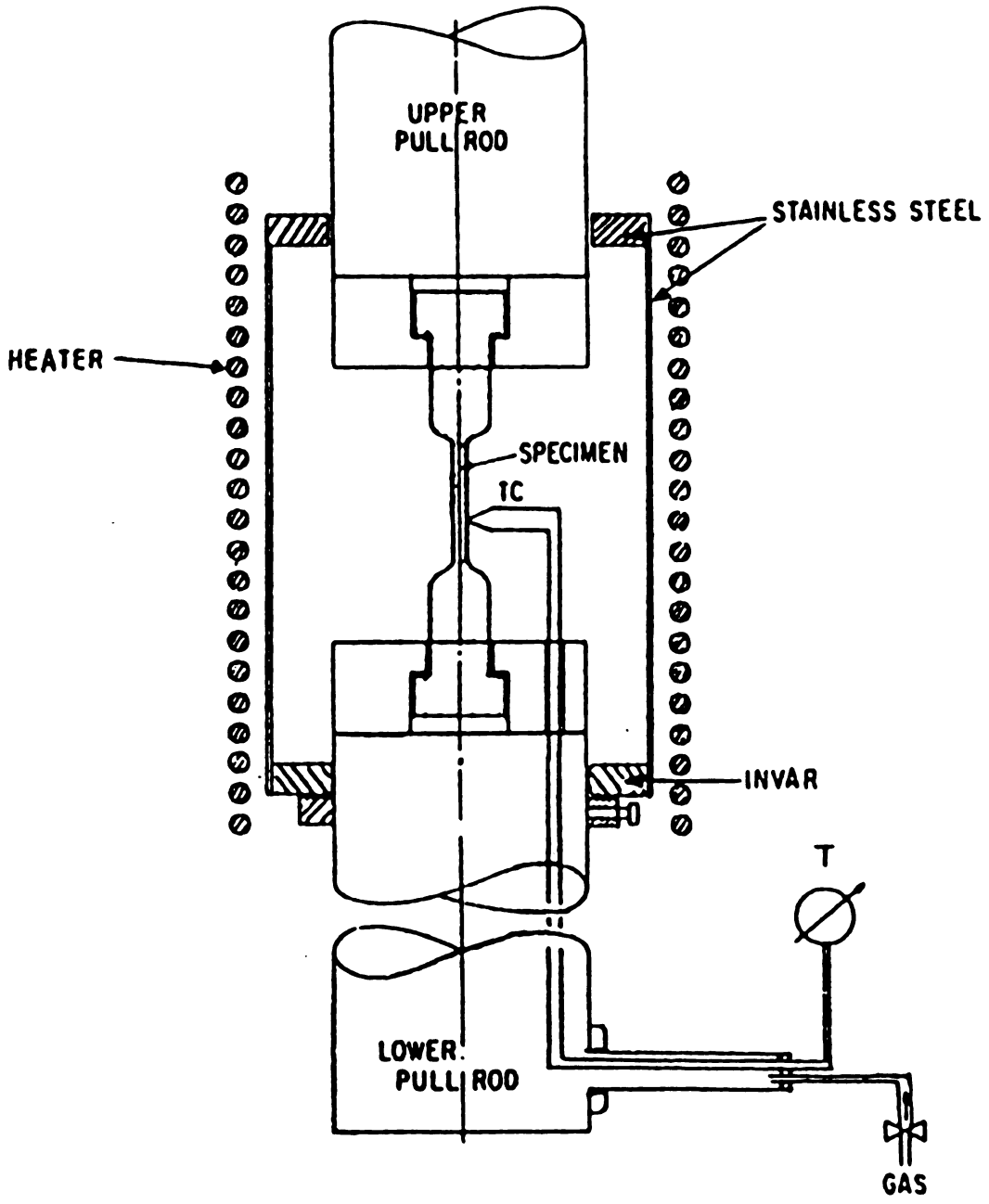

Fig. 3-10. Arrangement of the high temperature mechanical testing setup.

gas started burning at the top of the chamber, also it created an unwanted back pressure.

Computer codes were developed in house to control the Instron testing machine by the digital output from an IBM XT personal computer and for data aquisition by A/D conversion of the load cell signal. All the load-displacement data from the test then were stored at an interval chosen properly. The resolution of data aquisition was 4 μm per data set with an accuracy better than 0.1%. These data were then further processed to get the relevant information such as true stress-strain curves and work hardening coefficient vs. true stress curves,etc..

3.3.2 MTS Testing Machine

After July 1988, a new system was assembled. A schematic diagram showing the essential elements of the system is shown in Fig. 3-11.

The system includes a closed loop servohydraulic load frame (MTS 810) with a 10-100 kN (MTS 661.20A-03) or a 0.5-10kN (MTS 661.19) load cell, a 25.4mm gauge length water cooled high temperature extensometer with maximum strain range of 30% and minimum strain range of -10%, and equipped with a Centorr S-60 high vacuum high temperature furnace. The maximum resolution of the extensometer is 0.1 μm, but due to the limitation of 12 bit analog-digital converter (ADC), the actual resolution is 0.488 μm. The electronic noise arising from furnace further limits the resolution. To get better results, signal filtering circuit will be introduced to the system.

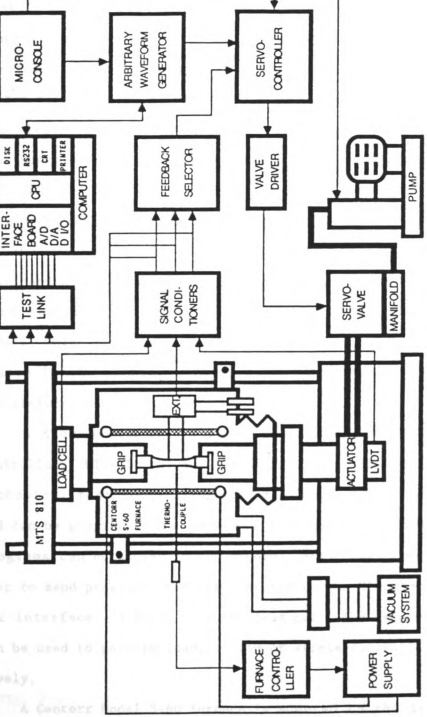

Fig. 3-11. Schematic diagram showing the basic elements of the computerized high temperature high vacuum servohydraulic test system.

For tension-compression fatigue tests, the crucial point is the grip design, this is especially important in a high temperature environment. The crossover phenomenon when changing from tension to compression can be solved by preloading against the bottom area of the specimen. This is accomplished by applying hydraulic pressure to a piston residing inside the pull rod. Such a grip assembly is shown in Fig. 3-12. The specimen gripping insert includes two pairs of collets, four tungsten pins and two extension pistons which are shown in Fig. 3-13. All parts inside the hot zone are made of high temperature molybdenum alloys (TZM). It contains approximately 0.5% Ti, 0.08% Zr and 0.01-0.04% C. The alloying elements give rise to both solid solution hardening and dispersion hardening. The current design is good for test temperatures up to 1000°C, but failed when trying to test at 1500°C, which is the desired temperature for this system. The major reason is the bonding between tungsten pins and TZM pull rods at high temperature under high pressure.

A MicroConsole (MTS 458.20), an AC controller (MTS 458.13), two DC controllers (MTS 458.11) and a MicroProfiler (MTS 458.91) compose the mechanical test controlling system. The MicroProfiler has 52KB memory and can be programmed to generate arbitrary waveforms. Ninety nine programs can be stored in the memory. Remote programability allows the user to send programs from the computer to the MicroProfiler via an RS 232 interface. Signals from the load cell, the extensometer or an LVDT can be used to perform load, strain or stroke controlled tests, respectively.

A Centorr Model S-60 furnace is mounted to the load frame of the MTS machine. Two bellows for 50.8mm diameter rods accommodate the

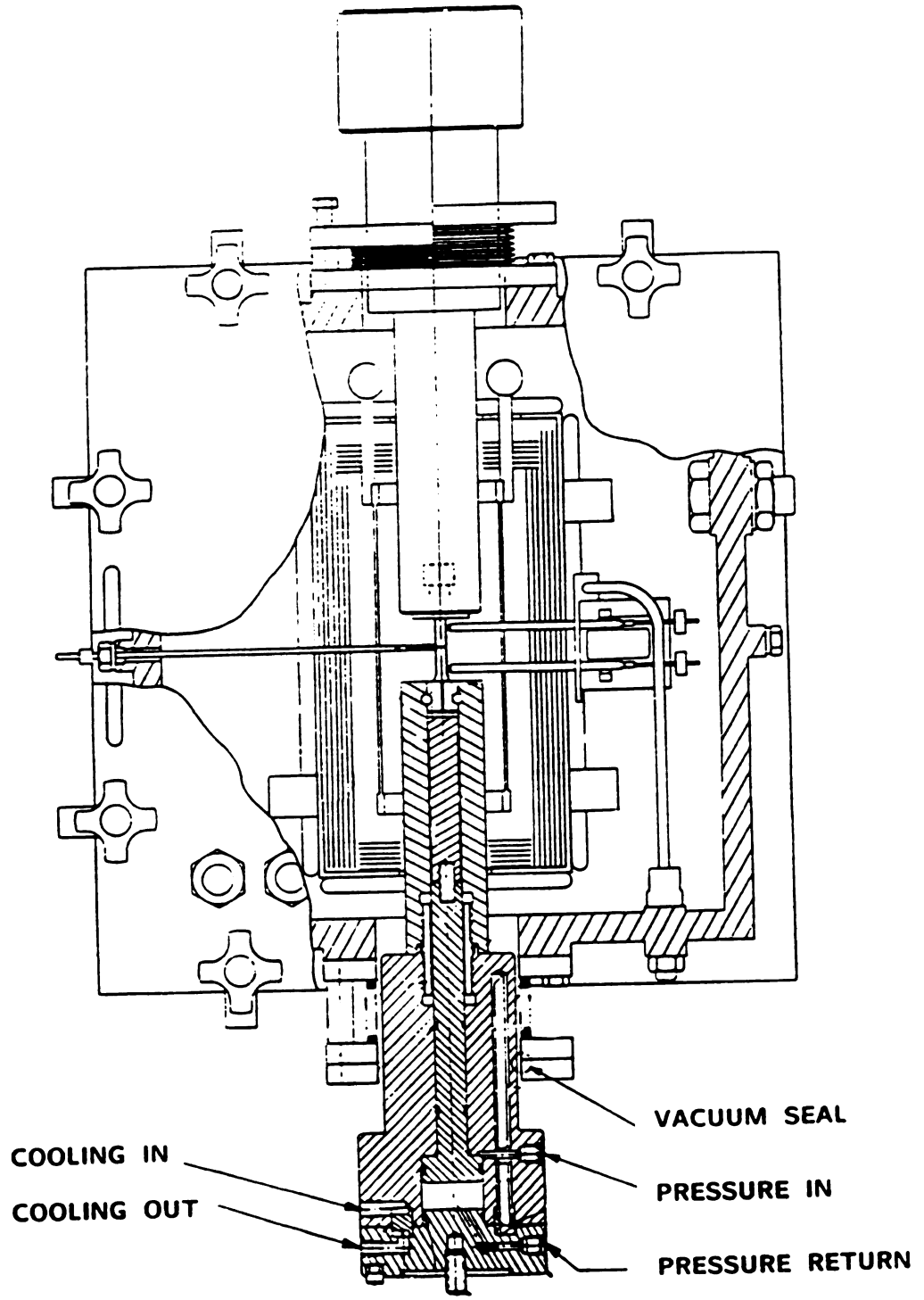

Fig. 3-12. A drawing showing the design of the pre-load grips for high temperature tension-compression fatigue test.

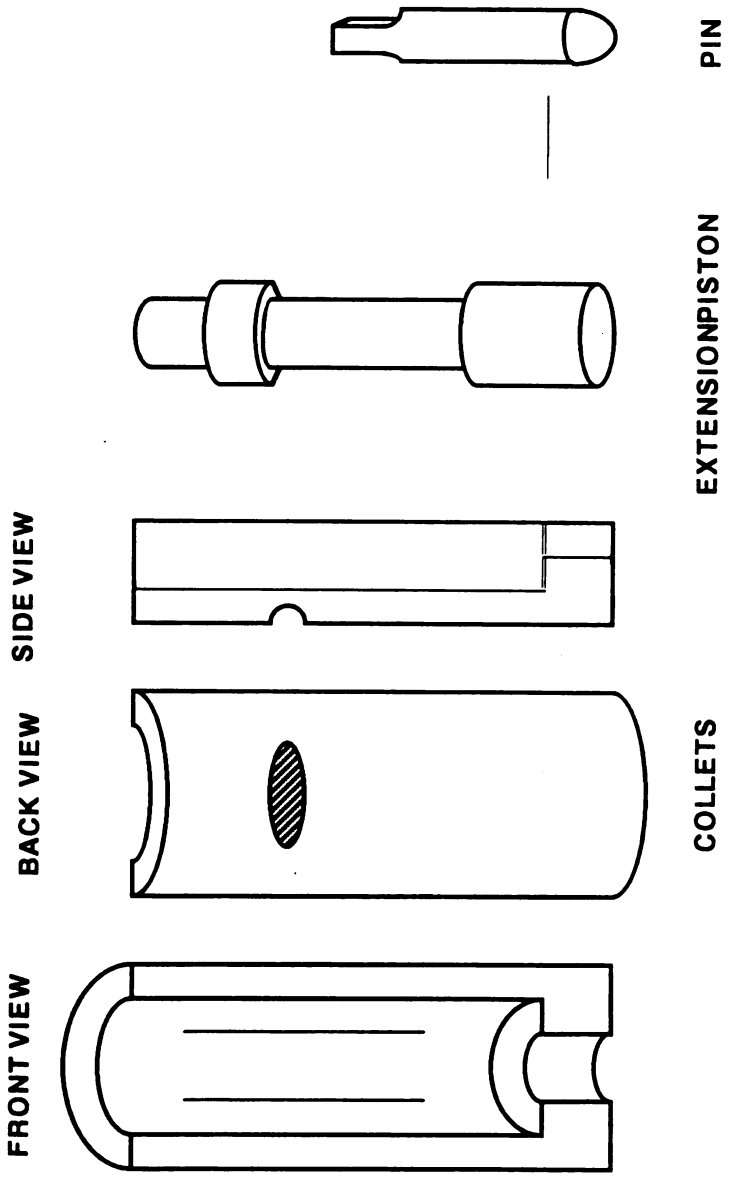

Fig. 3-13. Schematic diagram of the specimen gripping insert.

movements of the actuator up to 150 mm. The hot zone size is 76.2 mm diameter by 203.2 mm height with two halves of tungsten mesh heating elements. The radiation is blocked by six layers of heat shields made of tungsten and molybdenum. The furnace chamber is designed to also accommodate the MTS extensometer. The final setup for a test is shown in Fig. 3-14. The maximum operating temperature of the furnace is 2000°C in vacuum or in controlled inert gas (argon, nitrogen, helium) atmosphere. Two thermocouples of type "C" W5%Re/W26%Re are used as the temperature sensors and a Honeywell Universal digital PID controller with 20 programable segments controls the temperature. The temperature was stable within ±1°C. An over-temperature controller is installed to protect the system from over heating in case of a broken main thermocouple.

A Zenith AT compatible personal computer using Intel 80286 CPU and 80287 math coprocessors and equipped with 1 MB of main memory is used to perform the machine control and data acquisition. A high performance analog and digital I/O board (Data Translation DT 2818) is plugged into one of the system expansion slots in the personal computer backplane. The board can be programmed from the computer's compiled BASIC language to perform analog to digital (A/D) conversions; digital to analog (D/A) conversions; and digital input and digital output transfers. The DT 2818 has a 12 bit A/D converter with a maximum data sampling rate of 13.7 kHz. It uses a simultaneous sample and hold A/D converter, which permits up to four A/D channels to be sampled simultaneously. By using Direct Memory Access (DMA), the data can be moved directly into or out of BASIC variable arrays at high speeds. A real-time software package (PCLAB) containing a number of machine language routines designed to be

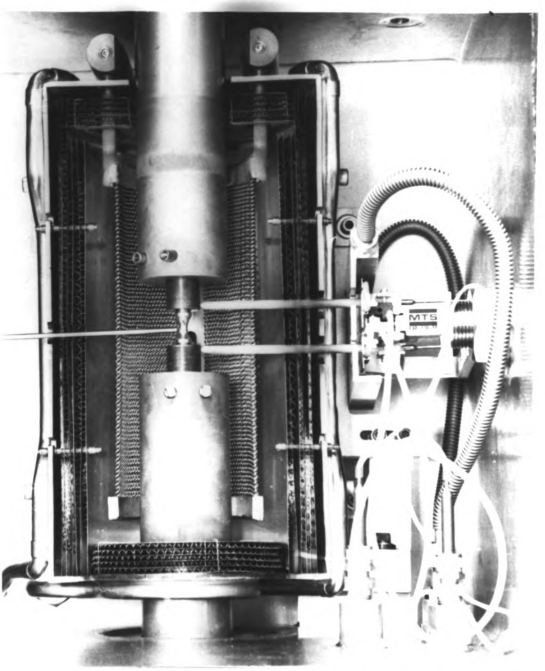

Fig. 3-14. Final setup inside a vacuum chamber with an extensometer attached for conducting a strain amplitude control fatigue test at high temperature.

called from the computer's compiled BASIC language greatly simplify the programming required to use the DT 2818 board and only high level routines for data acquisition and control needed to be written.

A lot of efforts were made to develop the software for test control and data acquisition. Because of various testing techniques adopted among the laboratory colleagues, several programs have been written in MicroSoft QuickBASIC language to meet individual need. Currently, programs for tension, compression, load controlled fatigue, strain controlled fatigue and user defined tests are available. Programs for plotting and printing the data are available, too. A listing of the programs used in current fatigue tests are included in appendix A.

Total strain amplitude (i.e. elastic + plastic strain) control was applied to all fatigue tests.

3.4 The Microhardness Test

The microhardness tester (Buehler Micromet) was adopted to measure the hardness of the microstructure. The diamond-pyramid hardness number (DPH) was determined from the following equation [56]

$$DPH = \frac{2P\sin(\theta/2)}{L^2} = \frac{1.854P}{L^2}$$

where P = applied load, kg

L = average length of diagonal, mm

θ = angle between opposite faces of diamond = 136°.

The applied load in the test was 0.3 kg; the loading speed was 70 μm/sec and the loading time was 20 seconds.

IV EXPERIMENTAL RESULTS

4.1 Mechanical Behavior

The test conditions are summarized in Table 4-1. The cyclic hardening curves of the Ni and Al specimens are shown in Fig. 4-1. These curves are plotted in terms of the stress amplitude as function of the number of cycles (Fig. 4-1(a)) or cumulative strains (Fig. 4-1(b)). The qualitative shape of the cyclic hardening curve is similar for all specimens. The true stress increases rapidly in the first few cycles due to the high initial strain hardening. With increasing number of cycles (N) the work hardening rate ($d\sigma/dN$) (σ-true stress) decreases. Eventually the hardening curve attains a maximum and exhibits continuous softening thereafter. The stress decrease at large cumulative strains indicates a strong softening mechanism to occur at large numbers of cycles. At a smaller total (elastic + plastic) strain amplitude, the maximum stress is smaller and attained at a higher number of cycles. With increasing strain rate (or cycle frequency), the stress level increases and the maximum stress is attained at a higher cumulative strain. The same result was observed when the test temperature was increased to 955°C. An increase in deformation temperature lowers the stress level and shifts the maximum stress to a higher cumulative strain. In fact, at the chosen test temperature of 955°C ($0.71T_m$) the hardening curve becomes very flat. Raising the total strain amplitude results in an increase of the stress level and an attainment of the maximum at a lower number of cycles. Al qualitatively shows the same

Table 4-1 Test conditions and results of low cycle fatigue.

Test No.	Material	Temperature (°C)	Shear modulus (G, MPa)	Total strains amplitude (%)	Cycle frequency (10^{-3} Hz)	Initial strain rate ($10^{-4}\,s^{-1}$)	Total No. of cycles	Cycle to maximum ($\simeq$)	Maximum stress (σ_{max}, MPa)	Cell size (μm)
1	Ni	600	60,800	0.375	20	1.5	840	450	42	—
2	Ni	600	60,800	0.5	13	1.5	510	140	50	3.9
3	Ni	600	60,800	1.7	4	1.5	310	60	54	3.34
4	Ni	600	60,800	1.0	70	15	550	110	63	2.84
5	Ni	955	51,900	1.0	7	1.5	460	170	13	16.0
6	Al	200	22,800	0.5	13	1.5	720	180	8.5	10.0
Tensile	Ni	600	60,800	—	—	1.5	—	—	78	2.16

behavior as Ni, but at a much lower stress level. Fig. 4-1(c) shows the stress decrease rate ($(d\sigma/G)/dN$) (G-shear modulus) as a function of number of cycles. At the same homologous temperature and the same total strain amplitude the average rate of stress decrease in Al ($\simeq 1.152\times10^{-7}$) is much smaller than that of Ni ($\simeq 5.723\times10^{-7}$).

It is finally noted that at the end of a test the specimen usually had not failed or would reveal macroscopic cracking, except for two Ni specimens, one deformed at the higher strain rate and the other with 0.5% total strain amplitude. This is also noticeable on the hardening curve by a strong softening toward the end of the test.

4.2 Microstructural Development

Substantial microstructural changes due to extensive grain boundary migration were found when comparing the microstructures before (Fig. 3-4) and after (Fig. 4-2) the test. For a more quantitative evaluation one specimen was machined flat on one side surface (Fig. 3-9) such that the grain structure could be easily examined by optical microscopy. The specimen was deformed to a specific number of cycles, air cooled to room temperature, dismounted, examined in a microscope, remounted and reheated at 10°C/min, further deformed etc.. A series of micrographs taken directly from the planar side surface of the specimen after each specific stage are shown in Figs. 4-3(a)-(j). All these micrographs show the same area which was parallel to the loading direction. Fig. 4-3(a) is the microstructure of the annealed state. There are many small grains

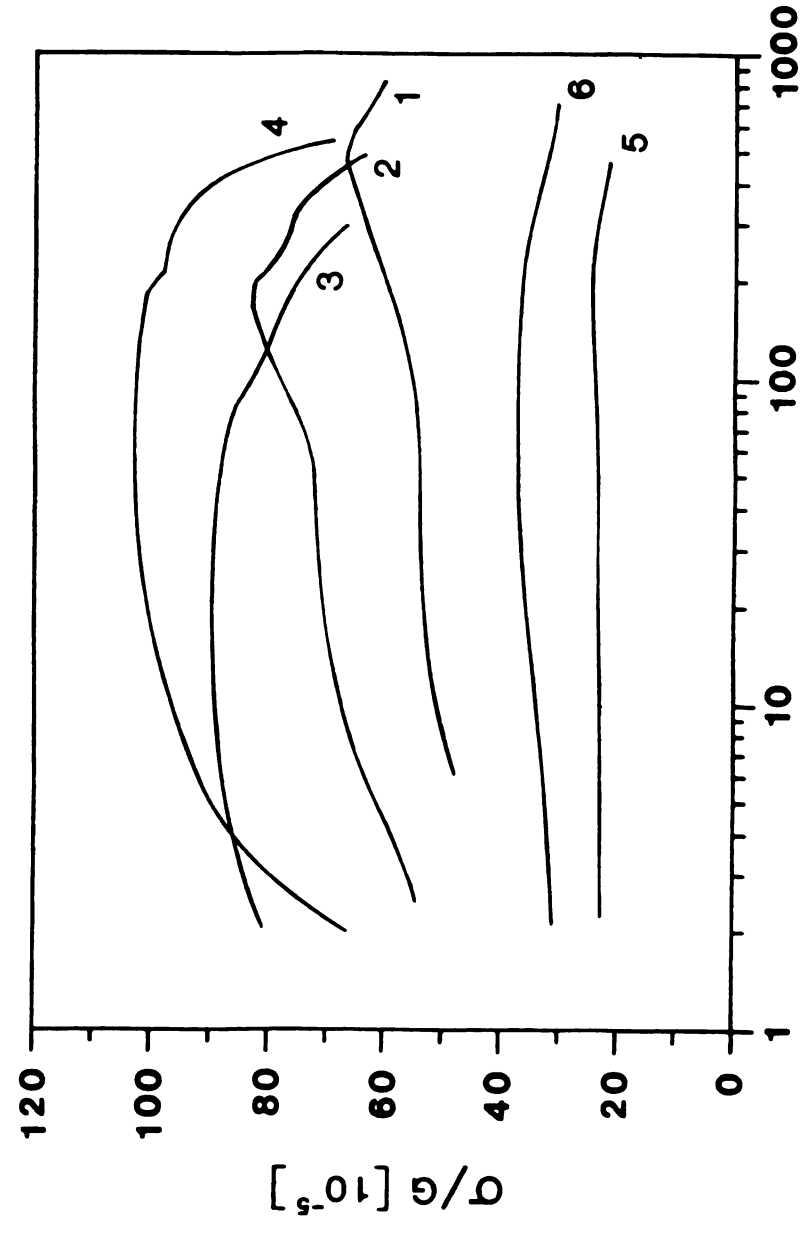

Fig. 4-1. (a)-(b) Cyclic hardening curves for Ni and Al at high temperature with various total strain amplitudes and cycle frequencies; (c) stress decrease rate vs. number of cycles. (The numbers of the curves corresponds to the test numbers in Table 4-1).

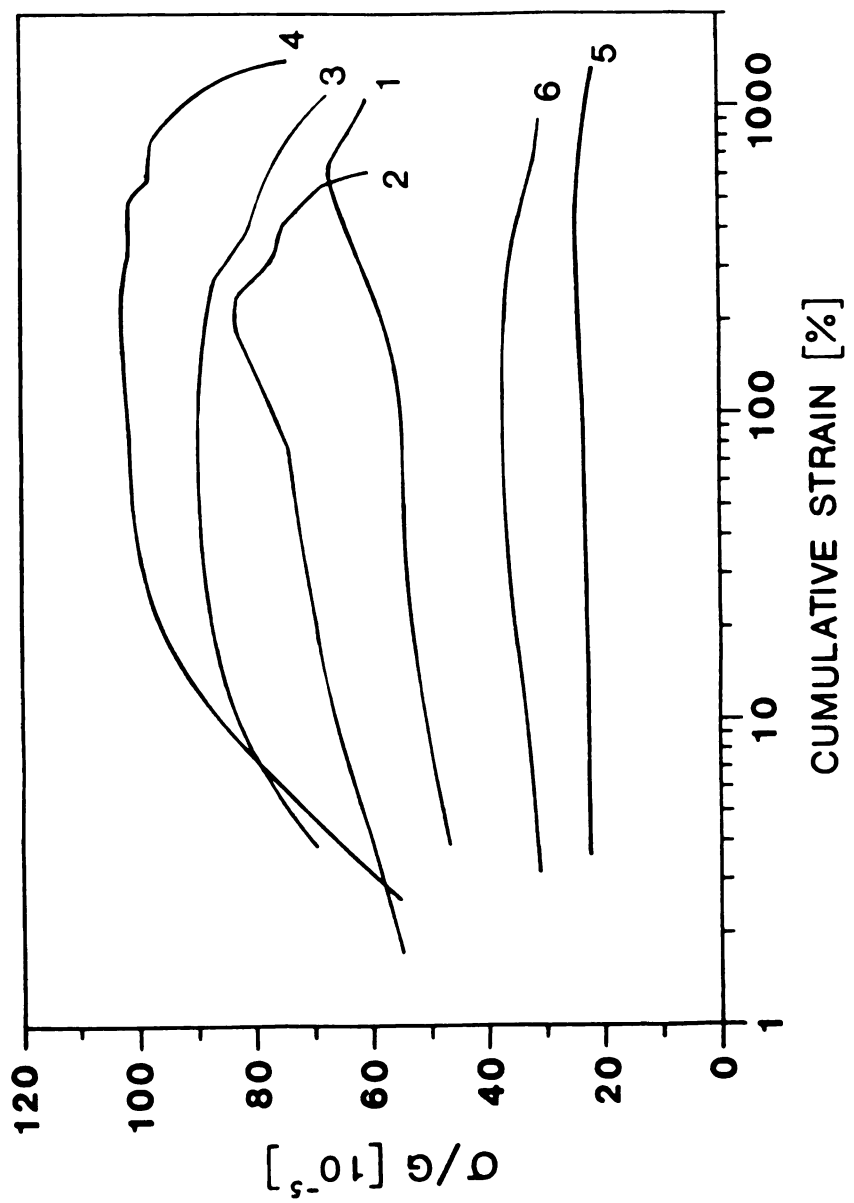
σ/G [10⁻⁵]
120
100
80
60
40
20
0
1
10
100
1000
CUMULATIVE STRAIN [%]
1
2
3
4
5
6

(b)

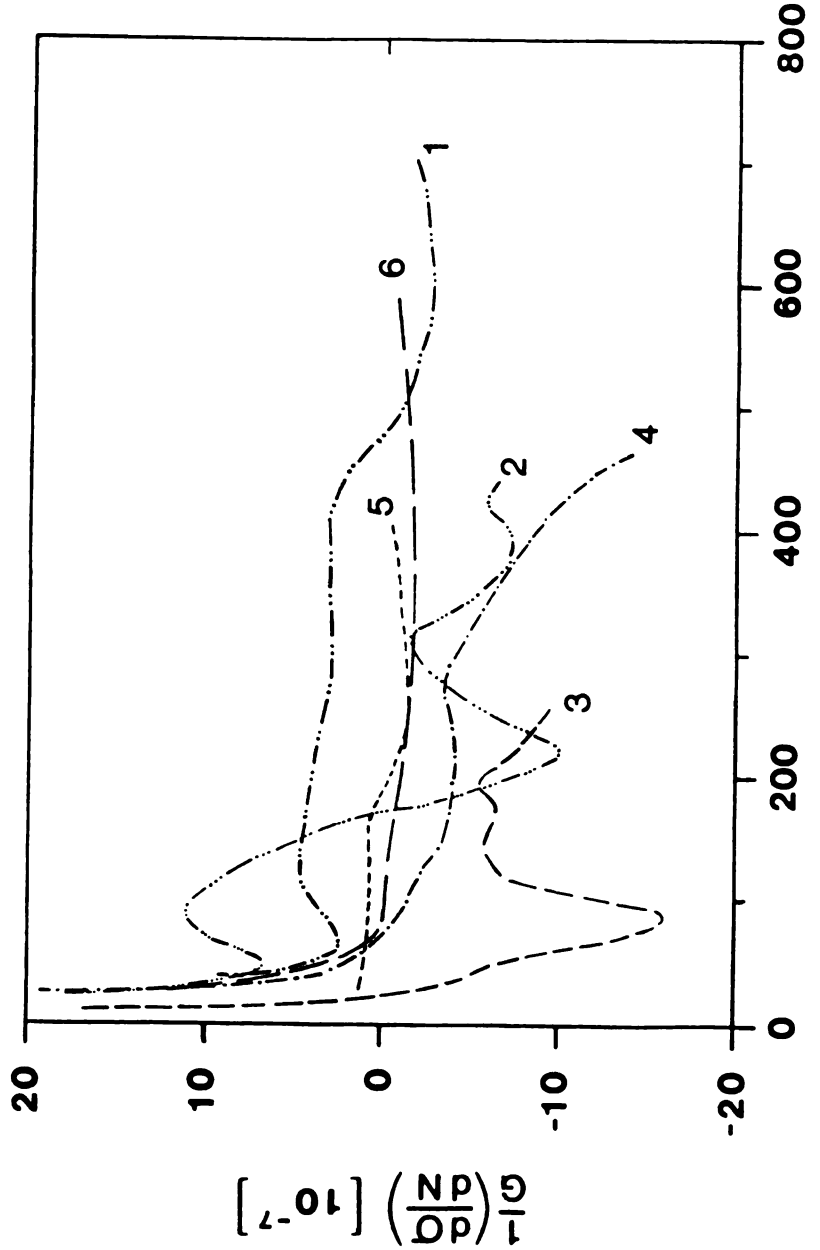
20
10
0
-10
-20
0
200
400
600
800
NUMBER OF CYCLES
1
2
3
4
5
6
$G_1\left(\frac{dQ}{dN}\right)$ [10^{-7}]

(c)

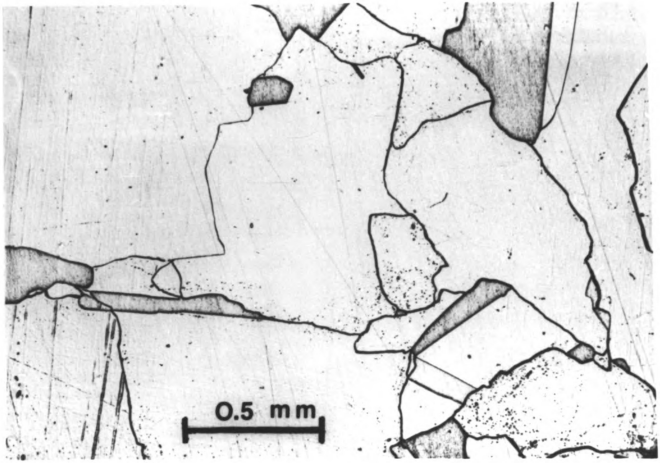

Fig. 4-2. The microstructure of a Ni after 200 cycles with 0.5% total strain amplitude at 600°C.

embedded between large ones in this annealed state. Fig. 4-3(b) is the microstructure after 10 complete cycles. Position A, B and D reveal extensive grain boundary migration. One grain boundary disappeared and a twin boundary formed at position C. About 25 μm thickness was removed by polishing in the sequence from Fig. 4-3(a) to Fig. 4-3(b). Comparing these two microstructures, it is evident that the small grains tend to shrink. Fig. 4-3(c) is the microstructure taken immediately after 10 cycles. The distribution of migration distance is inhomogeneous in that some areas show much stronger grain boundary migration than others. The sample was slightly etched again such that the boundary position before and after deformation could be seen simultaneously. Fig. 4-3(d) is the result after etching. The grain boundary at position B in Fig. 4-3(c) reveals a series of approximately parallel markings in front of this grain boundary. The new grain boundary position can be seen in Fig. 4-3(d). Those markings delineated the positions of the boundaries at the end of each stress cycle. Evaluation reveals that there is a one-to-one correspondence between the number of grain boundary markings and the total number of whole cycles imposed on the specimen. A more detailed structure of surface markings is shown in Fig. 4-4. The same procedure was followed for the investigation at higher numbers of cycles. Figs. 4-3(e)-(g) are the microstructures after 40 cycles. They show qualitatively the same phenomenon, but the migration rate has decreased compared to the first 10 cycles. The positions indicated by arrows make obvious that the grain boundaries tend to migrate such as to align under 45° with respect to the stress axis as has been shown previously by Langdon and coworkers [20-23]. This will facilitate the grain boundary sliding and is believed to cause cavity formation [49]. Figs. 4-3(h)-(j)

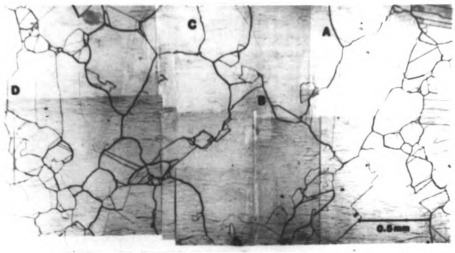

(a)

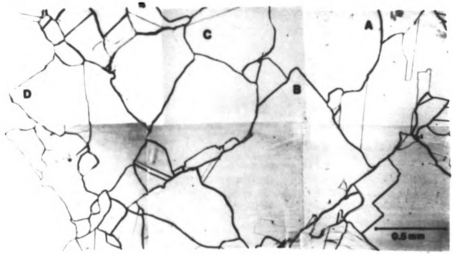

(b)

Fig. 4-3. The microstructures of a Ni in a plane parallel to the loading direction after cyclic deformation with 0.5% total strain amplitude at 600°C (a) Annealed at 900°C for 5 hours; (b) after 10 complete cycles at 600°C, slightly polished and etched again to reveal the new grain boundary positions;

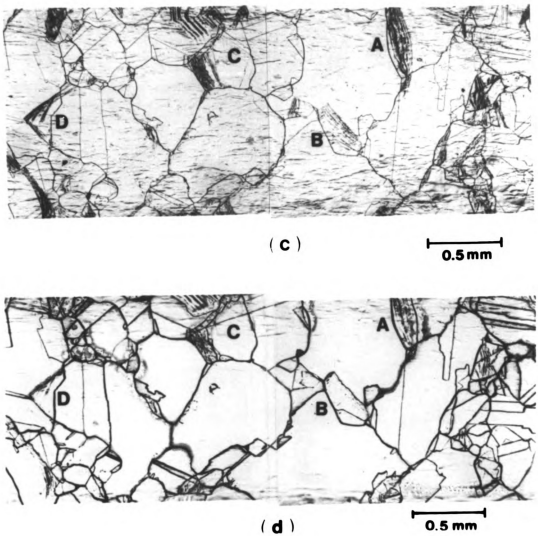

Fig. 4-3(c) after 10 complete cycles, positions A,B,C and D indicate inhomogeneous strain distribution on the surface; (d) etched to reveal the positions of new and original grain boundaries simultaneously;

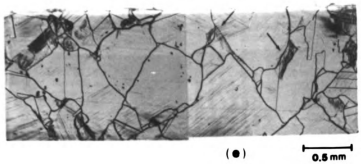

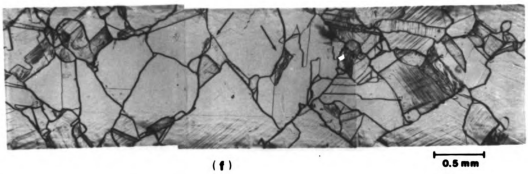

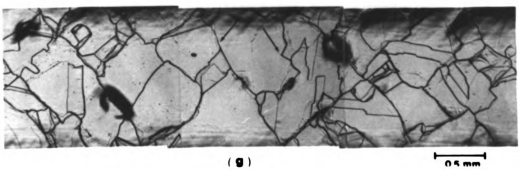

Fig. 4-3(e) **after 40 cycles; (f) the positions of new and original grain boundaries after etching again; (g) slightly polished and etched again, only new grain boundaries can be seen;**

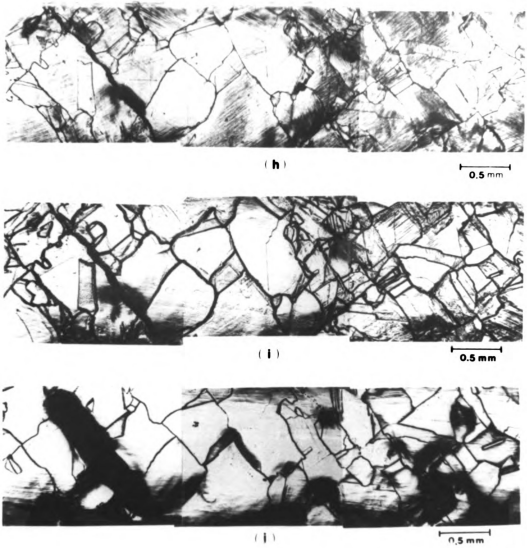

Fig. 4-3. (h) right after 160 cycles; (i) after etching; (j) after polishing and etching.

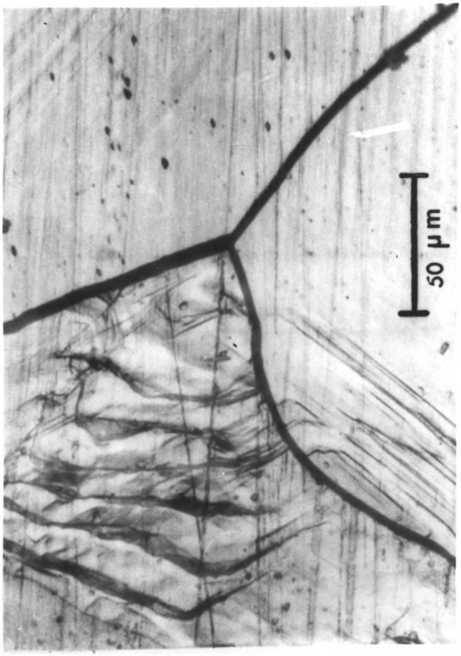

Fig. 4-4. Detailed structure of surface markings after 10 cycles.

are the micrographs after 160 cycles. Although compared to Figs. 4-3(e)-(g) the sample had deformed another 120 cycles, Fig. 4-3(j) doesn't show much difference compared to the microstructure in Fig. 4-3(g), except most grain boundaries now are aligned under 45° to the stress axis. Grain boundary sliding was observed even during the early stage of cyclic deformation. An example is shown in Fig. 4-5. The specimen was fatigued at 600°C with 0.5% strain amplitude. A scratch was introduced accidentally during specimen dismounting after 10 cycles of test (Fig. 4-5(a)). Under further deformation to 20 cycles, a small offset can be seen in Fig. 4-5(b) as indicated by an arrow. The offset distance increases as numbers of cyclic deformation increase, which corresponds to higher degree of grain boundary sliding (Fig. 4-5(c), 40 cycles). Comparing Fig. 4-5(c) with Fig. 4-5(a), some grain boundaries show much more migration, but some don't, also some grains reveal higher density of slip bands.

Grain boundary migration was also observed in Al. The micrographs in Fig. 4-6 were taken after 720 cycles deformation. Actually, the micrograph reveals the whole cross sectional area perpendicular to the loading direction. The extent of grain boundary migration can be seen by comparison of Figs. 3-8 and 4-6. The deformed state (Fig. 4-6) shows curved grain boundaries instead of perfectly straight ones, as in the microstructure of the undeformed specimen (Fig. 3-8).

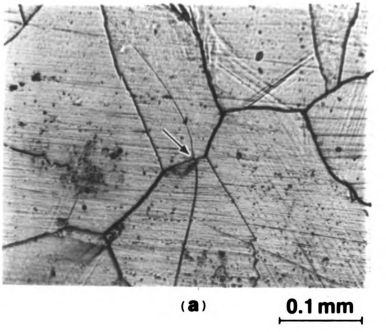

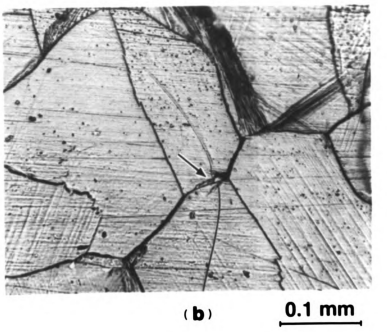

Fig. 4-5. The microstructure on the planar surface of a Ni after cyclic deformation with 0.5% total strain amplitude at 600°C for (a) 10; (b) 20 and (c) 40 complete cycles. The arrow indicates the offset of a scratch across the grain boundary due to grain boundary sliding.

(**b**) 0.1 mm

(**c**) 0.1 mm

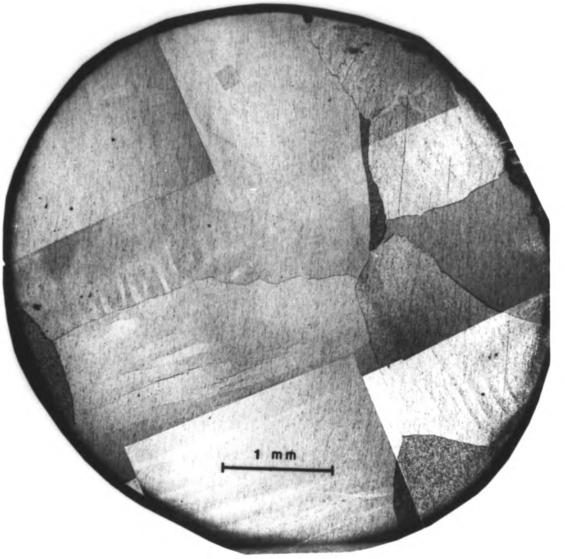

Fig. 4-6. The microstructure of an Al after 720 cycles with 0.5% total strain amplitude at 200°C.

4.3 Evidence Of DRX Under LCF

The occurrence of DRX in polycrystals is difficult to evidence, since the sample remains polycrystalline and the newly formed grains are rapidly deformed by concurrent deformation. It is particularly difficult in LCF because of the small driving forces and thus a small boundary migration rate. The occurrence of DRX, therefore, had to be indirectly confirmed by microscopic investigations. After deformation, the sample was cut perpendicular to the loading direction, and the microstucture was examined in detail under higher magnification. Special attention was paid to grain boundaries. They reveal serrations (Fig. 4-7(a)), sharp protrusions (Fig. 4-7(b)) and even new grains (Figs. 4-7(b)-(f)). These phenomena are characteristic for the nucleation of recrystallization at grain boundaries [24,36]. Figs. 4-7(b), (d)-(f) show the details near a twin. It occurs as if the twin in Fig. 4-7(d) and the grain at the twin boundary in Fig. 4-7(e) were created during deformation. This is important, since recrystallization twinning was found to be one of the major nucleation mechanisms of DRX in monotonic tests. In fact these observed phenomena are nucleation processes. This becomes clear from Fig. 4-8 which reveals that the microstructure contains areas with many small grains. While the migration processes observed in the beginning of deformation, are directed towards a coarsening of the microstructure, this micrograph, in contrast indicates a local refinement of the microstructure.

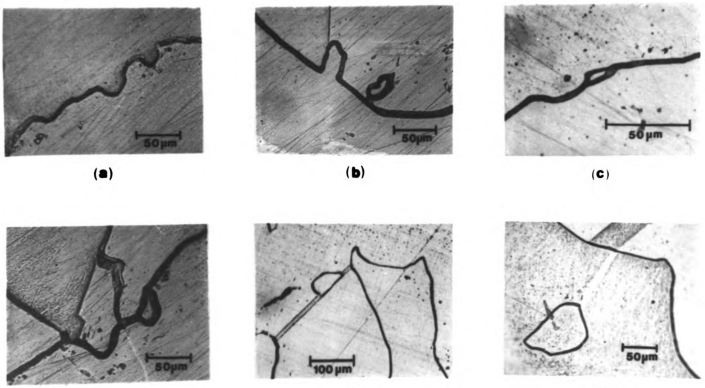

Fig. 4-7. In Ni (a) serrations of a grain boundary, nuber of cycles N = 200, total strain amplitude ϵ_t= 0.5% ; (b) a protrusion and a new grain at a grain boundary, N = 200, ϵ_t= 0.5%; a new grain formed (c) on the grain boundary, N = 510, ϵ_t= 0.5%; (d) near a twin, N = 200, ϵ_t= 0.5%; (e) at a twin boundary, N = 310, ϵ_t= 1.7%; (f) in the interior of a grain at the tip of a twin, N = 510, ϵ_t= 0.5%.

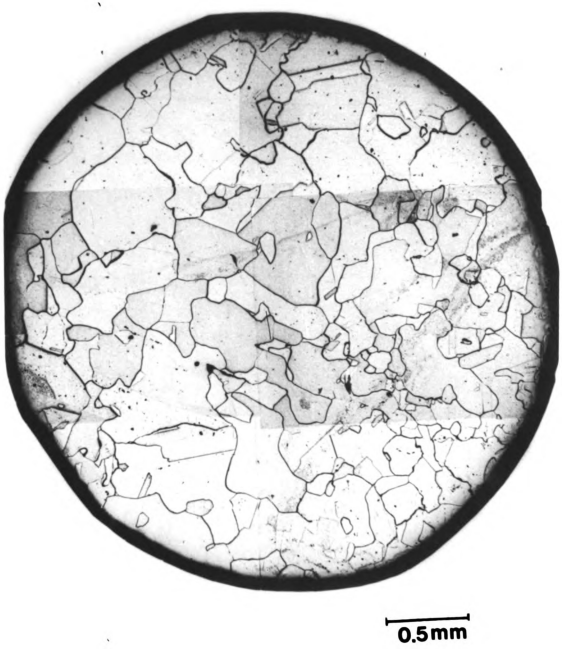

Fig. 4-8. The microstructure of a Ni after 510 cycles with 0.5% total amplitude. The whole cross sectional area perpendicular to the loading direction is revealed.

More evidence of DRX can be seen on the surface of fatigued specimen. Fig. 4-9 reveals the microstructure on the planar side surface of a specimen tested at 600°C with 0.5% strain amplitude for 80 cycles (Fig. 4-9(a)) and 120 cycles (Fig. 4-9(b)). Fig. 4-9(b) is the microstructure when slightly etching after test. Twins appear on the surface of the specimen as indicated by an arrow. In the same specimen, a new grain attached to the serrated grain boundary can be seen in Fig. 4-10(b) which is absent in Fig. 4-10(a).

A parallel study was conducted on Al. Due to the high stacking fault energy Al is not able to recrystallize dynamically. No small grains were detected in the fatigued structure (Fig. 4-6). Obviously without DRX the microstructure has a tendency to uniform coarsening. This further substantiates the conclusion that Ni polycrystals actually undergo DRX during LCF at high temperature.

4.4 Results of High Strain Amplitude Tests

Local grain refinement was observed during HTLCF with a small strain amplitude. By increasing the strain amplitude, the driving force for DRX may increase such that overall microstructural change which is similar to monotonic test may be possible.

One specimen was fatigued at 600°C with 5% strain amplitude for 55 cycles. The cyclic hardening curve is shown in Fig. 4-11. The stress becomes a maximum in the early cycles and then decreases. The

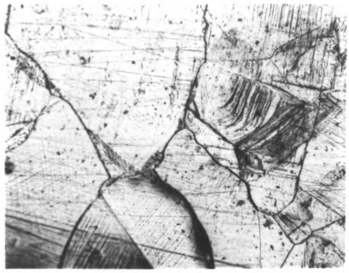

(a)

(b)

Fig. 4-9. The microstructure on the planar surface of a Ni after cyclic deformation with 0.5% total strain amplitude at 600°C. (a) after 80 cycles; (b) after 120 cycles and slightly etched. The arrow indicates the position where a twin was created.

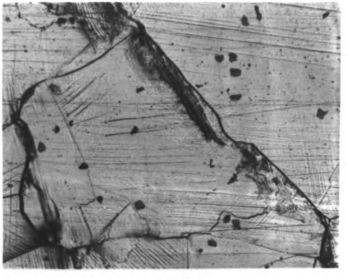

(a)

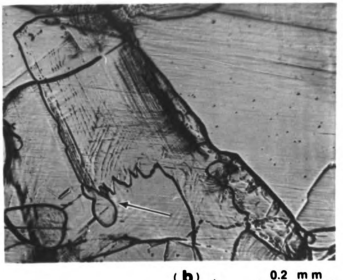

(b)

Fig. 4-10. The microstructure on the planar surface of a Ni after cyclic deformation with 0.5% total strain amplitude at 600°C. (a) after 80 cycles; (b) after 120 cycles and slightly etched. A new grain attached to the serrated grain boundary.

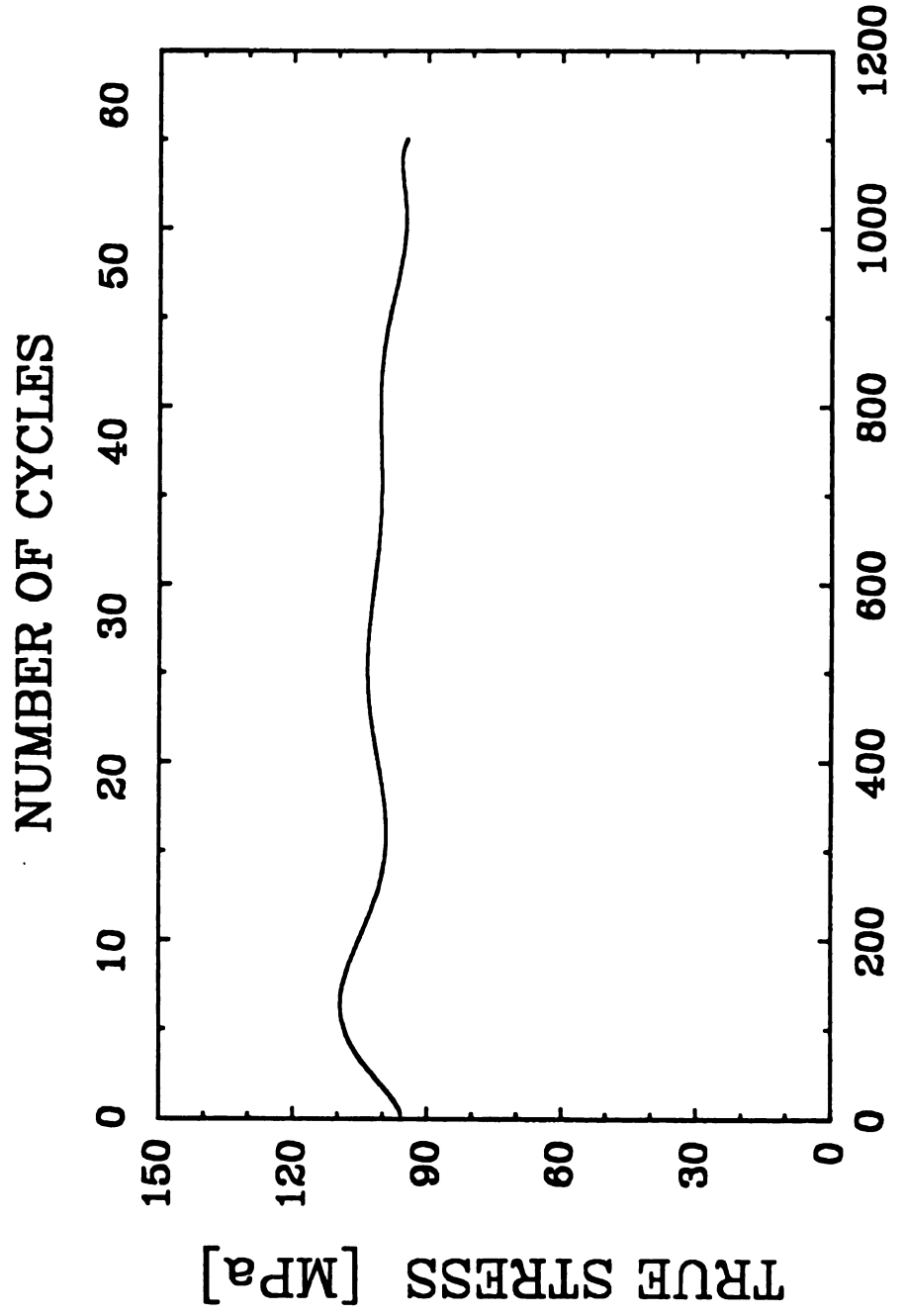

Fig. 4-11. Cyclic hardening curve of a Ni after 55 cycles with 5% total strain amplitude at 600°C.

microstructure after the test is shown in Fig. 4-12. This micrograph reveals the structure of the area which is parallel to the stress axis. The average grain size of the specimen gauge section is much smaller than that of the specimen shoulder area where at most elastic deformation occurred. The microstructure shown in Fig. 4-13(a) further indicates the overall microstructural change. The structure after annealing (Fig. 3-5) is totally replaced by a finer grain structure. This substantiates the occurrence of DRX during LCF with high strain amplitude. A higher magnification micrograph shows the recrystallization twins present in the new structure (4-13(b)). An hour-glass shape specimen with 6.35 mm radius of curvature and 5 mm smallest diameter was fatigued with 1% total axial strain amplitude at 600°C for 1013 cycles. The hardening curve also shows the stress to increase up to 100 cycles and then to decrease continuously (Fig. 4-14). The microstructure parallel to the stress axis is shown in Fig. 4-15. It is clearly evident that a finer grain structure in the center region had replaced the initial coarse grain structure shown in the area of specimen shoulder. Except for the fine grains, most grain boundaries had moved to a position aligned under 45° with respect to the stress axis. The grain morphology of the cross section near the smallest diameter of the specimen is shown in Fig. 4-16. It is quite different from the annealing structure. In this test, the deformation was confined to the very narrow region where the cross sectional area was small. One hour-glass shape specimen with 12.7 mm radius of curvature and 5.08 mm smallest diameter was fatigued at 600°C for 3645 cycles with 0.3% strain amplitude. The hardening curve is shown in Fig 4-14. The microstructure along the gauge length is shown in Fig. 4-17. The structure has

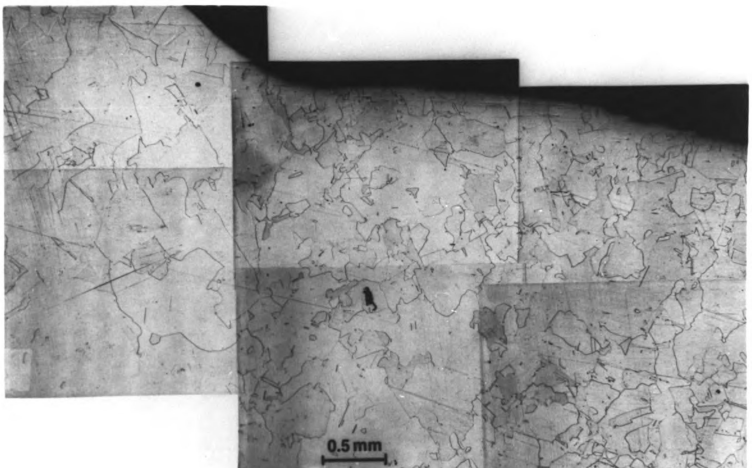

Fig. 4-12. **The microstructure of a Ni in a plane parallel to the loading direction after 55 cycles with 5% total strain amplitude at 600°C.**

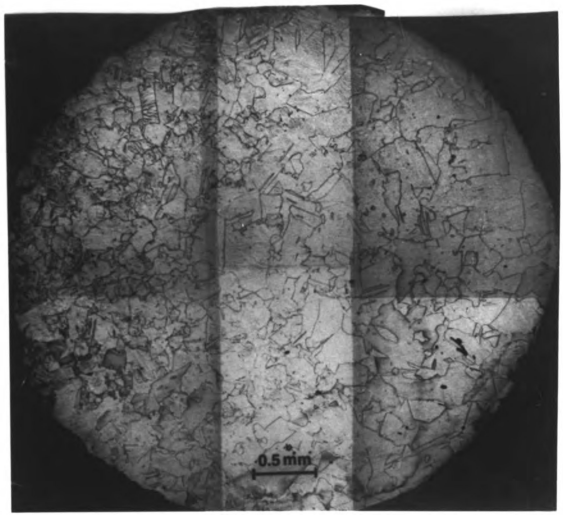

(a)

Fig. 4-13. (a) The microstructure of a Ni after 55 cycles with 5% total amplitude. The whole cross sectional area perpendicular to the loading direction is revealed; (b) higher magnification of the structure in (a)

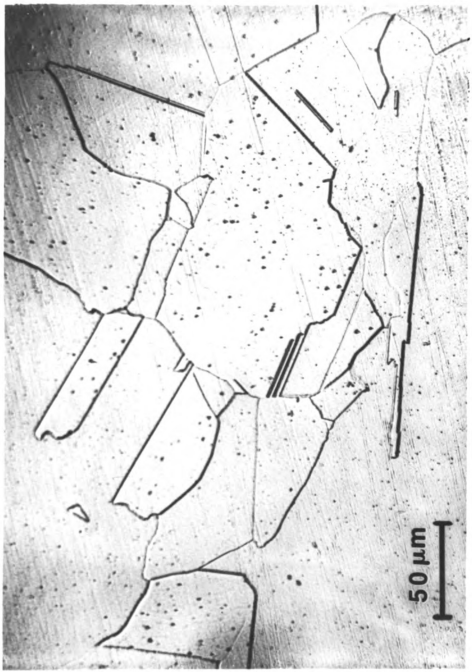

(b)

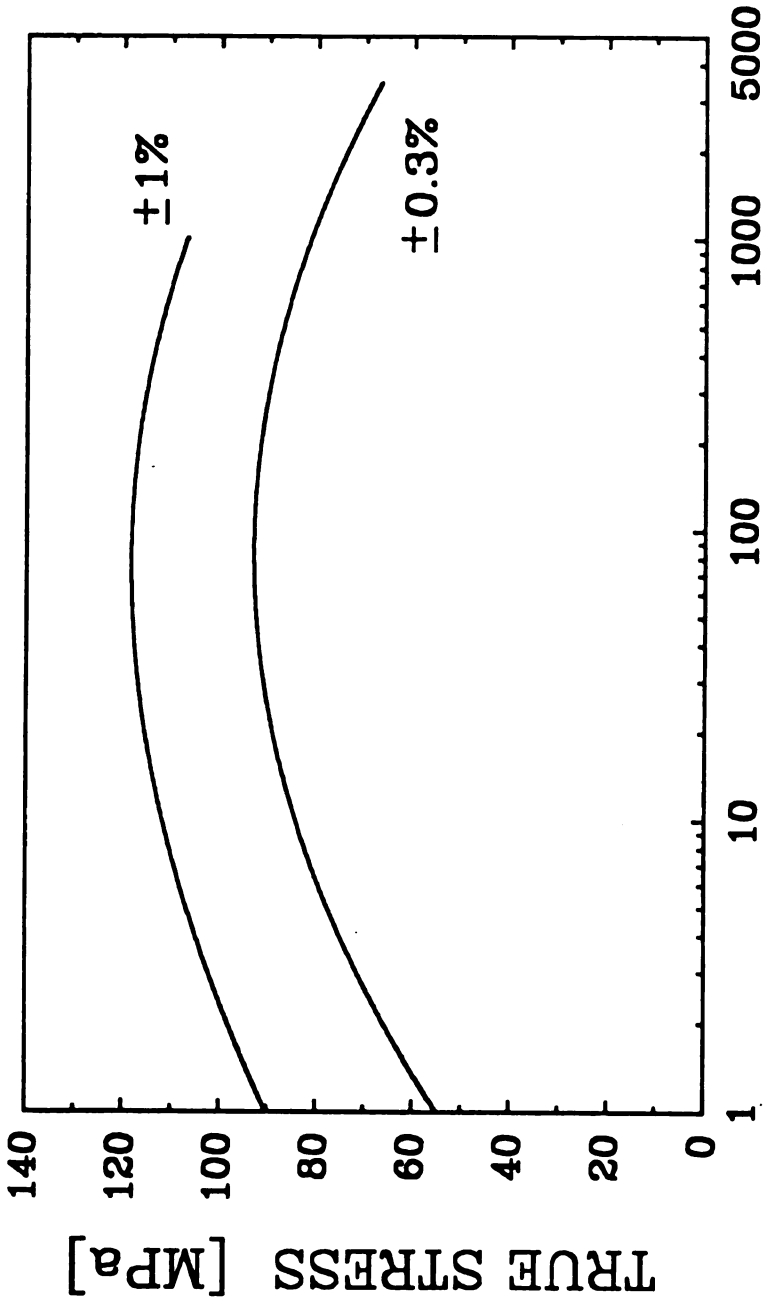

Fig. 4-14. Cyclic hardening curves of two Ni hour-glass shape specimens with 0.3% and 1% total strain amplitudes at 600°C.

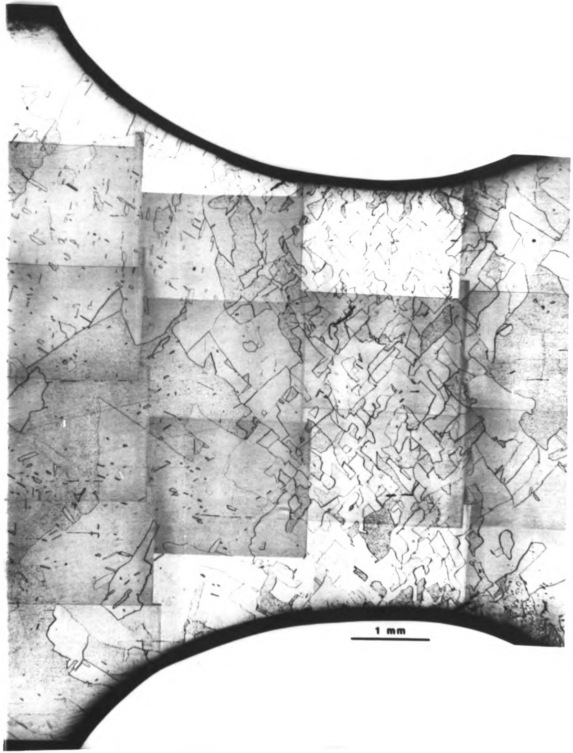

Fig. 4-15. The microstructure in a plane parallel to the loading direction of an hour-glass shape Ni fatigued at 600°C with 1% total axial strain amplitude.

Fig. 4-16. The microstructure in a plane perpendicular to the loading direction and containing the smallest diameter region of an hour-glass shape Ni fatigued at 600°C with 1% total axial strain amplitude.

changed due to DRX, but not drastically as shown in Fig. 4-15. The deformation region is wider than in the previous test because of the smaller gradient of the cross sectional area along the stress axis. Grain boundaries migrate to the position aligned under 45° with respect to the stress axis. A crack has initiated and propagated along grain boundaries. The strain amplitude in the smallest diameter region is estimated approximately 3 to 5 times of the strain amplitude imposed to the whole gauge length.

The irregular and large initial grain structure was utilized to investigate the effect of a high strain amplitude. From the microstructure observed after test, DRX and subsequent the grain boundary migration can be distinguished without ambiguity.

4.5 Results on Cu Single Crystals

Cu single crystals were tested at 400°C (0.5 T_m) and room temperature at a strain rate of $1.6 \times 10^{-4} s^{-1}$ and total strain amplitudes of 1% corresponding to a cyclic frequency of 6.2×10^{-3} Hz.

The cyclic hardening curve of a <169> oriented Cu single crystal cycled at 400°C is shown in Fig. 4-18. After initial hardening the flow stress reaches a maximum and declines thereafter slightly but continuously. Despite very careful inspection of the specimen, however, no recrystallized grains could be detected, neither on the surface nor in the interior of the single crystal. The dislocations are arranged in a

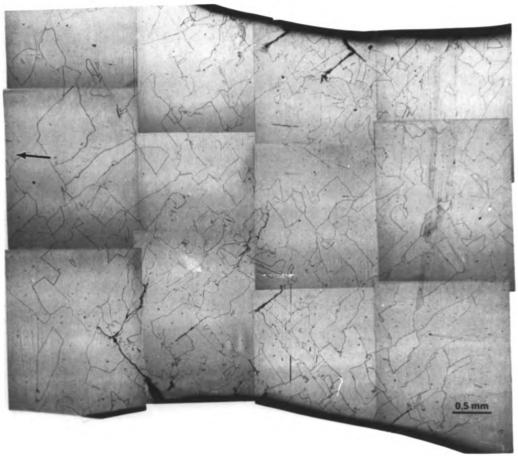

Fig. 4-17. The microstructure in a plane parallel to the loading direction of an hour-glass shape Ni fatigued at 600°C with 0.3% total axial strain amplitude.

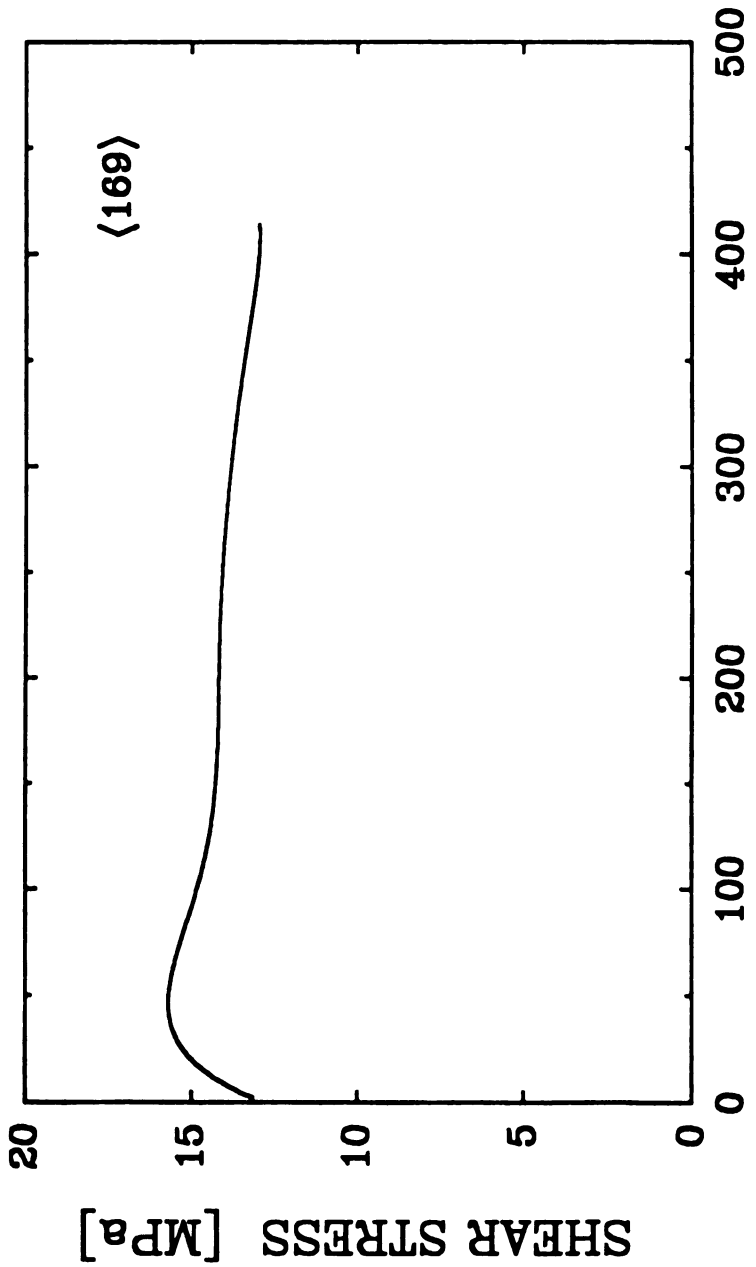

Fig. 4-18. Cyclic hardening curve of a Cu single crystal tested at 400°C with 1% total strain amplitude.

well defined cell structure (Fig. 4-19), and the substructure does not reveal indications of viable recrystallization nuclei. Hence, the flow stress behavior has to be attributed entirely to the dislocation structure development and cannot be associated with DRX or grain boundary motion phenomena. Consequently, the occurrence of DRX during HTLCF in polycrystals has to be interpreted as a grain boundary effect. Also, the results confirm that cyclic softening is not necessarily indicative for DRX. This was shown before for Al polycrystals, where cyclic softening was associated with grain growth.

It was further studied whether fatigued dislocation structures in single crystals are at all prone to recrystallization. A single crystal was deformed at room temperature for 110 cycles with 1% strain amplitude. After initial hardening the cyclic hardening curve reaches a plateau stress (Fig. 4-20) as has been established in many previous investigations [57,58]. Slip lines could clearly be seen on the surface of the fatigued specimen (Fig. 4-21). Upon isochronal annealing for 30 min between 200°C and 850°C in a vacuum furnace, the microhardness decreases strongly in the temperature range between 500°C and 700°C (Fig. 4-22). Annealing at temperatures above 800°C essentially restores the single crystals yield stress. Different slices of specimen cut perpendicular to the stress axis from the gauge section were used for different annealing conditions. After each annealing the specimen was examined using optical microscopy. While the observed kinetics are very akin to recrystallization behavior, the absence of recrystallized grains after annealing at different temperatures indicate that no recrystallization occurred. Some specimens were then further prepared for TEM.

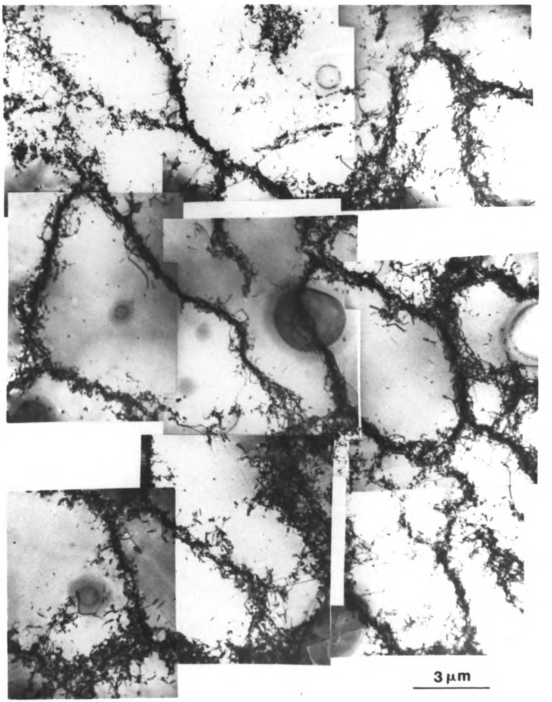

Fig. 4-19. Dislocation structure of a Cu single crystal tested at 400°C with 1% total strain amplitude for 420 cycles.

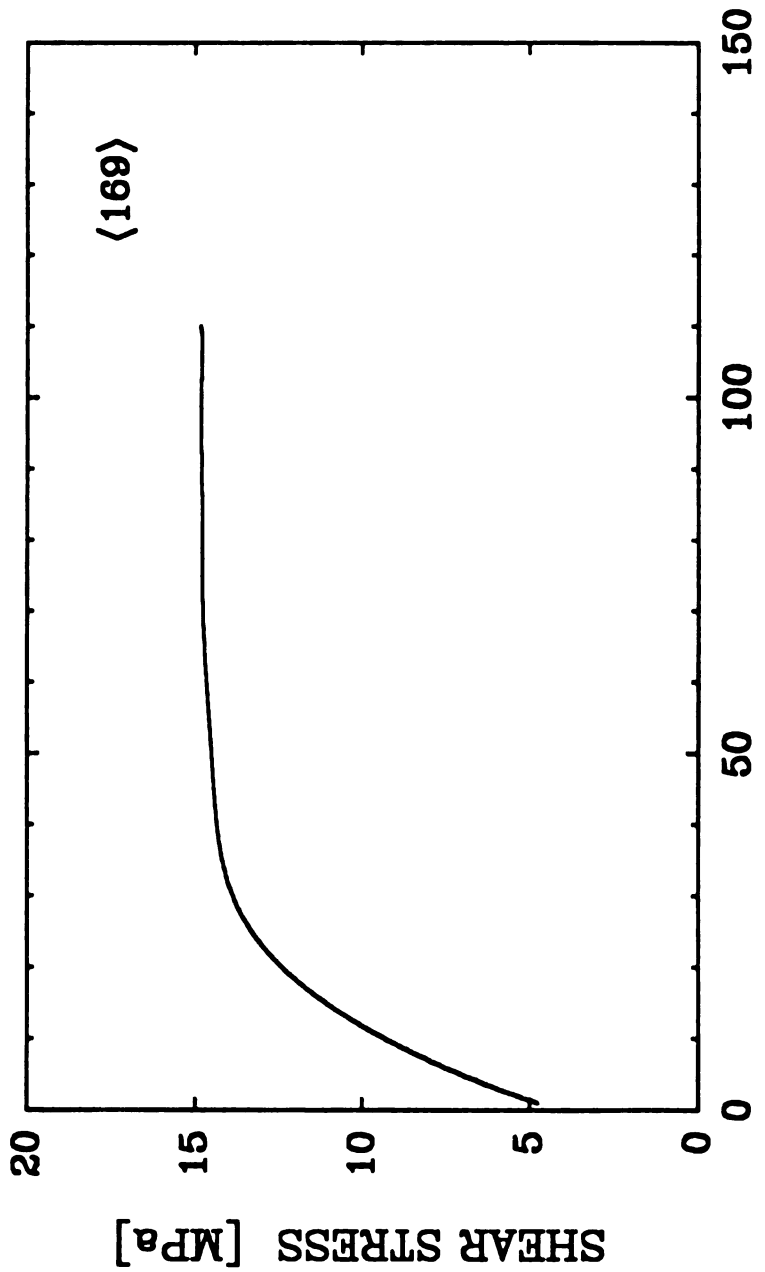

Fig. 4-20. Cyclic hardening curve of a Cu single crystal tested at room temperature with 1% total strain amplitude.

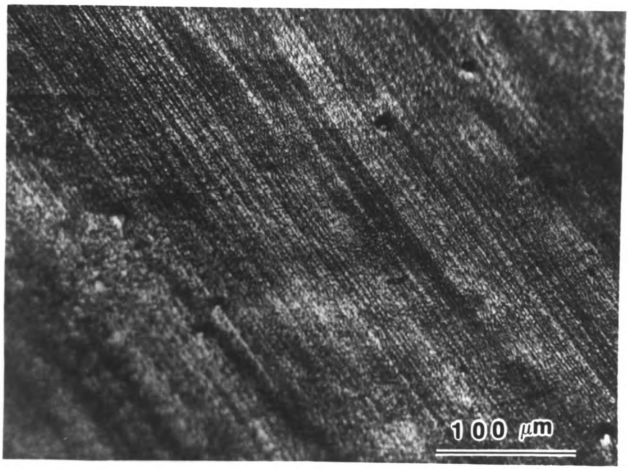

Fig. 4-21. Surface markings on a Cu single crystal after 110 cycles with 1% total strain amplitude at room temperature.

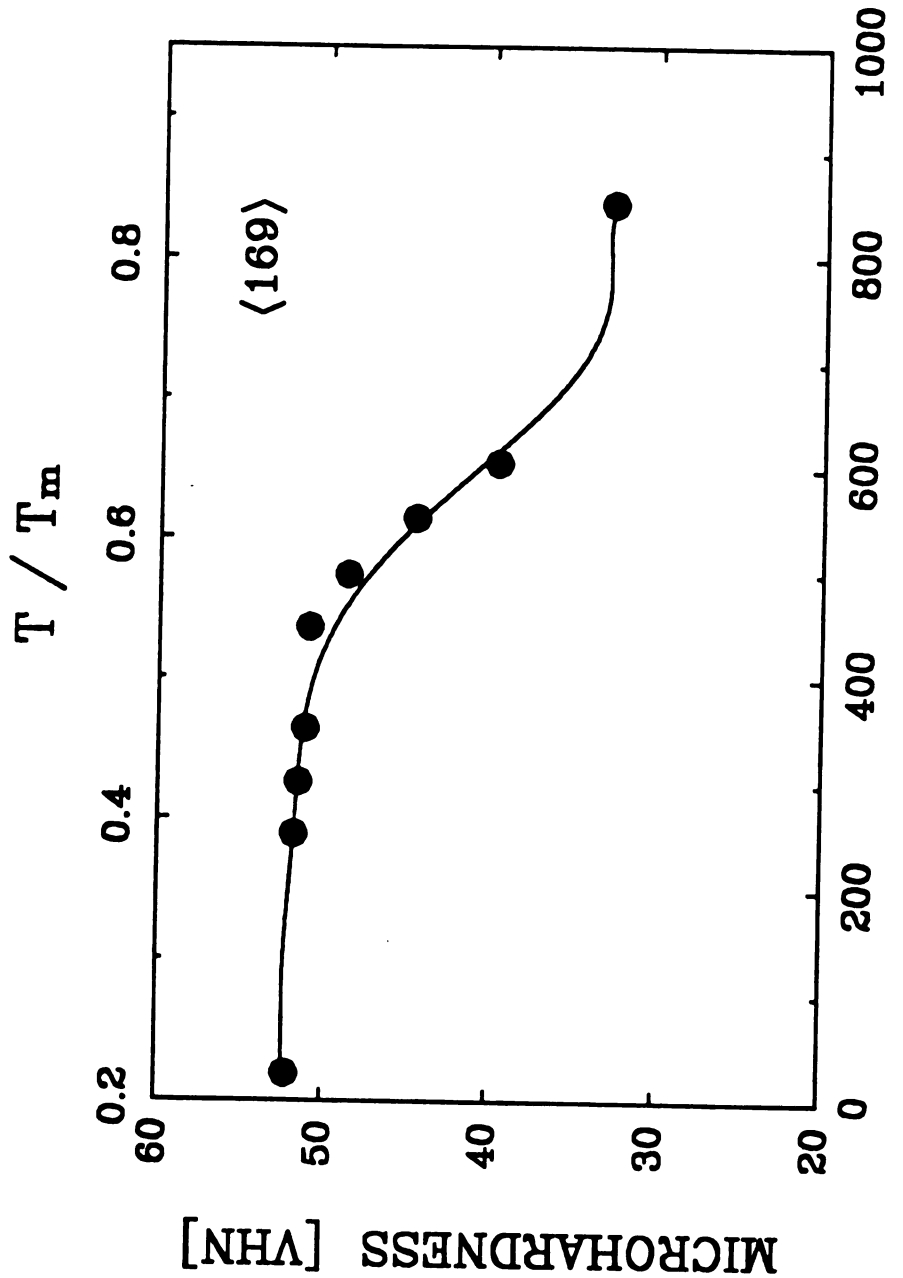

Fig. 4-22. Microhardness during isochronal annealing of a Cu single crystal fatigued at room temperature with 1% total strain amplitude.

A typical dislocation structure which consists of dense multipolar arrangement of primary edge dislocations, referred to as veins, which are separated by dislocation poor regions, can be seen in Fig. 4-23(a). Upon subsequent annealing at 250°C for 30 min, the density of dislocation between veins decreases due to recovery (Fig. 4-23(b)). Further annealing at 552°C which is in the region of decreasing microhardness, reduces the dislocation density inside the veins (Fig. 4-23(c)). The final state of recovery which was annealed at 852°C leads to the formation of almost perfect dislocation networks (Fig. 4-23(d)), with obviously negligible flow stress contribution.

Thus, even deformation at room temperature to a stress level comparable to that at 400°C fails to provide viable recrystallization nuclei upon annealing.

4.6 Dislocation Structures

Transmission electron microscopy was applied to examine the dislocation arrangement and its development during LCF. Fig. 4-24(a) shows the dislocation structure of Ni after 310 cycles with 1.7% total strain amplitude (σ_{max}= 54 MPa). The micrograph reveals a well developed cell structure inside a grain. Compared to a monotonic test prior to the onset of DRX (σ_{max}= 78 MPa) at the same temperature and strain rate (Fig. 4-24(b)) the structure of cycled specimens appears more strongly recovered.

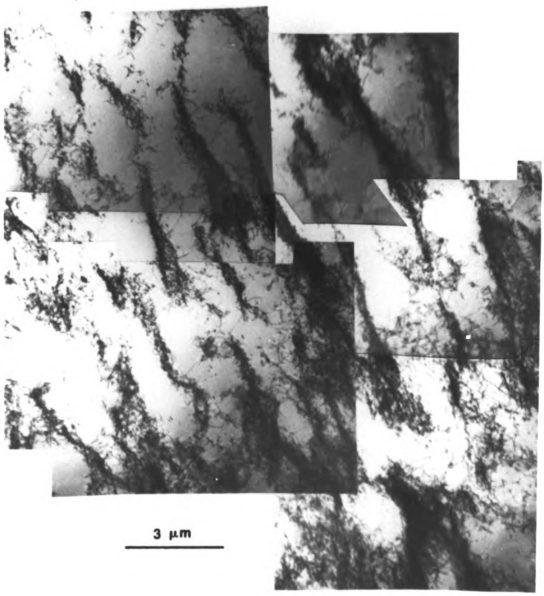

(a)

Fig. 4-23. Dislocation structure of a Cu single crystal fatigued at room temperature. (a) as deformed; deformed and then annealed at (b) 250°C; (c) 552°C and (d) 850°C for 30 min.

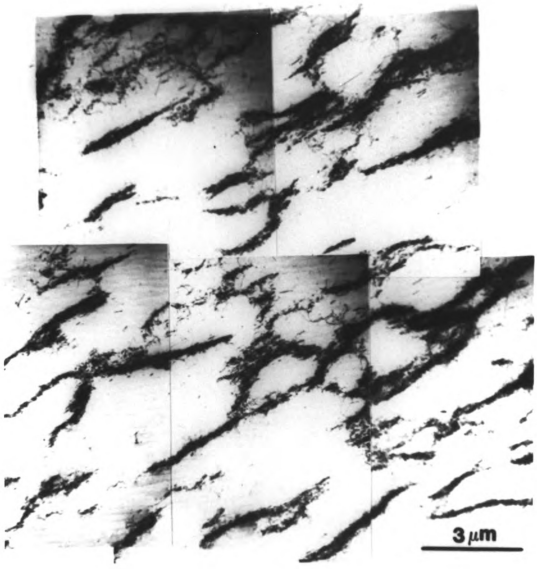

(b)

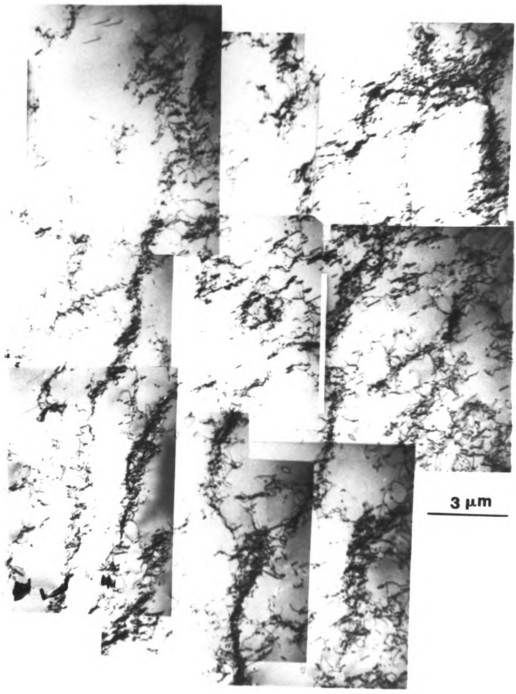

(c)

(d)

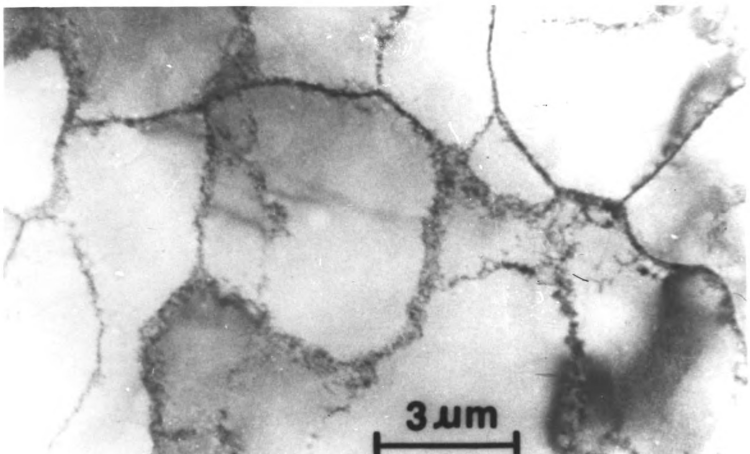

(a)

Fig. 4-24. The dislocation structure inside a Ni grain after (a) 310 cycles with 1.7% total strain amplitude; (b) monotonic

(b)

Because of the observed extensive grain boundary migration, special efforts were made to observe the dislocation structure around grain boundaries. Fig. 4-25 shows the dislocation arrangement in a Ni polycrystal after 310 cycles with 1.7% total strain amplitude. The grain boundary seems to migrate down to the right corner. In front of the grain boundary, dislocations form a distinct cell structure, but are not as heavily tangled as in large strain monotonic tests (Fig. 4-24(b)), rather they are loosely arranged in cell walls. Immediately behind the serrated boundary segment, the dislocation structure is poorly recovered, the cell interior is not so neat, and the cell walls are more diffuse. Such an arrangement is more typical for the beginning of cell formation and the arrangement indicates that it represents the new formation of a cell structure after the boundary swept the volume and eliminated the original structure. In contrast, a well recovered cell structure is observed in front of or a little farther behind the serrated part of the boundary.

The results from single crystals indicate that grain boundaries play an important role in DRX during HTLCF. Extensive grain boundary migration also occurred during cyclic deformation. It is interesting to see how dislocation structures develop during the test, especially around the grain boundaries. Fig. 4-26 shows the cyclic hardening curve of samples deformed at 600°C with a total strain amplitude $\Delta\epsilon = 0.5$ % and cycle frequency 1.3×10^{-2} Hz. The corresponding microstructures are given in Figs. 4-27 to 4-30. After 10 cycles the development of a cell structure is evident (Fig. 4-27). The grain boundary in Fig. 4-27(b) reveals heavy activity in terms of steps, curvature and considerable dislocation

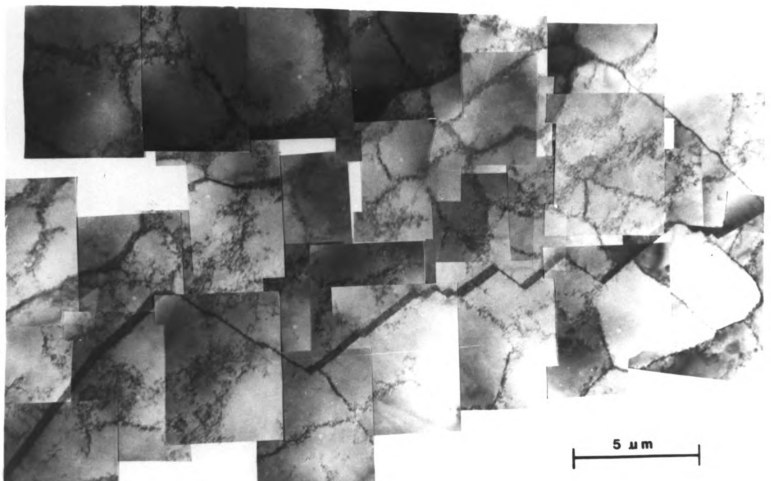

Fig. 4-25. The dislocation structure in a Ni of a larger area around
[illegible] boundary after 310 cycles with 1.7% total strain amplitude.

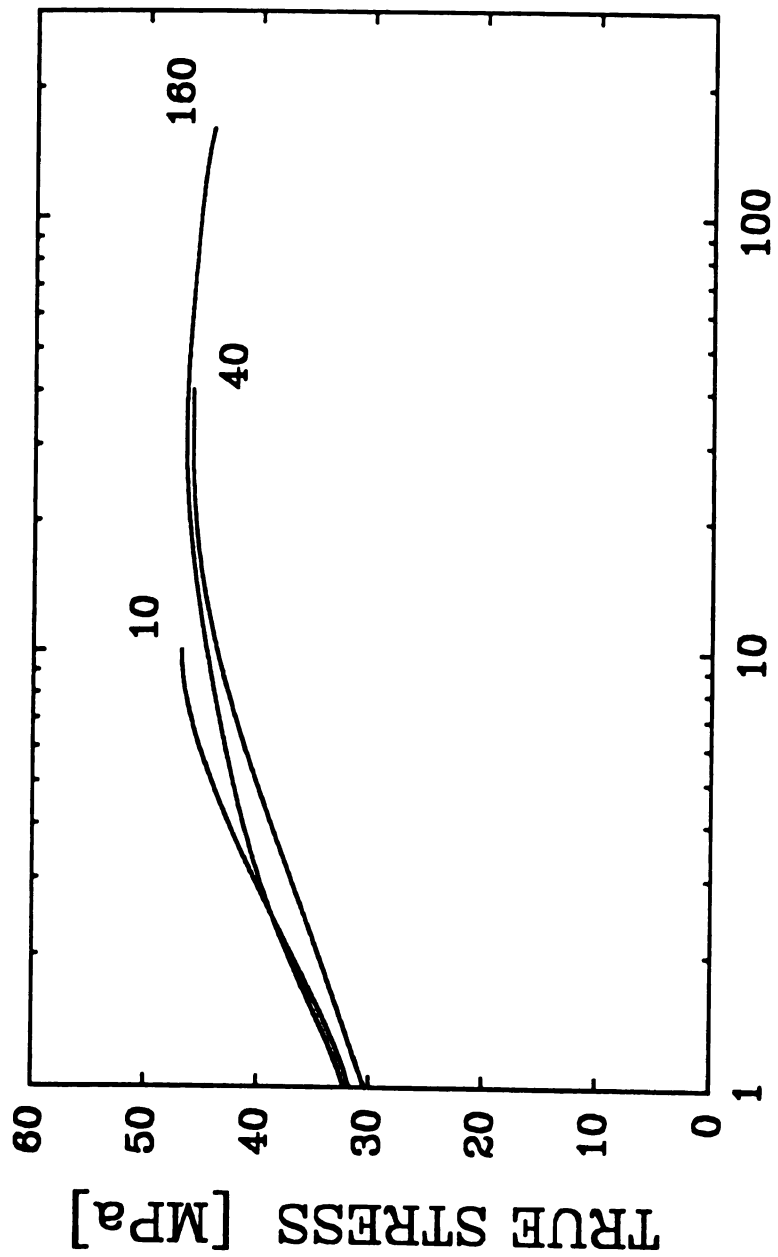

Fig. 4-26. Cyclic hardening curve of a Ni tested at 600°C with 0.5% total strain amplitude.

content in the boundary. In contrast to the cell interior (Fig. 4-27(a)), the cell structure in the vicinity of the boundary is only poorly developed with incomplete cell wall sections and frequent debris in the cell interior. After 40 cycles, the cell structure in the grain interior is now very well developed and much more distinct than after 10 cycles, although far from being uniform (Fig. 4-28). There are areas with narrow, condensed cell walls and essentially dislocation free cell volumes (Fig. 4-28(a)), but other areas comprise much less orderly arranged dislocations (Fig. 4-28(b)).

The dislocation structure after 160 cycles (Fig. 4-29) is akin to the structure after 40 cycles. Most dislocations are arranged in constricted cell walls, enclosing regions completely denuded of dislocations, but locally patches of less orderly dislocation patterns are apparent. The area around a grain boundary is shown in Fig. 4-30. The boundary curvature indicates recent grain boundary motion. Far away from the grain boundary the cell structure is very pronounced and well recovered. In close proximity to the boundary, however, the dislocation structure is quite different, namely very little organized and only incipient of cell formation.

The dislocation density and arrangement gradients produced by grain boundary migration during cyclic deformation may actually be the cause for DRX phenomena during HTLCF. The microstructure in Fig. 4-31 is due to a Ni polycrystal deformed at a large strain amplitude, namely $\Delta\epsilon$ = 1.7%, to 300 cycles. The cyclic hardening curve (Fig. 4-1 #3) indicates the occurrence of DRX and grain boundary migration as apparent from the

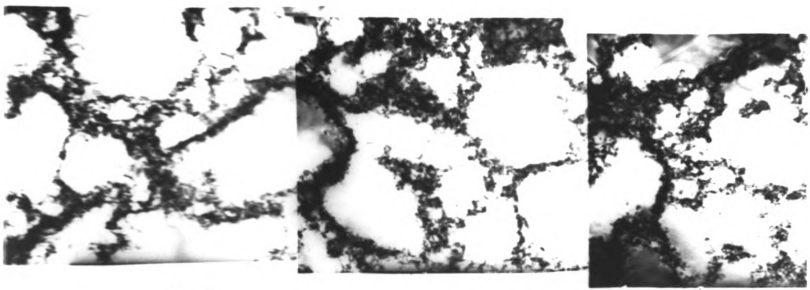

Fig. 4-27. Microstructure of a Ni after testing at 600°C with 0.5% total strain amplitude for 10 cycles. (a) grain interior, (b) around a grain boundary.

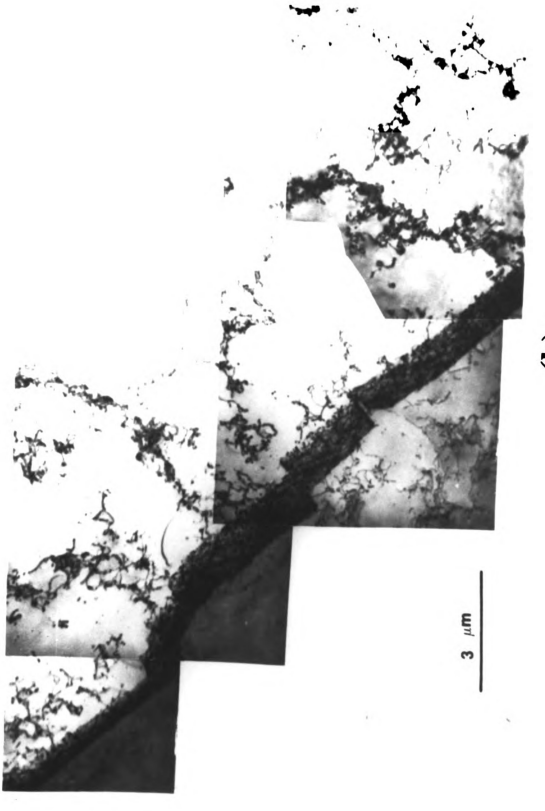
3 μm
(b)

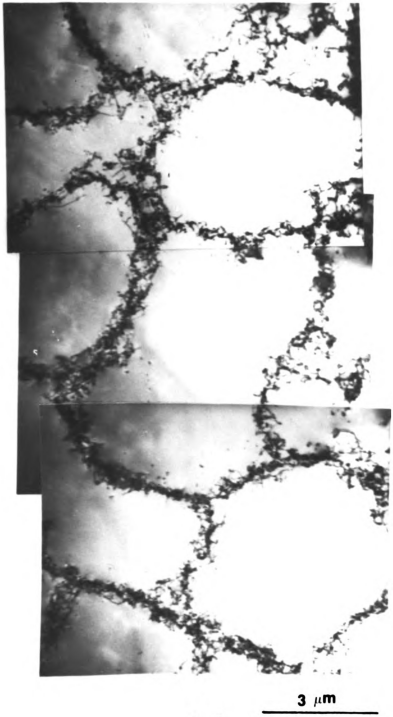

(a)

Fig. 4-28. Microstructure of a Ni after testing at 600°C with 0.5% total strain amplitude for 40 cycles. (a) and (b) different areas in the same specimen. Note difference in structure.

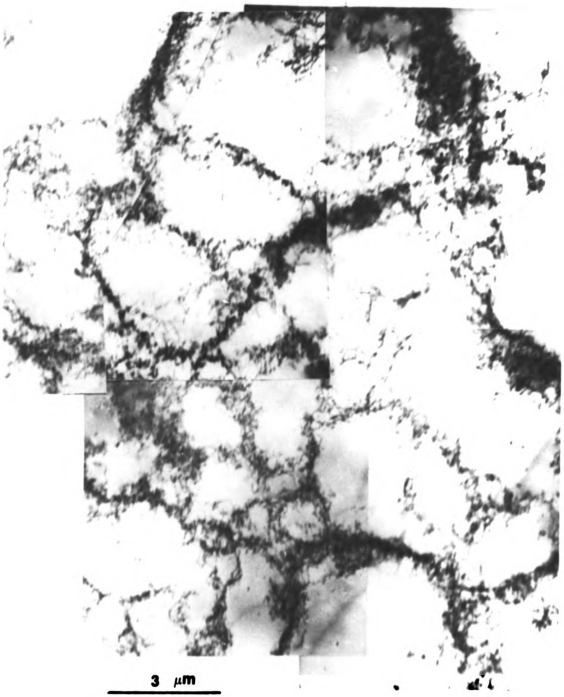

(b)

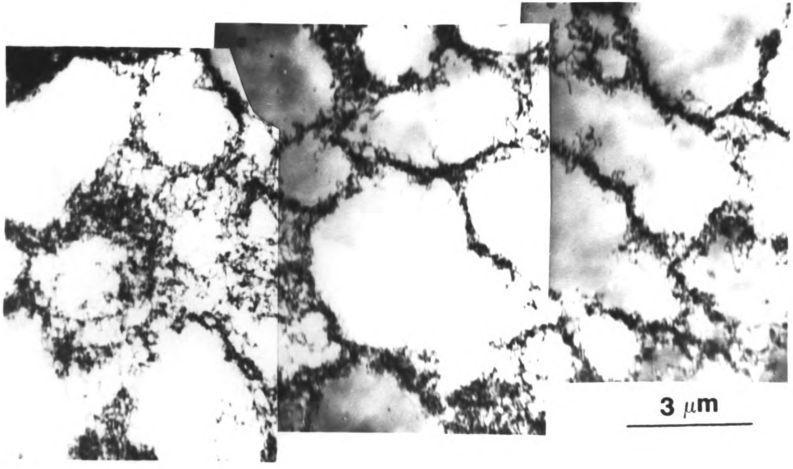

Fig. 4-29. Dislocation structure in the grain interior of Ni after testing at 600°C with 0.5% total strain amplitude for 160 cycles.

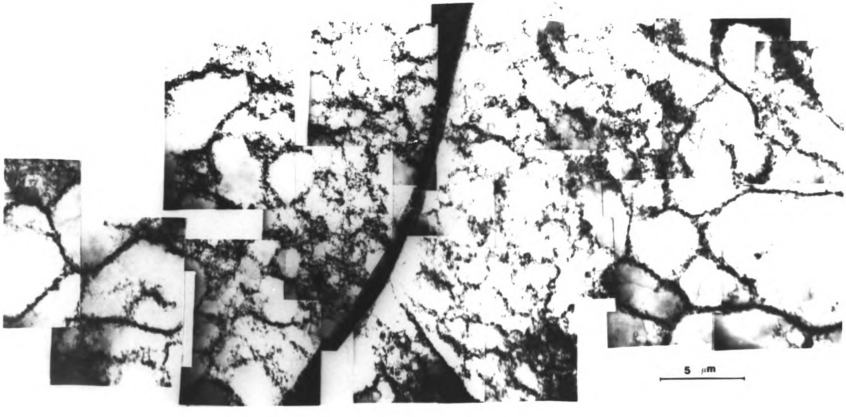

Fig. 4-30. Dislocation structure around a grain boundary of a Ni after testing at 600°C with 0.5% total strain amplitude for 160 cycles.

distinct maximum of the flow curve. The vicinity of the vertical boundary in Fig. 4-31 comprises areas with more recovered cell arrangements (left to the boundary, especially at the bottom) and more disorderly arranged dislocations (to right of boundary, especially at the top). In the latter area a twin is created at a triple junction - most likely during the migration of the vertical grain boundary to the left - and the steps in the twin boundary indicate migration activity. Also interesting is the area next to the junction of the twin boundary with the horizontal boundary. A small grain seems to have developed there right adjacent to a heavily tangled dislocation arrangement. The resemblance of this arrangement with nucleation phenomena observed in dynamically recrystallizing Ni during HTLCF is obvious (Fig. 4-7(d)), and supports the hypothesis that DRX phenomena are due to the structure gradients in the wake of moving grain boundaries. This argument would also comply with the observation that DRX does not occur during HTLCF of single crystals.

Of particular interest with regard to the stability of dislocation structures is their accommodation of strain path changes, especially if such changes lead to a different steady state dislocation arrangement. Fig. 4-32 gives an example that dislocation rearrangements due to changes of strain path can occur without disruption of the previously established structure. After 1218 cycles at 600°C and $\Delta\epsilon = 0.5$ % deformation was continued only in tension to $\epsilon = 8$% (actually incidentally due to malfunction of the machine control). The maximum of the tensile flow curve indicates the occurrence of large scale DRX at 6% tensile strain (Fig. 4-32(a)). The dislocation structure after this additional

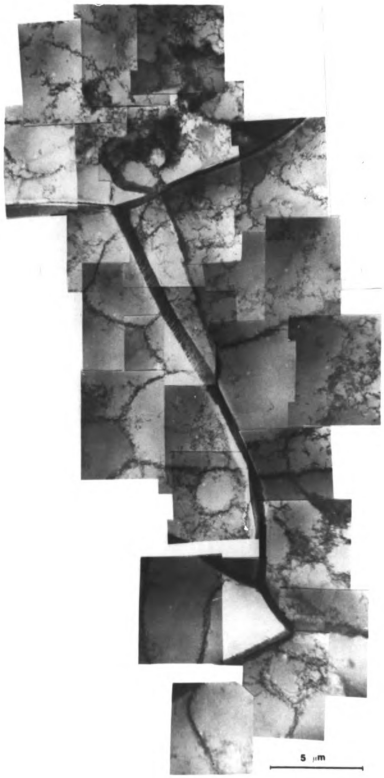

Fig. 4-31. Dislocation structure around a grain boundary of a Ni tested at 600°C with 1.7% total strain amplitude.

tensile strain (in the unrecrystallized volume, of course) reveals the superposition of two cell structures. The well recovered cell structure was produced during cyclic deformation and is still retained, while a new cell structure, still much less recovered, is generated within the old structure. The new cell structure tends toward a smaller cell size than the fatigued structure, because of the higher flow stress [3,14]. No disruptions or discontinuities of the previous structure are apparent, rather both structures seem to be able to coexist, and gradually the former cell walls become incorporated in a new homogeneous arrangement. Hence, Fig. 4-32(b) reveals actually two different stages of dislocation cell structure development and indicates that the specimen actually retains a 'temporal memory' of its strain history in terms of its dislocation arrangement, until a new structure is fully developed.

4.7 Effect of DRX on Mechanical Properties

In ductile materials, crack propagation is accompanied by plastic deformation in the wake of the crack tip. Prenotched specimens were tested at room temperature first to study the crack tip plastic deformation zone. Table 4-2 lists the test conditions for the samples referred in this section. The microstructure of a sample which was fatigued for 440 cycles with 0.5% total strain amplitude is shown in Fig. 4-33. The micrograph shows the microstructure of the deformed state with a crack extending through about half of the gauge diameter. The micrograph reveals the structure in the center of the specimen parallel to the stress axis indicated by an arrow. The crack propagates transgranularly

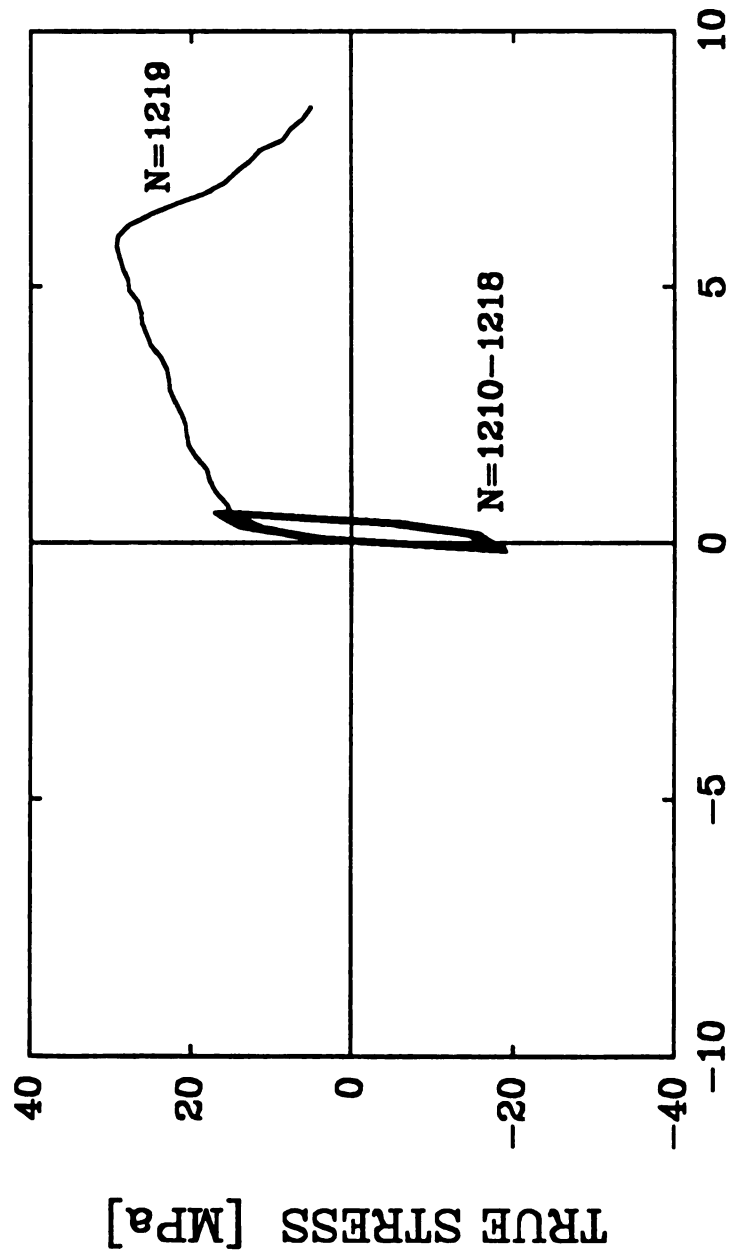

Fig. 4-32. (a) True stress vs. true strain curve during cycles 1210-1218 and (b) corresponding dislocation structure of Ni tested at 600°C with 0.5% total strain amplitude. The test was terminated during the extended tensile cycle number 1219.

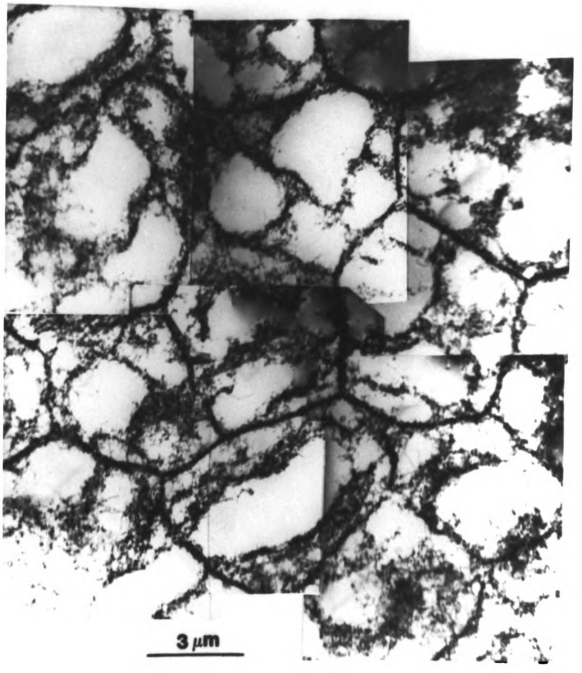

(b)

Table 4-2 Summary of the test conditions

Test No.	Test conditions
CRK00K	$\dot{\epsilon}=2\times10^{-4}s^{-1}$, T=25°C, $\Delta\epsilon=\pm0.5\%$, N=440 single edge notch specimen.
CRK00F	$\dot{\epsilon}=2\times10^{-4}s^{-1}$, T=25°C, $\Delta\epsilon=\pm0.8\%$, N=380 single edge notch specimen.
CRK00A	$\dot{\epsilon}=2\times10^{-4}s^{-1}$, T=600°C, $\Delta\epsilon=\pm0.5\%$, N=600 single edge notch specimen.
CRK00E	$\dot{\epsilon}=2\times10^{-4}s^{-1}$, T=600°C, $\Delta\epsilon=\pm0.5\%$, N=880 single edge notch specimen.
CRKHF01	$\dot{\epsilon}=2\times10^{-3}s^{-1}$, T=600°C, $\Delta\epsilon=\pm0.5\%$, N=744 single edge notch specimen.
CRK6001	$\dot{\epsilon}=5\times10^{-4}s^{-1}$, T=600°C, $\Delta\epsilon=\pm0.5\%$, occasionally 1%, -5% for several cycles, single edge notch specimen.
CRK6011	$\dot{\epsilon}=5\times10^{-4}s^{-1}$, T=600°C, $\Delta\epsilon=\pm0.75\%$, for 710 cycles, occasionally $\Delta\epsilon=\pm5\%$ for several cycles, single edge notch specimen.
CRK6021	$\dot{\epsilon}=5\times10^{-4}s^{-1}$, T=600°C, $\Delta\epsilon=\pm0.5\%$ for 425 cycles, $\Delta\epsilon=\pm1\%$ for 619 cycles, circumferential notch specimen.
CRK6031	$\dot{\epsilon}=5\times10^{-4}s^{-1}$, T=600°C, $\Delta\epsilon=\pm1\%$ for 605 cycles, circumferential notch specimen.
CRK6041	$\dot{\epsilon}=5\times10^{-4}s^{-1}$, T=600°C, $\Delta\epsilon=1\%$ for 280 cycles, hour glass shape specimen with an edge notch.
CRK6051	$\dot{\epsilon}=5\times10^{-4}s^{-1}$, T=600°C, $\Delta\epsilon=\pm0.5\%$ for 4300 cycles, +5%, -1% for 31 cycles, $\Delta\epsilon=\pm0.5\%$ for 284 cycles, +5%, -1% for 13 cycles, $\Delta\epsilon=\pm0.5\%$ for 93 cycles, circumferential notch specimen.
CRK6071	$\dot{\epsilon}=5\times10^{-4}s^{-1}$, T=600°C, +5%, -1% for 20 cycles then $\Delta\epsilon=\pm0.5\%$ for 200 cycles, repeat this waveform until fracture at 1114 cycles, circumferential notch specimen.
CRK6081	$\dot{\epsilon}=5\times10^{-4}s^{-1}$, T=600°C, +0.5%, -5% for 5 cycles then $\Delta\epsilon=\pm0.5\%$ for 500 cycles, repeat this waveform until fracture at 5512 cycles, double edge notch specimen.
CRK6091	$\dot{\epsilon}=5\times10^{-4}s^{-1}$, T=600°C, $\Delta\epsilon=\pm0.5\%$, fracture at 10943 cycles, double edge notch specimen.

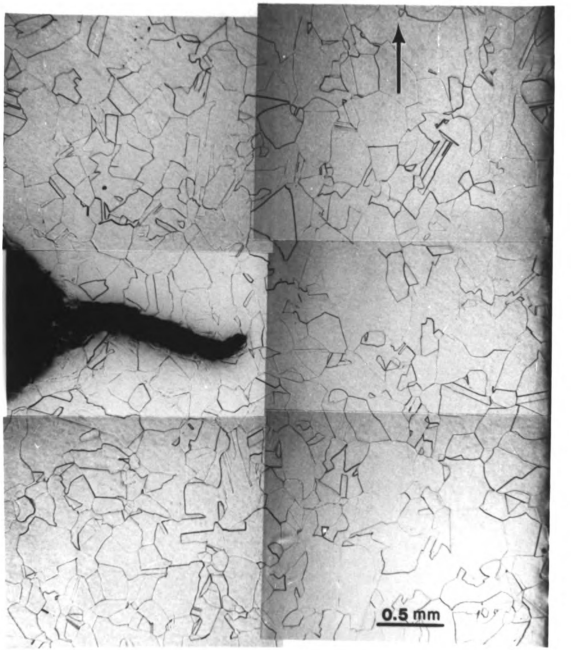

Fig. 4-33. The microstructure of a prenotched Ni fatigued at room temperature with 0.5% total strain amplitude. The arrow indicates the stress direction.

and approximately perpendicular to the applied stress. A slice of the fatigued sample was then annealed at 764°C ($0.6T_m$) for one hour. Fig. 4-34 shows the microstructure after annealing. The overall microstructure has changed due to grain growth, probably owing to strain induced grain boundary migration. However, the area very close to the crack surface reveals finer grains as the result of static recrystallization. This becomes clearer when annealing at a lower temperature. Fig. 4-35 shows the same crack as in the previous micrograph but after annealing at 418°C ($0.4T_m$) for one hour. The plastic zone around the crack can now be easily distinguished by the many small statically recrystallized grains along crack surface. This micrograph clearly shows the large plastic deformation zone associated with the crack. This plastic flow might be sufficient to initiate dynamic recrystallization during high temperature fatigue.

Several tests with 0.5% total strain amplitude were conducted at 600°C for 600 to 1000 cycles. Fig. 4-36 shows the microstructure parallel to the stress axis of a notched specimen after 880 cycles. The results of extensive grain boundary migration can be seen in this micrograph. Most grain boundaries are now oriented under approximately 45° to the stress axis. Structural grain coarsening resulted from grain boundary migration. In contrast to room temperature deformation, the crack does not propagate transgranularly, but advances along the grain boundaries, and the propagation direction is close to 45° with respect to the stress axis. This crack propagation under 45° should not be confused with or attributed to the maximum shear stress in this direction. Rather it is due to the easy crack opening (or small energy

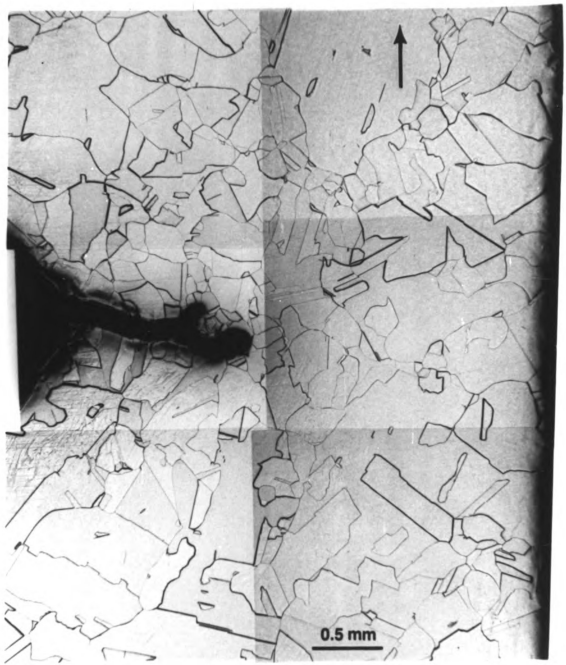

Fig. 4-34. The microstructure of a prenotched Ni fatigued at room temperature with 0.5% total strain amplitude and after annealing at 764°C ($0.6T_m$) for 1 hour.

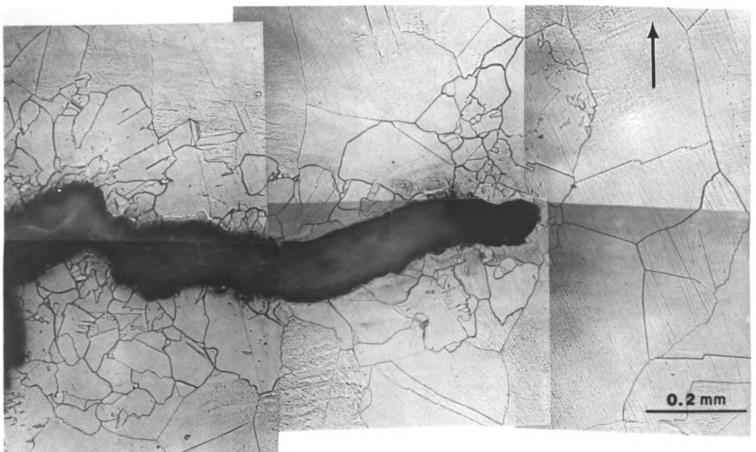

Fig. 4-35. The microstructure of a prenotched Ni fatigued at room temperature with 0.5% total strain amplitude and after annealing at 418°C ($0.4T_m$) for 1 hour.

release rate) along the boundaries, which are aligned under 45° owing to previous migration, but contain cavities as a result of grain boundary sliding. This is for instance substantiated by the crack which propagated under 45° into a grain and got arrested as indicated by an arrow. That the crack extended into the grain at all is most likely due to the fact that a grain boundary was previously located in this position and produced cavities because of grain boundary sliding. When the boundary moved on, it left the cavities behind. While the overall microstructure has undergone substantial grain coarsening due to grain boundary migration, there is noticeable grain refinement along the crack surface and near the crack tip area (Figs. 4-36, 4-37). A branch of the crack is shown in Fig. 4-38. It is obvious that these small grains attached to the crack were created during test since they appear individually and separately which is quite atypical for static recrystallization. The small grains along the cracks in Figs. 4-36 and 4-37 also have to be understood as the product of dynamic recrystallization during crack propagation.

A sample was fatigued at higher strain rate ($2\times10^{-3}s^{-1}$) with 0.5% strain amplitude for 744 cycles. The microstructure is shown in Fig. 4-39. The crack propagated along the grain boundary for a short distance compared to Fig. 4-36 which was tested at lower strain rate ($2\times10^{-4}s^{-1}$) for 880 cycles with 0.5% strain amplitude. The average grain size is smaller which corresponds to a small degree of grain boundary migration and sliding under higher strain rate (i.e., higher cycle frequency).

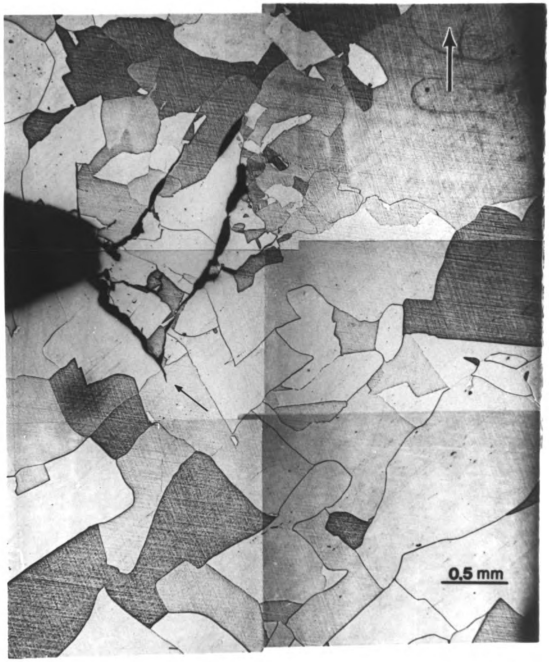

Fig. 4-36. The microstructure of a prenotched Ni fatigued at 600°C with 0.5% total strain amplitude. The arrow indicates the stress direction.

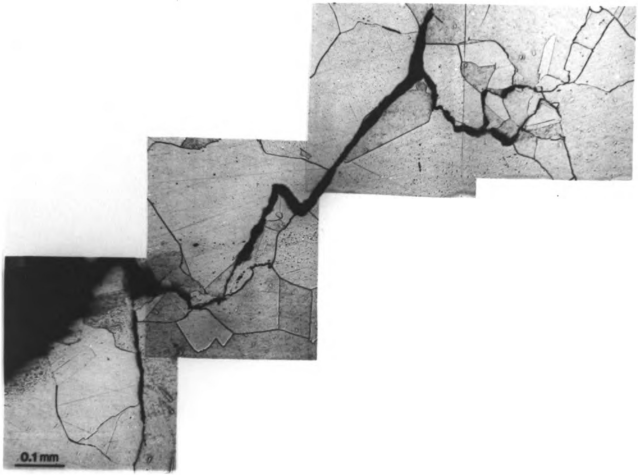

Fig. 4-37. The microstructure of a prenotched Ni fatigued at 600°C with 0.5% total strain amplitude. The arrow indicates the stress direction.

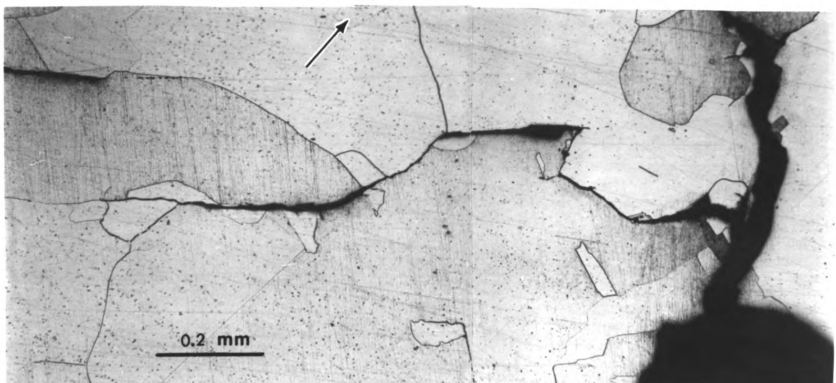

Fig. 4-38. The microstructure around a branch of a crack of a Ni fatigued at 600°C with 0.5% total strain amplitude. The arrow indicates the stress direction.

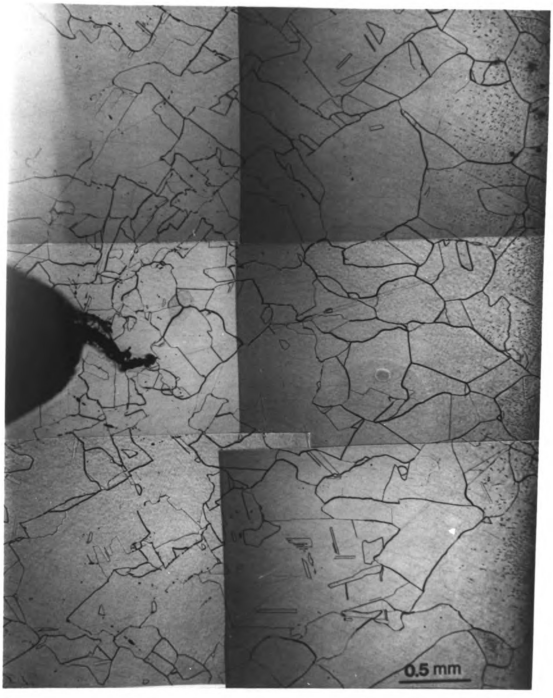

Fig. 4-39. The microstructure of a prenotched Ni fatigued at 600°C with 0.5% total strain amplitude and strain rate of $2\times10^{-3}s^{-1}$. The arrow indicates the stress direction.

Very pure Ni polycrystals were used to perform the current high temperature fatigue tests. The dislocation storage rate is fairly small because of easy dislocation movement which means high recovery rate. This low energy storage will limit the driving force for DRX which has been shown as the locally microstructural change during crack propagation. It is reasonable to speculate that it may be possible to retard crack propagation by a global rebuilding of the microstructure with dynamic recrystallization, i.e. by creation of new uncavitated boundaries. This might be achieved by intermittent overloads that would trigger global dynamic recrystallization which has been observed in section 4.4.

Several tests had been tried and are listed in Table 4-2. Fig 4-40 is the hardening curve of a sample tested at 600°C with 1% strain amplitude for 605 cycles. The curve gives the stress as a function of the strain amplitude in terms of cumulative displacement. A circumferential crack was used in order to concentrate the deformation within the area adjacent to the crack. According to previous results, the load decrease indicates the occurrence of DRX. The microstructure around the cracks is shown in Fig. 4-41. Owing to the nature of the circumferential crack and the higher strain amplitude imposed on the specimen, the stress highly concentrates in front of the crack, and dynamic recrystallization occurred in this area, which is indicated by the many small grains ahead of the crack tip. DRX most likely causes the initial load drop. The following load decreasing probably is due to the combination of DRX and less effective strain amplitude (part of the strain amplitude contribute to the crack opening displacement). The shape of

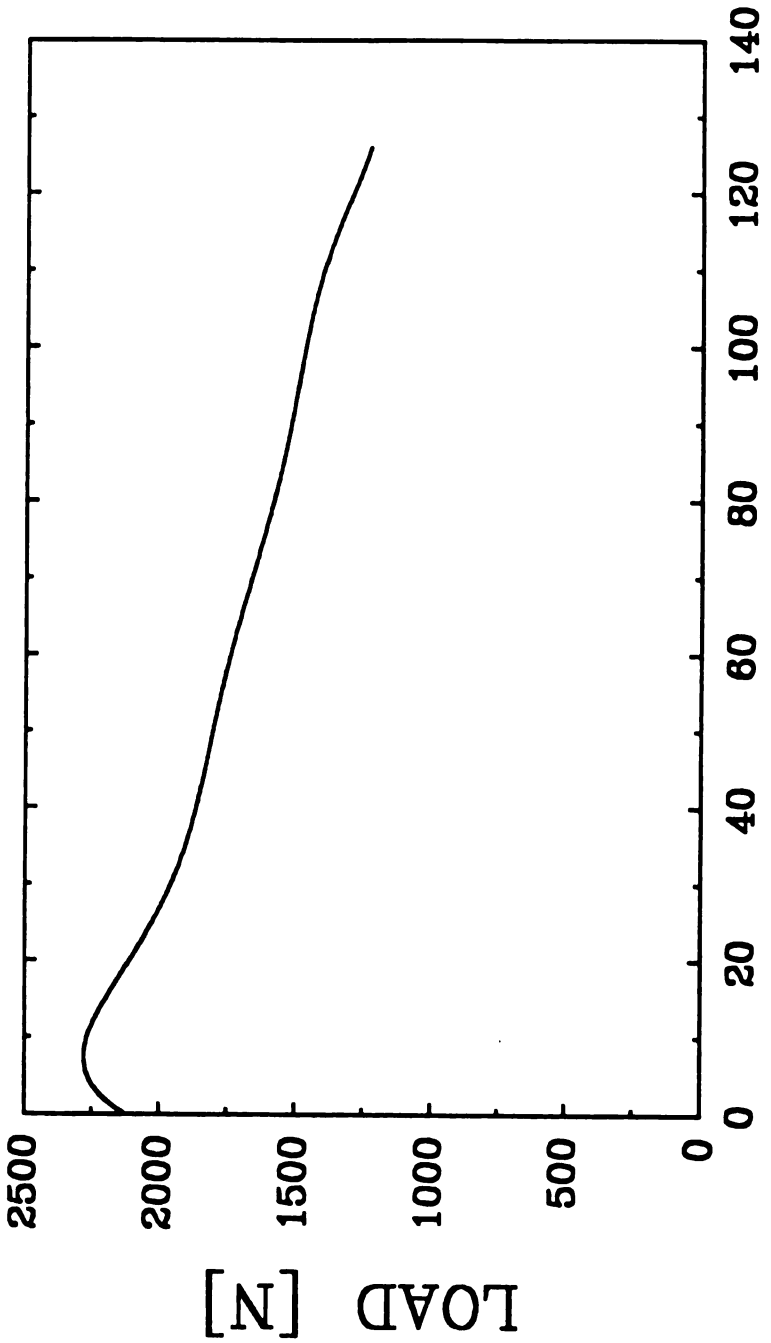

Fig. 4-40. Cyclic hardening curve of a Ni having a circumferential notch fatigued at 600°C with 1% total strain amplitude for 605 cycles.

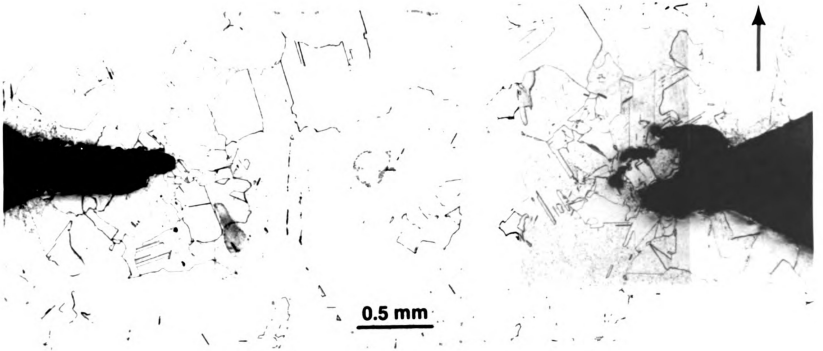

Fig. 4-41. The microstructure associated with crack propagation corresponding to the test indicated in the Fig. 4-40.

the crack tip (Figs. 4-42 & 4-43) suggests that the crack has been blunted and the stress concentration has been relieved by those newly formed small grains. This is further substantiated by a sample with a circumferential notch elongated at 600°C. The corresponding load-displacement curve is shown in Fig. 4-44. The initial grain structure can be visualized as the left hand area away from the notch which contains a high density of annealing twins embedded among large grains. The notch was enlarged and became blunt due to dynamic recrystallization as shown in Fig. 4-45.

The result on a sample fatigued at 600°C for 605 cycles with 1% strain amplitude (Test No. CRK6031, Fig. 4-41) indicates that the microstructural change was limited around the crack tips, therefore, occasionally higher strain amplitudes are necessary to set off DRX in the entire cross section. Such a test is listed in Table 4-2 (CRK6051) and the hardening curve is shown in Fig. 4-46. The peaks in the curve show the positions where higher strain amplitudes were applied. Thirty one cycles of +5%, -1% strain amplitude were imposed to the specimen in the first peak. The load decreases fast and steadily. This unusual load decrease is due to the occurrence of DRX across the entirely region and the propagation of cracks because a high tensile strain was applied for a large number of cycles. The microstructure of the center area which is parallel to the stress axis is shown in Fig. 4-47. The first impression about this micrograph is that the overall microstructure has been changed. Because of stress relief due to DRX, the crack on the right hand side of the micrograph has been blunted and no main direction of propagation could be revealed. This test provides the information

Fig. 4-42. A higher magnification micrograph showing part of the structure around a crack in Fig. 4-41.

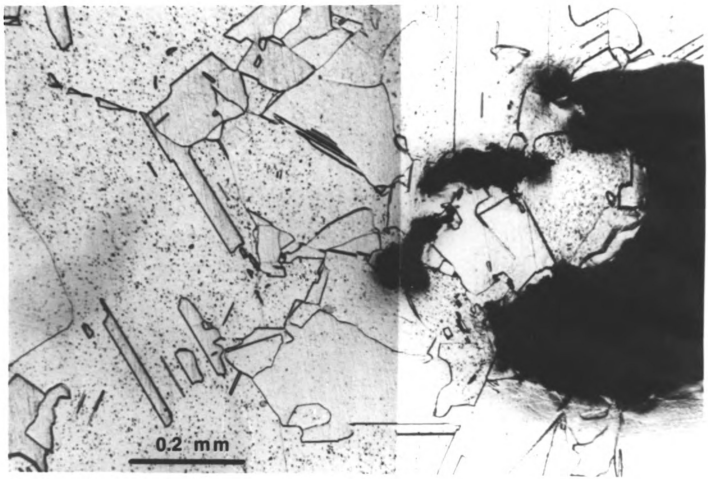

Fig. 4-43. A higher magnification micrograph showing part of the structure around a crack in Fig. 4-41.

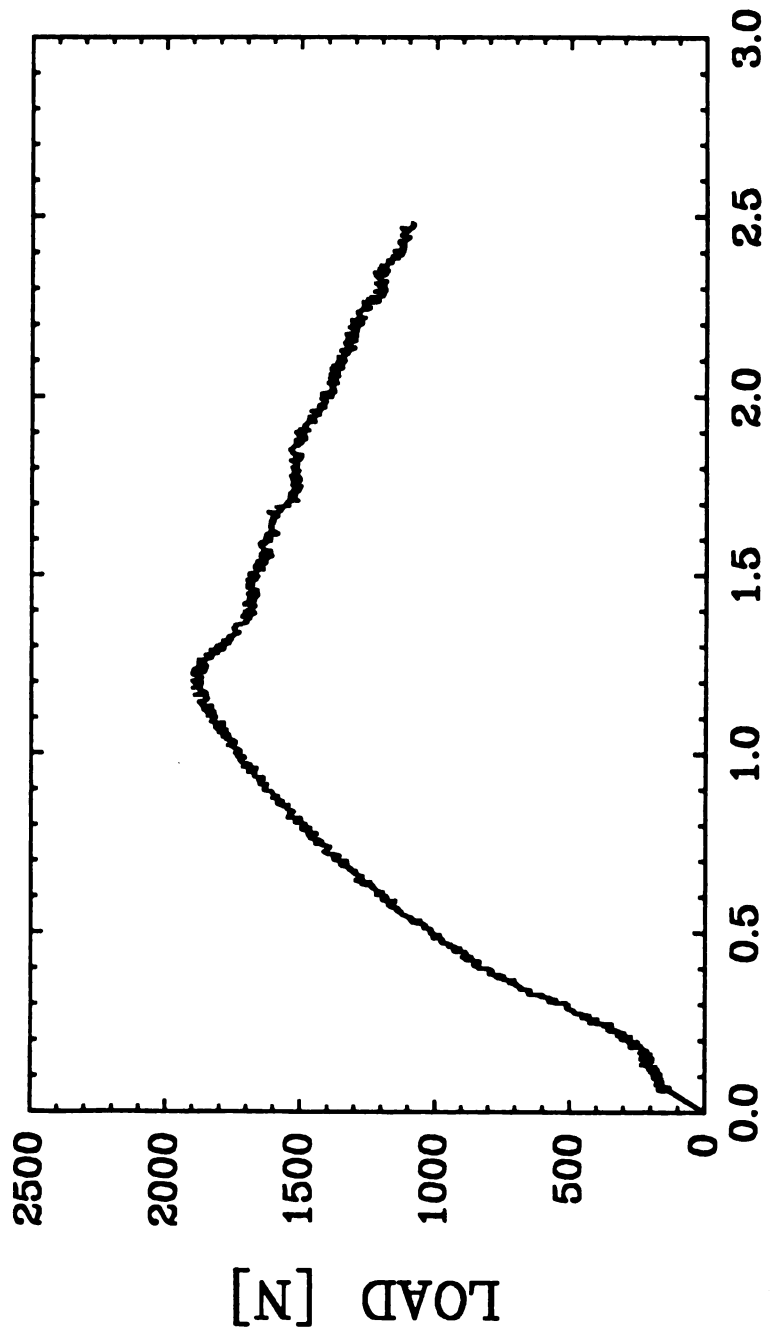

Fig. 4-44. Flow curve of a Ni having a circumferential notch elongated at 600°C with an initial strain rate of $2 \times 10^{-4} s^{-1}$.

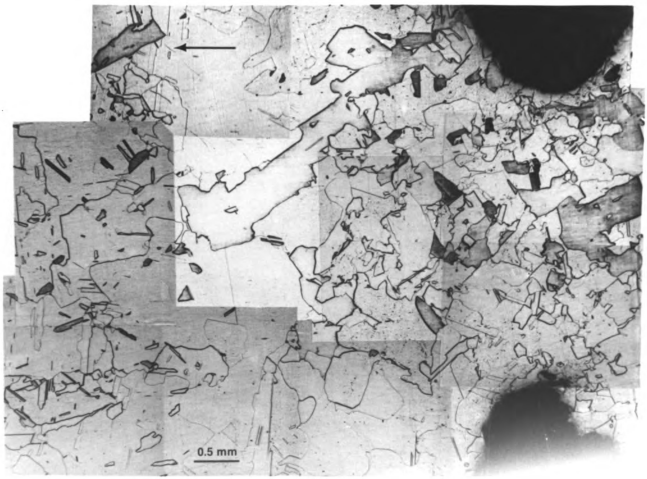

Fig. 4-45. The microstructure associated with crack propagation corresponding to the test indicated in the Fig. 4-44.

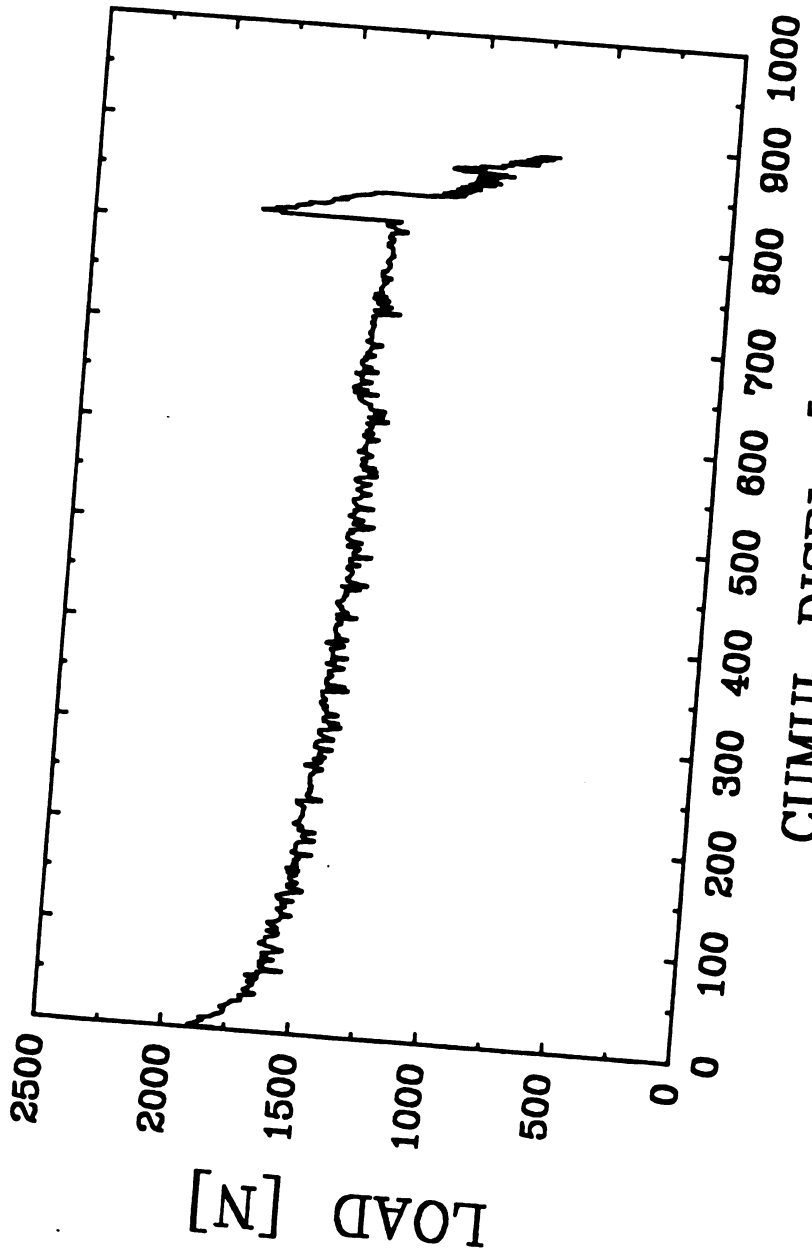

Fig. 4-46. Flow curve of a Ni having a circumferential notch fatigued at 600°C with ±0.5% total strain amplitude and occasional over-straining with +5%, -1% total strain amplitude.

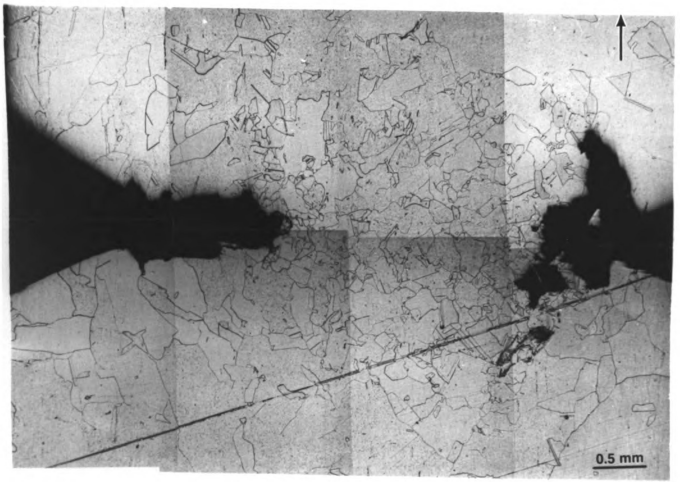

Fig. 4-47. The microstructure associated with crack propagation corresponding to the test indicated in the Fig. 4-46.

about the occurrence of DRX if +5%, -1% strain amplitude was applied. Another specimen was subjected to a more complex waveform, consisting of +5%, -1% strain amplitude for 20 cycles then followed by ±0.5% for 200 cycles. The circumferential notch specimen was tested at 600°C (Test No. CRK6071) until fracture occurred after 1114 cycles. The flow curve is shown in Fig. 4-48. The microstructure and fracture surface observations are seen in Figs. 4-49 and 4-50, respectively. The microstructure (Fig. 4-49) reveals small grains extending from the fracture surface downward along the stress axis. The area included by two arrows indicates the final fracture part. An SEM micrograph shows the fracture surface of the whole cross sectional area (Fig. 4-50(a)). A higher magnification of the final fracture area is given in Fig. 4-50(b). The very clean surface indicates an intergranular fracture mode. The crack propagation region is imaged in Fig. 4-50(c).

Because of the high tensile strain imposed on the specimen, DRX has occurred completely along the notched plane, however, the crack propagation speed is also influenced by the high tensile strain. Therefore, it is difficult to distinguish the effect of DRX on the crack propagation under a small symmetrical strain amplitude (e.g.. ±0.5%). A waveform composed of +0.5%, -5% for 5 cycles and then ±0.5% for 500 cycles was applied repeatly to a sample (CRK6081) until fracture occurred at cycle 5512). A double edge instead of circumferential notch specimen was used to allow deformation to occur along the whole gauge length. The flow curve is shown in Fig. 4-51. The microstructure (Fig. 4-52) is quite different from the previous one (Fig. 4-49). Grain boundary migration had caused grain coarsening. The crack propagated mostly along grain

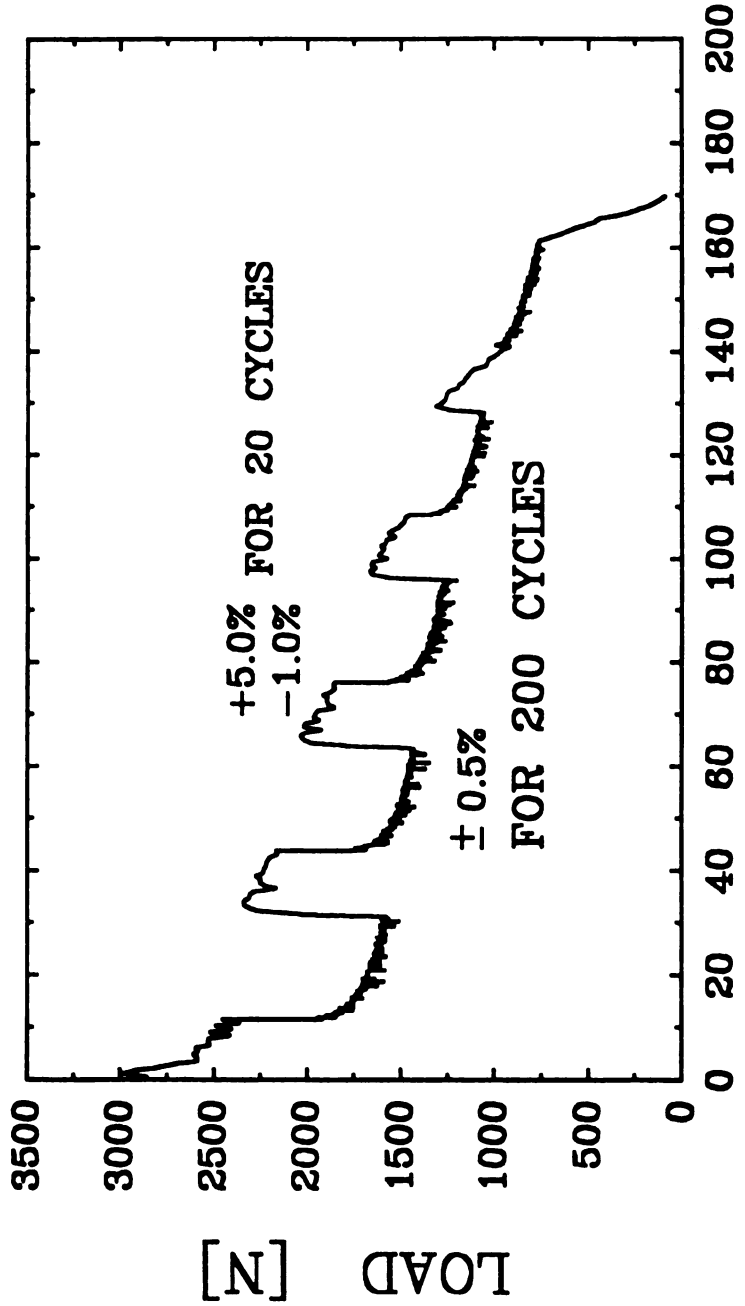

Fig. 4-48. Flow curve of a Ni having a circumferential notch fatigued at 600°C alternatively with +5%, -1% total strain amplitude for 20 cycles and ±0.5% total strain amplitude for 200 cycles until fracture at cycle number 1114.

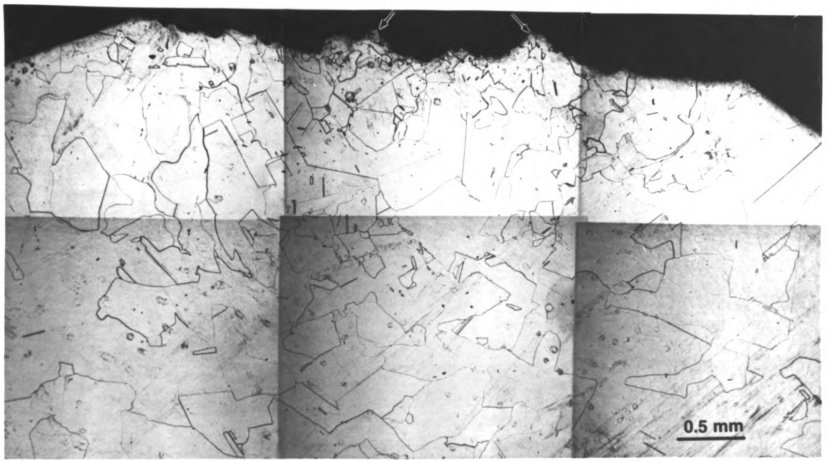

Fig. 4-49. The microstructure associated with crack propagation corresponding to the test indicated in the Fig. 4-43.

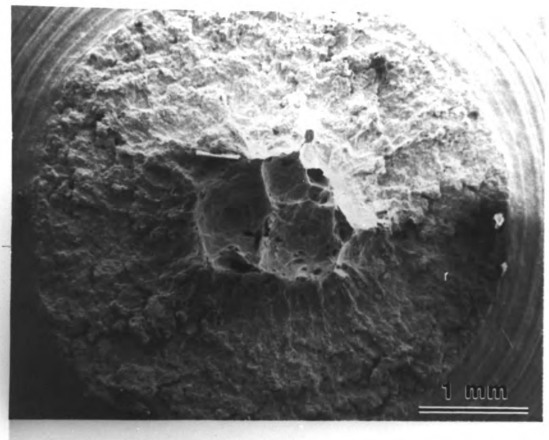

Fig. 4-50. SEM micrographs of the fracture surface after the test indicated in the Fig. 4-48.

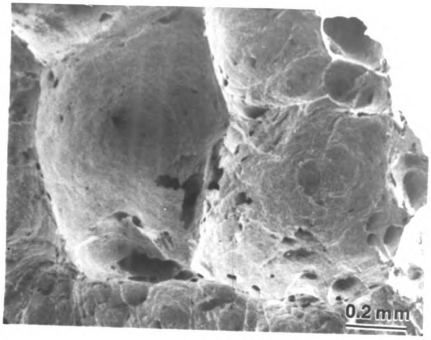

(b)

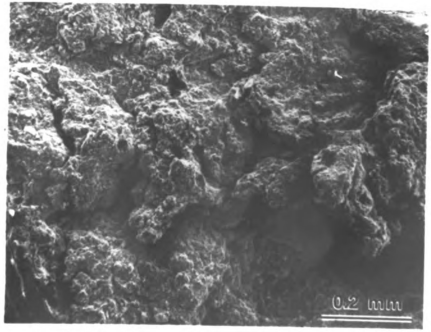

(c)

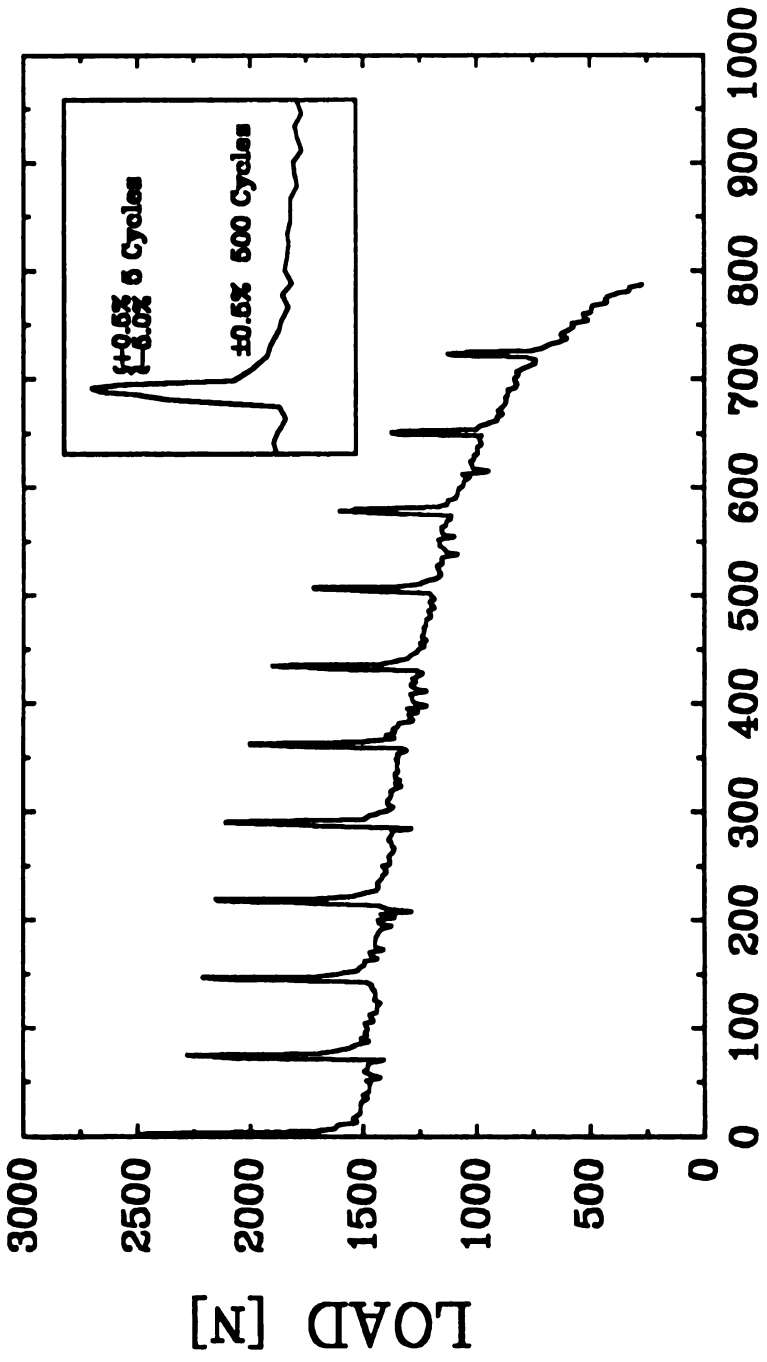

Fig. 4-51. Flow curve of a Ni having double edge notches fatigued at 600°C alternatively with +0.5%, -5% total strain amplitude for 5 cycles and ±0.5% total strain amplitude for 500 cycles until fracture at cycle number 5512.

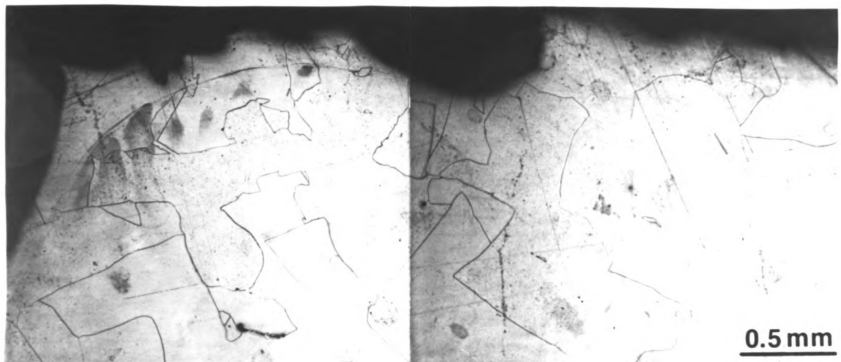

Fig. 4-52. The microstructure associated with crack propagation corresponding to the test indicated in the Fig. 4-51.

boundaries which can be seen in the fractograph (Fig. 4-53(a), magnified in Fig. 4-53(b)) near the notches, which is characterized by many facets on the fracture surface. Subsequently, transgranular crack propagation takes over which is revealed in Fig. 4-53(c) by the striations on the fracture surface. A sample with similar notches was tested at 600°C with ±0.5% strain amplitude until fracture at cycle 10943 (CRK6091) for comparison with the result of the overload test. The flow curve is shown in Fig. 4-54. After initial strain hardening, the stress reaches a maximum and then decreases continuously (Fig. 4-54(b)). The fatigue life of this specimen is about two times longer than that of the previous specimen. The microstructure is shown in Fig. 4-55. The notation S is defined as the normalized distance away from the plane parallel to the stress axis and through the center of the specimen (S=0). The maximum value of S is 1 which denotes the plane of the surface of the gauge section. Fig. 4-55(a) shows the microstructure at S=3/4. Besides the major cracks which propagate along the notches, two other large cracks can be seen in this micrograph. DRX is clearly revealed by the many small grains near the fracture surface and around crack tip. Fig. 4-55(b) shows the microstructure at S=1/2. The structure is similar to Fig. 4-55(a), only the recrystallization phenomenon is not so obvious as in Fig. 4-55(a). On the interior at S=0 (Fig. 4-55(c)), the microstructure shows only a few large grains. Fig. 4-56 are SEM micrographs of the fracture surface. The brighter area reveals the final fracture surface. The microstructures of Figs. 4-55(a) and 4-55(b) correspond to this area where a high stress due to the small cross sectional area in final stage induced a high degree of deformation such that DRX is apparent in this area. Fig. 4-56(b) shows the intergranular crack

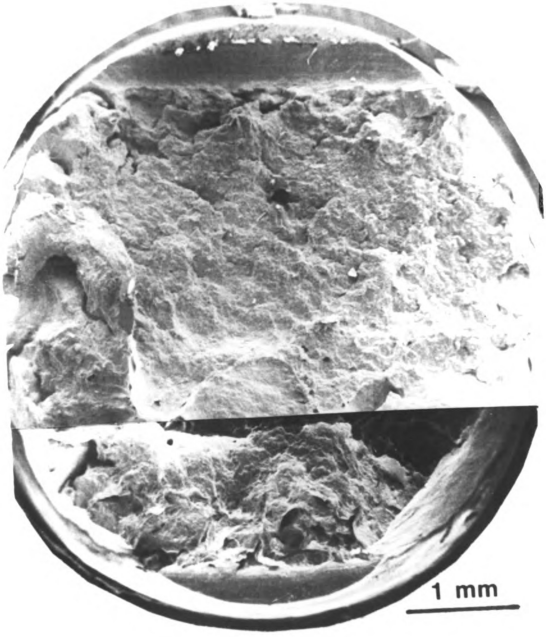

(a)

Fig. 4-53. SEM micrographs of the fracture surface after the test indicated in the Fig. 4-51.

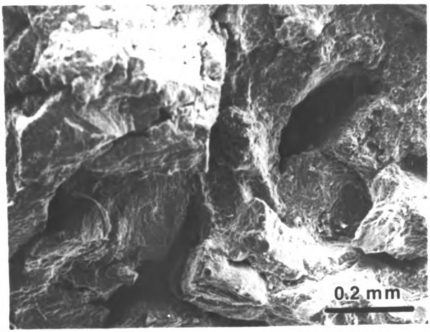

(**b**)

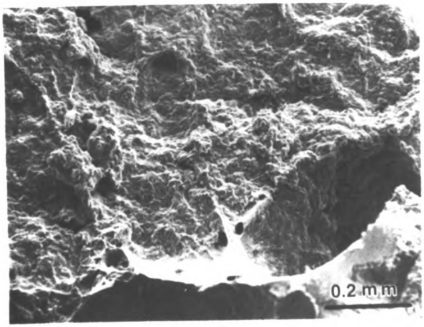

(**c**)

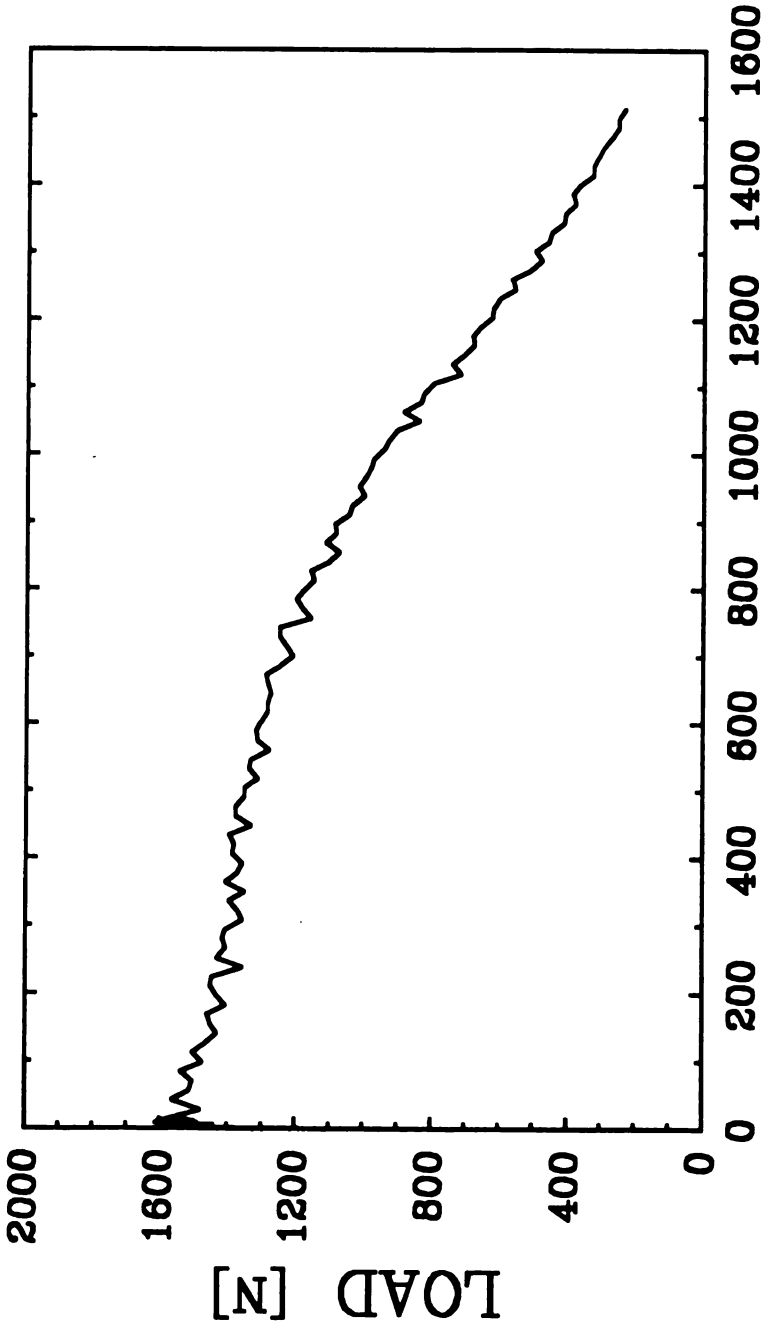

Fig. 4-54. Flow curve of a Ni having double edge notches fatigued at 600°C with ±0.5% total strain amplitude until fracture at cycle number 10943.

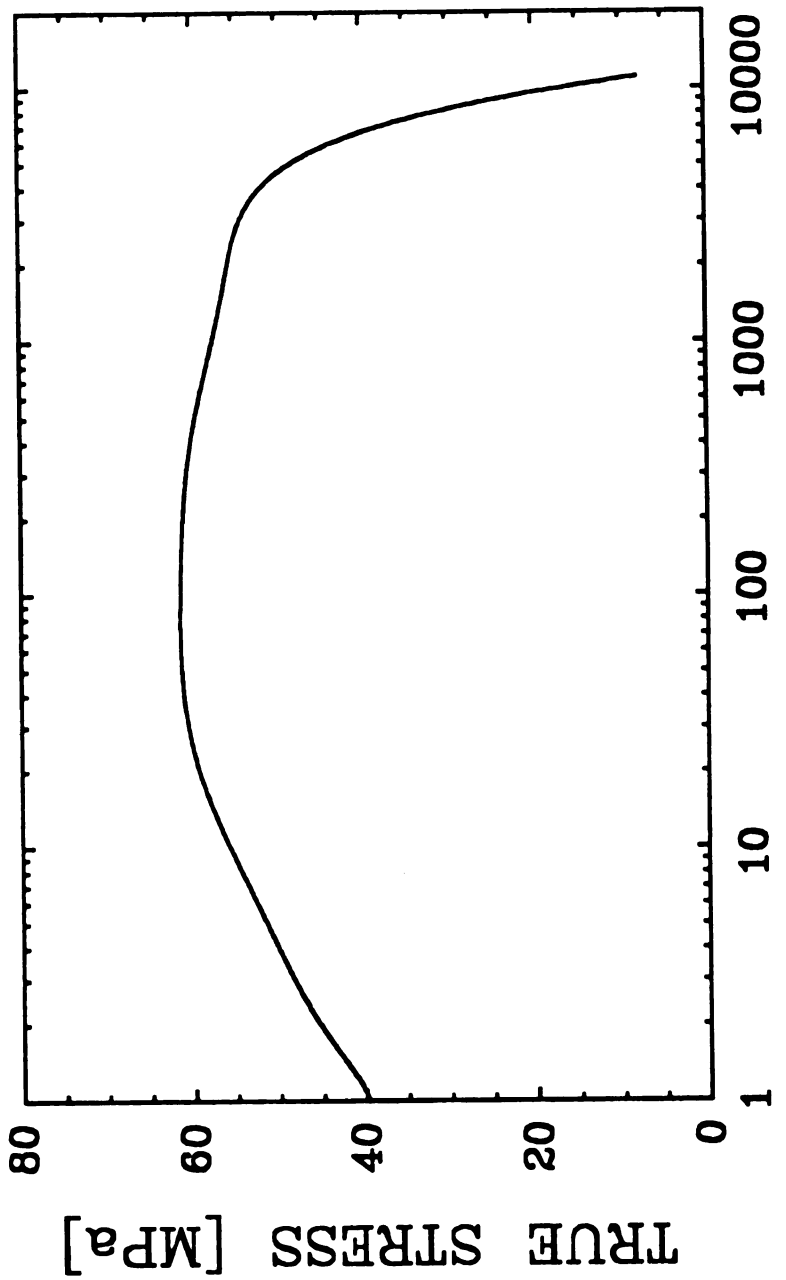
TRUE STRESS [MPa]
0
20
40
60
80
1
10
100
1000
10000
NUMBER OF CYCLES

(b)

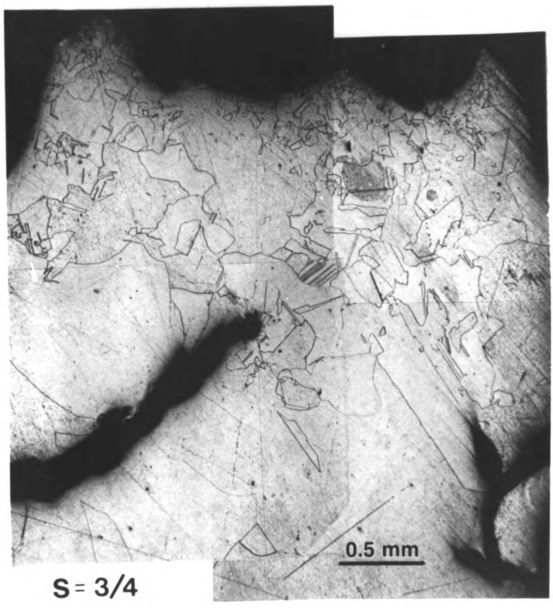

(a)

Fig. 4-55. The microstructures associated with crack propagation corresponding to the test indicated in the Fig. 4-54. (a) S=3/4; (b) S=1/2 and (c) S=0.

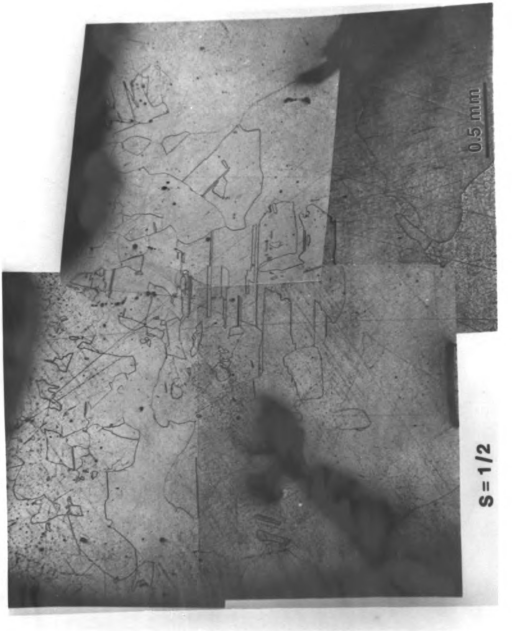

(b)

(c)

propagation from the surface in the early stage of crack growth. Fig. 4-56(c) reveals the microstructure in the center region of the fracture surface. The striations indicate that plastic deformation due to transgranular crack propagation has occurred which becomes even clearer in higher magnification (Fig. 4-56(d)).

(a)

(b)

Fig. 4-56. SEM micrographs of the fracture surface after the test indicated in the Fig. 4-55.

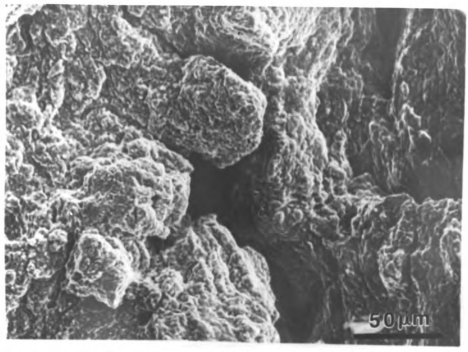

(c)

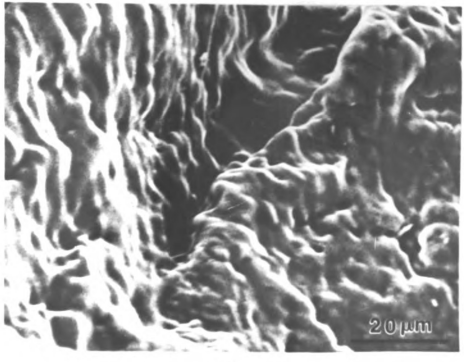

(d)

V DISCUSSION

5.1 Mechanical Behavior and DRX

All cyclic hardening curves (Fig. 4-1(a)) reveal a maximum followed by a continuous decrease of the true stress. The number of cycles to the flow stress maximum is the smaller the larger the cyclic total strain amplitude. This behavior indicates a strong softening mechanism that occurs at large cumulative strains. It is proposed to attribute this softening to grain boundary migration (grain coarsening) and DRX. In monotonic tests DRX is known to occur at relatively large strains and to make itself felt by a drastic decrease of the flow stress [7,37]. The softening observed in the current cyclic tests is much less spectacular, because the net driving force for DRX in cyclic tests is much smaller than in monotonic tests. The microstructural observations evidence extensive grain boundary migration (Fig. 4-3) and the occurrence of new grains (Figs. 4-7,4-9,4-10) during LCF. Since grain boundaries are known to absorb dislocations during migration, this process will decrease the total dislocation density and thus, the flow stress. With increasing strain the specimen continues to strain harden, but the strain hardening coefficient decreases owing to dynamic recovery, and DRX becomes increasingly stronger. This will finally lead to a maximum of the flow stress and a continuous stress decrease at larger accumulated strains.

The stress maximum is not sufficient, however, to infer the occurrence of DRX. Al also shows a hardening curve with a stress maximum,

although the average stress decrease rate is much smaller than that of Ni. (Note also that σ is considerably smaller for Al, under the same conditions). Al is known not to recrystallize dynamically due to its high stacking fault energy. In this case the stress maximum has to be attributed totally to dynamic recovery and grain coarsening during cyclic deformation. This is evident from the microstructure which reveals huge grains after cyclic deformation of Al (Fig. 4-6). In contrast, when the materials exhibits DRX, then grain refinement due to DRX will reduce the softening effect caused by grain coarsening, but even in this situation Ni still shows a larger stress decrease rate. This substantiates that DRX is the major softening mechanism in Ni.

High temperature LCF on Ni-200 and dispersion strengthened (DS) Ni was investigated by Bhat and Laird [14,15]. No DRX was found during cyclic deformation, in contrast to their results in monotonic tests. This is not in contradiction to the current findings, though. Bhat and Laird draw their conclusions exclusively from TEM results, where it is difficult to establish the rather localized occurrence of DRX. Also they confined their cyclic testing to only 100 cycles, while our specimens were subjected to 300 cycles and more, and the maximum generally was attained at cycle numbers in excess of 100. Furthermore their specimens - even the "pure" nickel - was much less pure than the material used in the current investigation. This is particularly evident from the distinctly higher flow stress of the specimens used by Bhat and Laird. It is a well known fact that recrystallization is delayed by the presence of impurities, owing to their retarding effect on dislocation recovery and grain boundary migration [59,60].

In monotonic tests, the onset of DRX can be associated with the drop of the flow stress. In cyclic tests this is doubtful, however, because the softening due to DRX is much smaller than in monotonic tests due to the low dislocation density, i.e., the low driving force. Also the concurrent deformation of the new grains will reduce the softening effect associated with these newly formed grains.

It is further noted that these results on DRX during cyclic deformation are also relevant for the understanding of DRX under monotonic conditions. During hot working, high strains and stresses are necessary to set off DRX, and it has been argued, whether DRX occurs nucleation or growth controlled [1,3,7,36]. The current observations show that DRX can be initiated at very low driving forces but dislocation production rates comparable to monotonic tests. This suggests that the nucleation is the triggering process for the initiation of DRX. Once nucleated, the grain will grow even at very small driving forces and thus, small growth rates despite concurrent dislocation production. With increasing critical stress, i.e. increasing dislocation density or, equivalently, driving force, the growth rate only controls the grain size in competition with the nucleation rate so that at very high critical stresses and singular nucleation events in monotonically deformed single crystals very large recrystallized grains are obtained [32].

Usually, it was found that a certain critical strain (in the order of 15% or so) (or stress), had to be exceeded in order to set off DRX in monotonic tests. For high strain amplitude (in the order of 5%), an

overall microstructural change has been observed (Figs. 4-12, 4-13, 4-15, 4-17) due to the large driving force for DRX which is comparable to monotonic tests. According to the mechanical test results from current research, the stress maximum occurs in the order of 100% in terms of cumulative strain that stands for the sum of the strain (elastic + plastic, negative + positive) imposed on the specimen, under the strain rate of $10^{-4}s^{-1}$ (cycle frequency in the order of 10^{-2}Hz depending on the strain amplitude) at $0.5T_m$.

The results from two hour-glass shape specimens are of particular interest. The microstructure (Figs. 4-15, 4-17) indicates grain refinement and grain boundary migration. The final grain size is apparently smaller than the original value. From the Hall-Petch relation, the smaller grain size should give rise to a higher flow stress. The stress decrease in Fig. 4-14, therefore, can be only attributed to softening owing to the occurrence of DRX. The recrystallized grains contain fewer dislocations which is the real determinant of the flow stress. From the results of DRX in monotonic tests, the size of dynamically recrystallized grains will reach a steady state value, i.e. the grain size will remain constant during progressing deformation. However, the stress is observed to continually decrease in the current case. This may indicate a reduction of the effective strain due to the action of grain boundary sliding, when the grain boundaries become aligned under 45° with respect to the stress axis. For instance, in an hour-glass shape specimen (Fig. 4-15) only a small crack was detected which can not cause the high magnitude of flow stress decrease. Further evidence can be gained by examining the hysteresis loops at various critical points on the cyclic

hardening curve. Fig. 5-1(a) is the hardening curve of a Ni specimen fatigued at 600°C with 0.5% strain amplitude. The stress reaches a maximum at about 100 cycles, and then decreases continuously. The hysteresis loops are plotted in Fig. 5-1(b). These loops share a line within the elastic region with a common slope quite well. This suggests the lack of macrocavities within the specimen. The significant stress decrease, therefore, indicates that the softening phenomena observed are mainly due to microstructural changes.

5.2 Grain Boundary Migration and Dislocation Structure

From the test results on Cu single crystals, it was concluded that DRX during HTLCF is a grain boundary effect and, thus, occurs only in polycrystals. The grain boundary becomes important in the initiation of DRX. Most grain boundaries in Ni and Al were found to show extensive migration during the test. Langdon et al. reported the same behavior in Al and Pb [20-23] and they assumed that the boundary migration is stress-induced in response to the cyclic loading, since the boundaries tend to align parallel to the plane of maximum shear stress. Since grain boundary migration will annihilate the dislocations in the swept volume, there ought to be a substantial difference in dislocation density in front of and behind a moving grain boundary. All TEM investigations failed to substantiate a drastic gradient in dislocation density across a boundary. Only qualitative differences in dislocation arrangements were noticed (Fig. 4-25). This does not mean though, that the grain

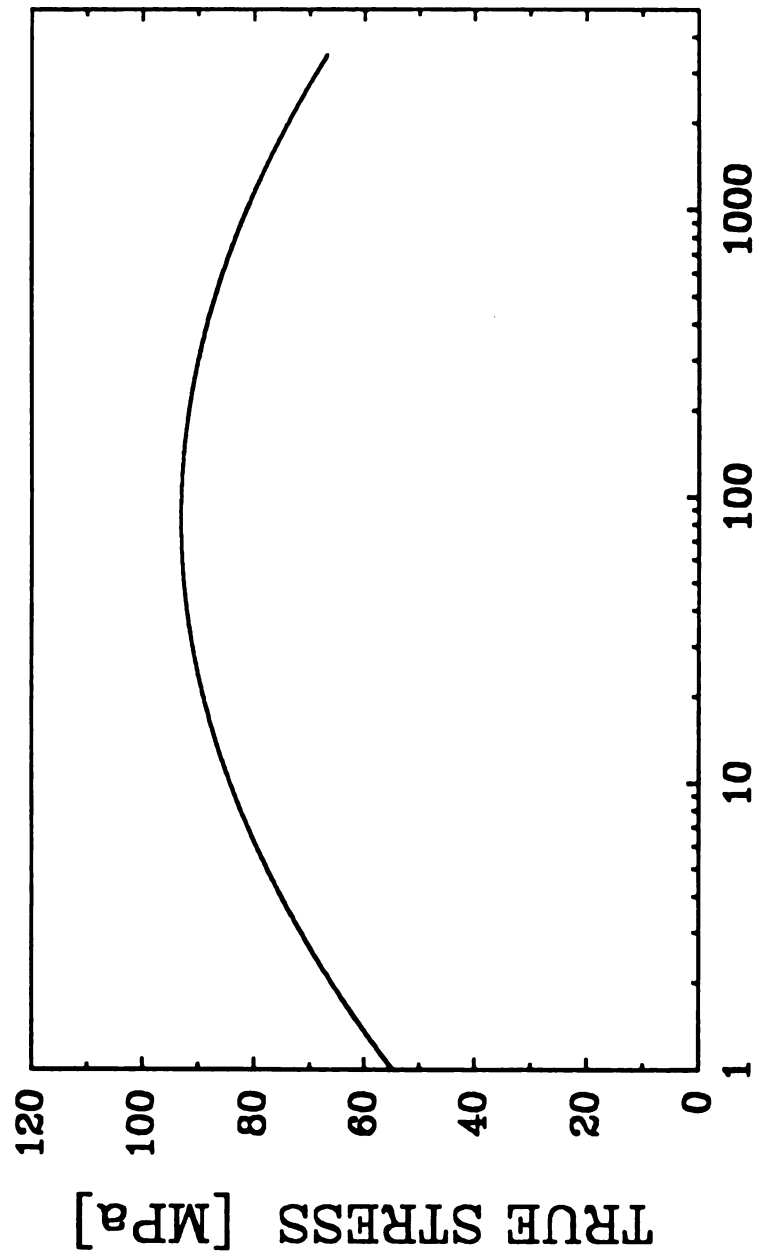

Fig. 5-1. (a) Cyclic hardening curve of a Ni tested at 600°C with 0.5% total strain amplitude; (b) the hysteresis loops corresponding to the various cycle numbers at curve (a) which is indicated in the graph.

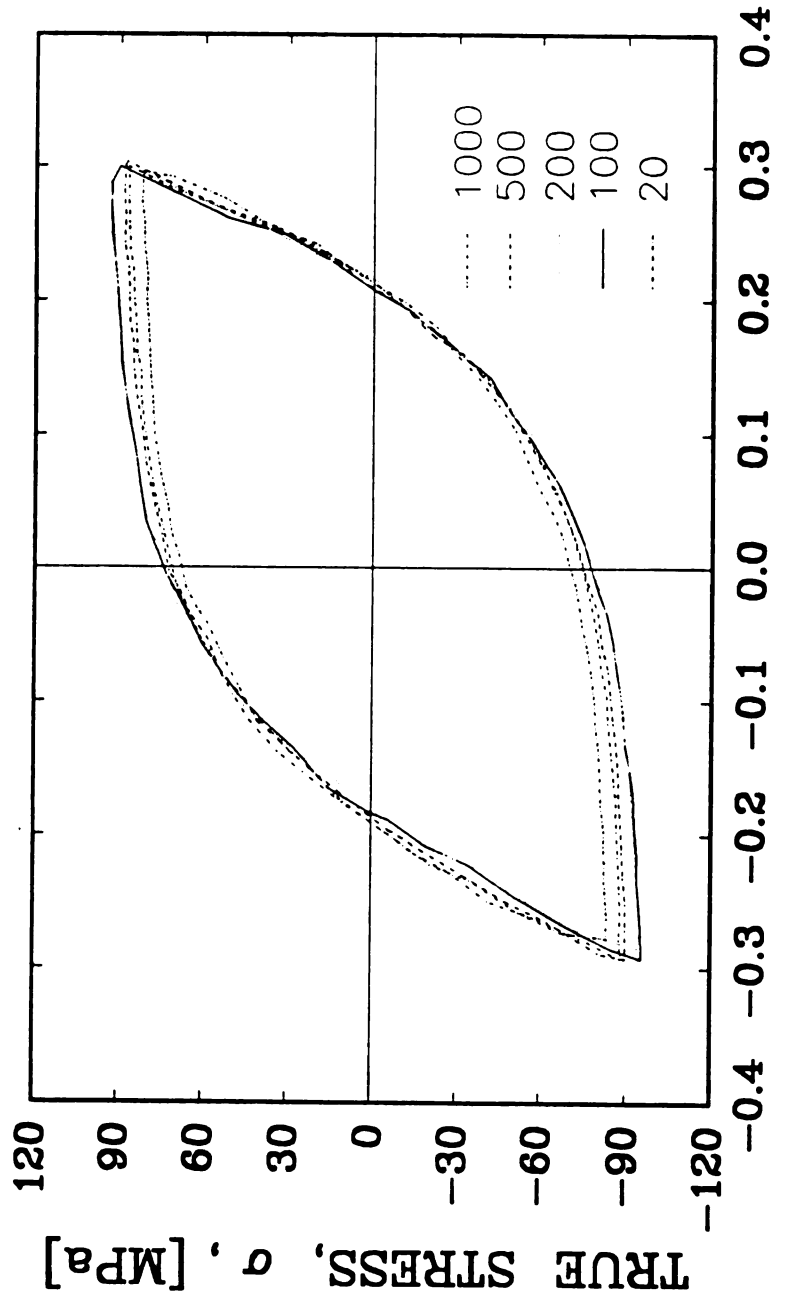
TRUE STRESS, σ, [MPa]
120
90
60
30
0
−30
−60
−90
−120
−0.4
−0.3
−0.2
−0.1
0.0
0.1
0.2
0.3
0.4
TRUE STRAIN, ε, [%]
1000
500
200
100
20

(b)

boundaries do not absorb dislocations. Rather it has to be taken into account that

(1) Grain boundary migration takes place gradually and continuously, but the concurrent deformation constantly produces dislocations, and thus, replaces annihilated dislocations.

(2) DRX progresses very slowly because of a very small driving force compared to monotonic test where the boundaries of new grains move very fast that usually dislocation free region can be observed if properly quenched the specimen at the time DRX occurs.

From the results of dislocation observations during different number of cycles, it was found that the dislocation structure in grain interior is quite different from the dislocation structure in the wake of the boundary (Fig. 4-30). The structure development during the progress of the fatigue test suggests that the structure close to grain boundary corresponds to a very early state of cell structure development. and thus, has to be interpreted as the rebuilding of a cell structure which was eliminated during grain boundary migration.

In essence it is concluded that from the observation of the structural gradient along a path perpendicular to the grain boundary, that boundary migration leads to the destruction of the previously formed dislocation cell structure, which subsequently is rebuilt through all stages of cell development. By analogy, one may conjecture that the patchwise occurrence of disorderly arranged dislocations in the grain interior may also be the result of dynamic changes in the microstructure owing to concurrent deformation.

A quantitative measure of the high temperature deformation structure is the size of the subgrains. The flow stress σ is usually found inversely related to the average subgrain size d [61]

$$\frac{\sigma}{G} = K \frac{b}{d} \quad \text{(b-Burgers vector, K-constant).}$$

Fig. 5-2 gives the relationship between subgrain size and flow stress of Ni. The data roughly join a straight line with slope -0.75 (Bhat and Laird) , -0.86 (current study) and -1.03 (all data). In this figure, Young's modulus (E) was used instead of the shear modulus (G) in order to compare the current results with data reported by Bhat and Laird [14].

One of the most important questions in the current investigation is "What is the driving force for grain boundary migration ?"

The scale of grain boundary migration under HTLCF is extremely large (a few hundred microns [19]). If the specimens were tested under the same conditions in monotonic loading, one would not observe grain boundary migration or at most on a small scale in some special cases (ex. creep). In contrast to the assumption made by Langdon and coworkers, I propose adopt the explanation given by Snowden [19]: "Different amounts of deformation were built up on each side of boundaries so that the migration is produced by unequal numbers of dislocations on opposite sides of boundaries", which also corresponds to the terminology: "Strain induced boundary migration (SIBM)". According to Taylor [62] five independent slip systems are necessary to maintain shape compatability at the boundary between grains which can undergo arbitrary deformation. For simplicity, only one favorable slip system

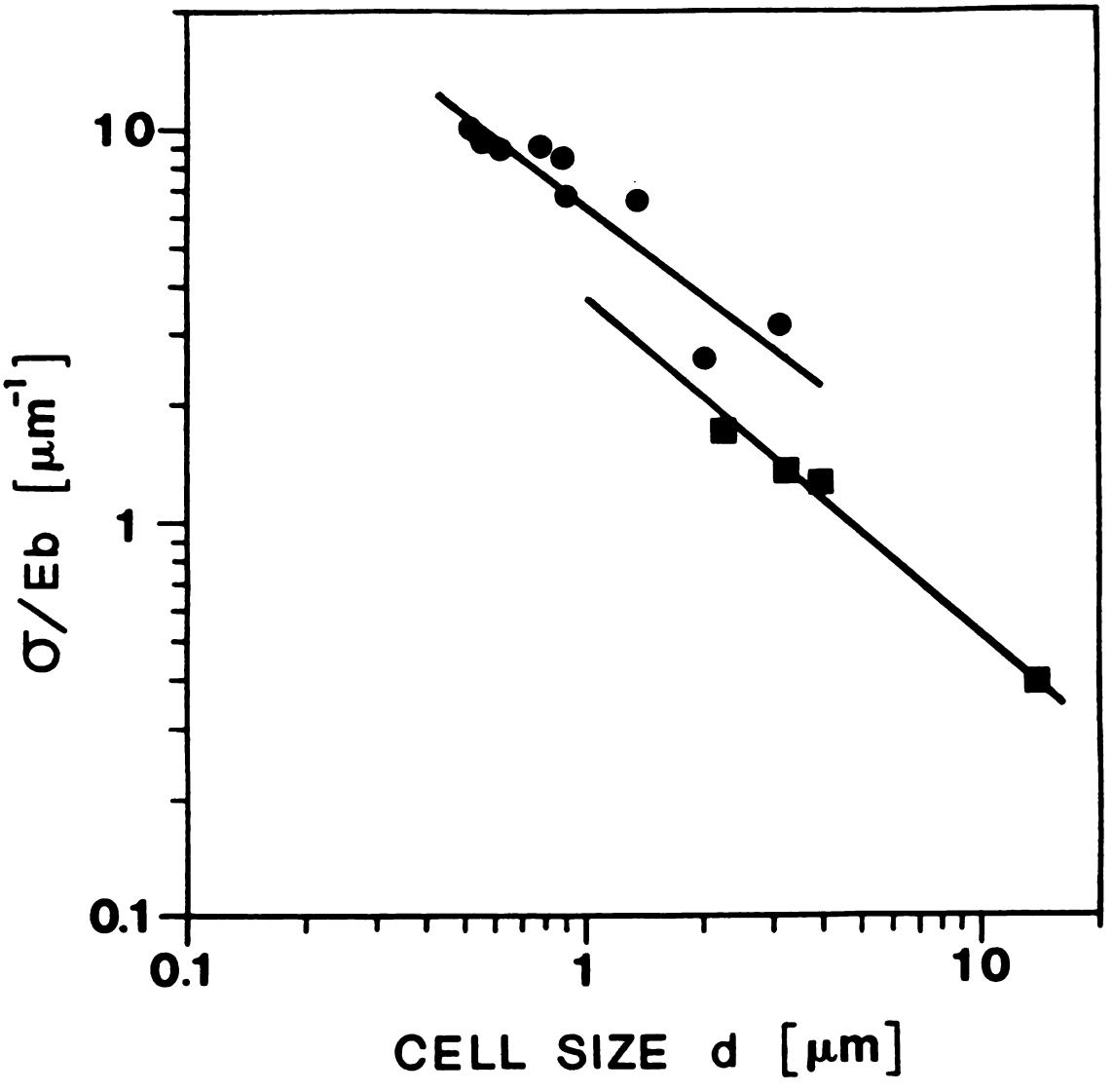

Fig. 5-2. Normalized true stress vs dislocation cell size in Ni for cyclic deformation at various temperatures, ■ - current investigation, ● - result of Bhat and Laird [14].

is shown in Fig. 5-3. During the tensile loading, the grain with higher resolved shear stress will produce higher density of dislocations, provided the resolved shear stress is larger than the critical shear stress. But the difference between the dislocation density is not so high, and one more important factor is that the stress acting on the grain boundary is in the same direction as the gradient of dislocation density. That means the energy difference between both grains due to dislocation gradient is somehow balanced by the pile-up stress of dislocation against the grain boundary. Upon changing loading direction from tension to compression, the dislocation will move toward the center of grains. Due to higher dislocation density in grain A, the elastic stress coming from other dislocations will retard the motion of dislocations from moving away from the grain boundary area. However, in grain B the retarding stress is smaller which means the dislocation will move toward the center of grain easily. In the same time, more dislocation will be produced in grain B in order to obtain the overall strain externally. The difference of dislocation density between grains A and B is even higher and the stress acting on the grain boundary also changes the direction from B to A which assists the grain boundary migration. The new positions of grain boundaries are indicated as dotted lines in Fig. 5-3(b). The dislocation density in the region far away from grain boundary is similar for both grains after completing a cycle. At high temperature, recovery takes place and transfers the dislocations into cell structure as shown in Fig. 4-30. When the cycle finished, the load returned to zero then the dislocations relax from the external stress and back to the wake of grain boundary (Fig. 5-3(c)) which explains the very early state of cell structure development around grain boundary as

observed in Fig. 4-30. In conclusion, the driving force for grain boundary migration is the difference of dislocation density comes from the unequal amounts of deformation between grains under cyclic loading condition with a small strain amplitude.

5.3 Crack Propagation and DRX

From the crack propagation test results, it was found that the dynamically recrystallized zone does not extend to a larger size (Figs. 4-36, 4-37), that is, comparable to the zone observed for room temperature tests (Fig. 4-35). It was also found that the recrystallized zone is not contiguous but consists of isolated grains along the crack path (Fig. 4-38). The important difference between room temperature and elevated temperature deformation crack propagation is that during room temperature deformation the crack propagates transgranularly, that is perpendicular to the direction of the largest principal stress, while during a high temperature test, the crack propagates intergranularly, which is usually not perpendicular to the normal stress, but along the path of weakest resistance to crack growth owing to cavitation in the boundaries. A larger resistance to crack growth in a ductile material is equivalent to a large amount of plastic deformation, for instance in case of transgranular crack growth. Intergranular crack propagation can occur in two possible ways . Either the cavities grow and coalesce until they touch the crack, which means the crack advances without major plastic deformation. Or, the cavities nucleate and grow, but do not become contiguous. Then plastic deformation has to occur locally to

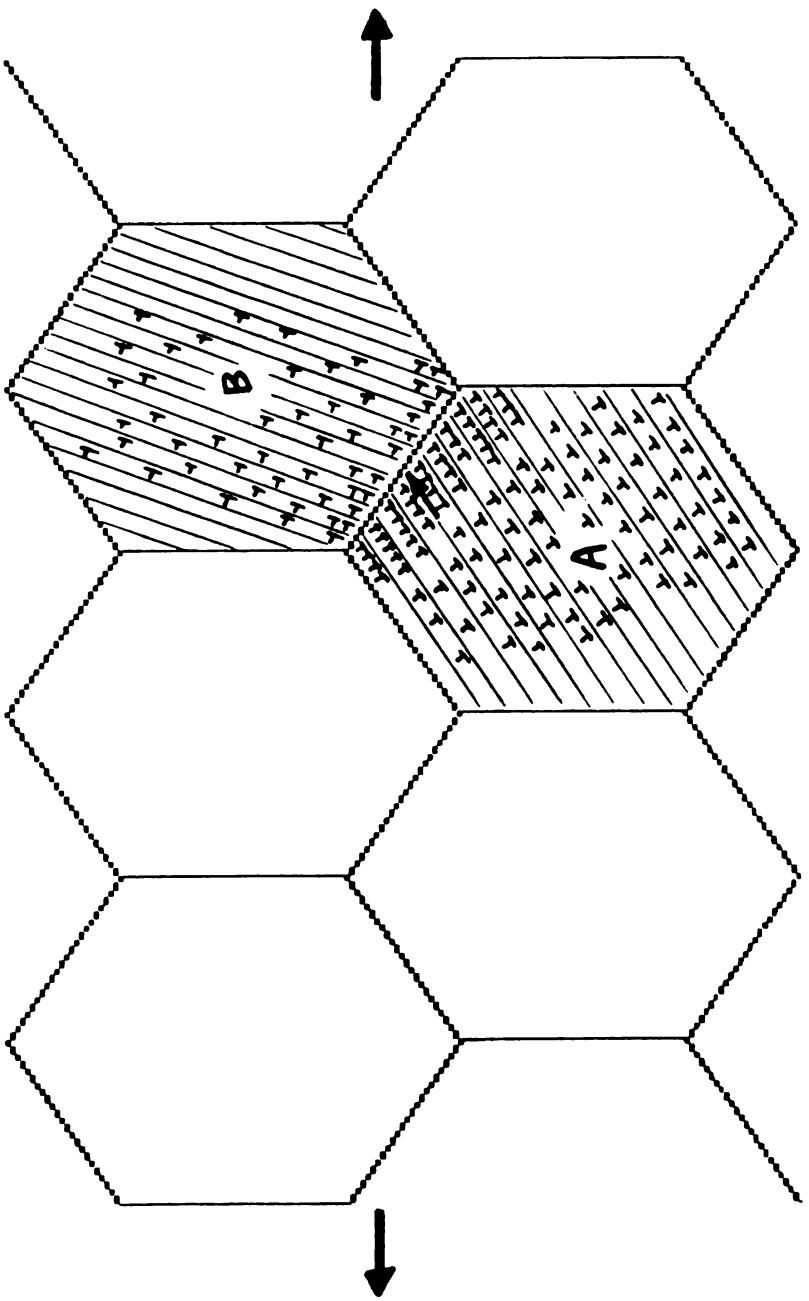

Fig. 5-3. Schematic sketch showing the strain induced grain boundary migration. Loading is in (a) tension; (b) compression and (c) returning to zero.

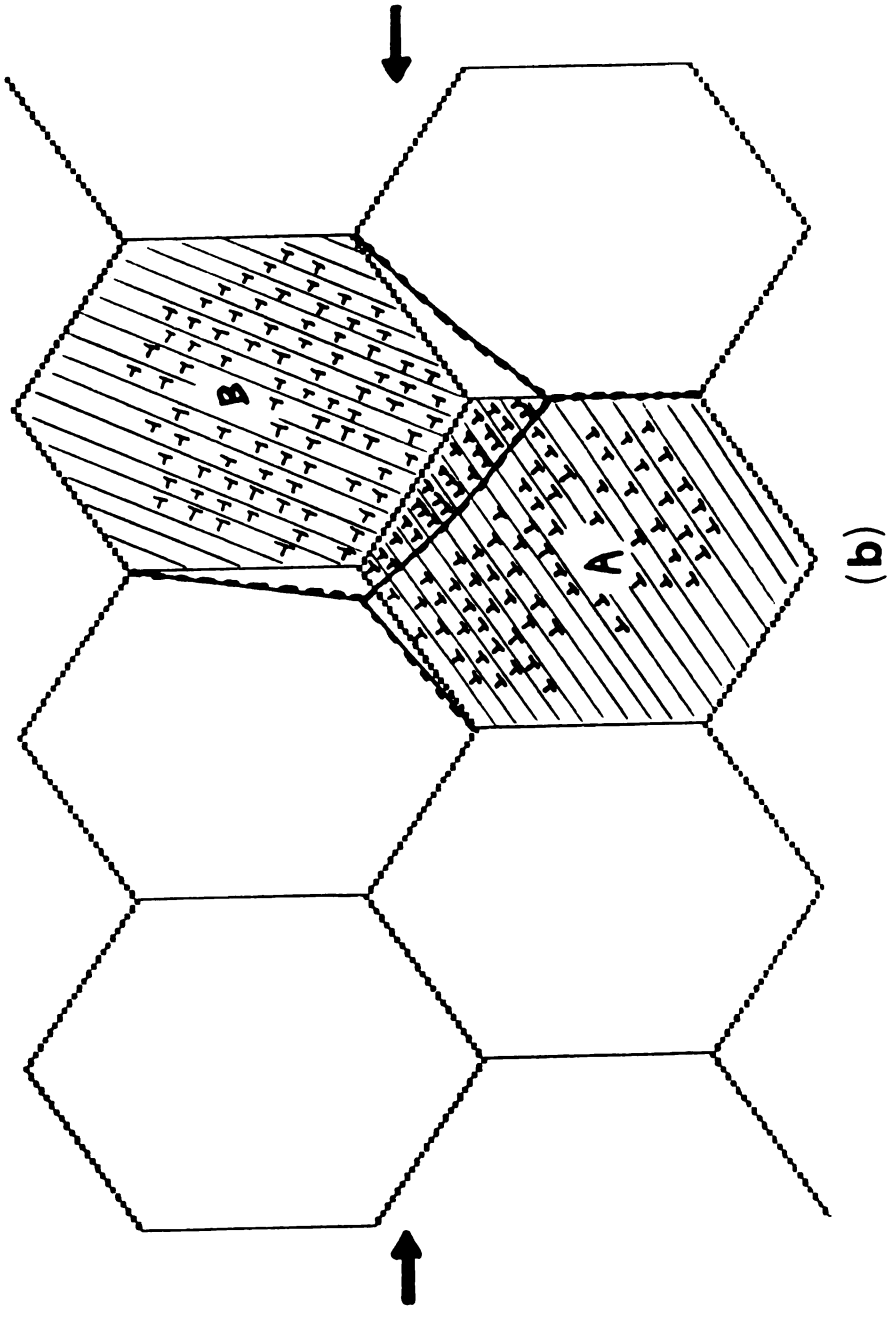

(b)

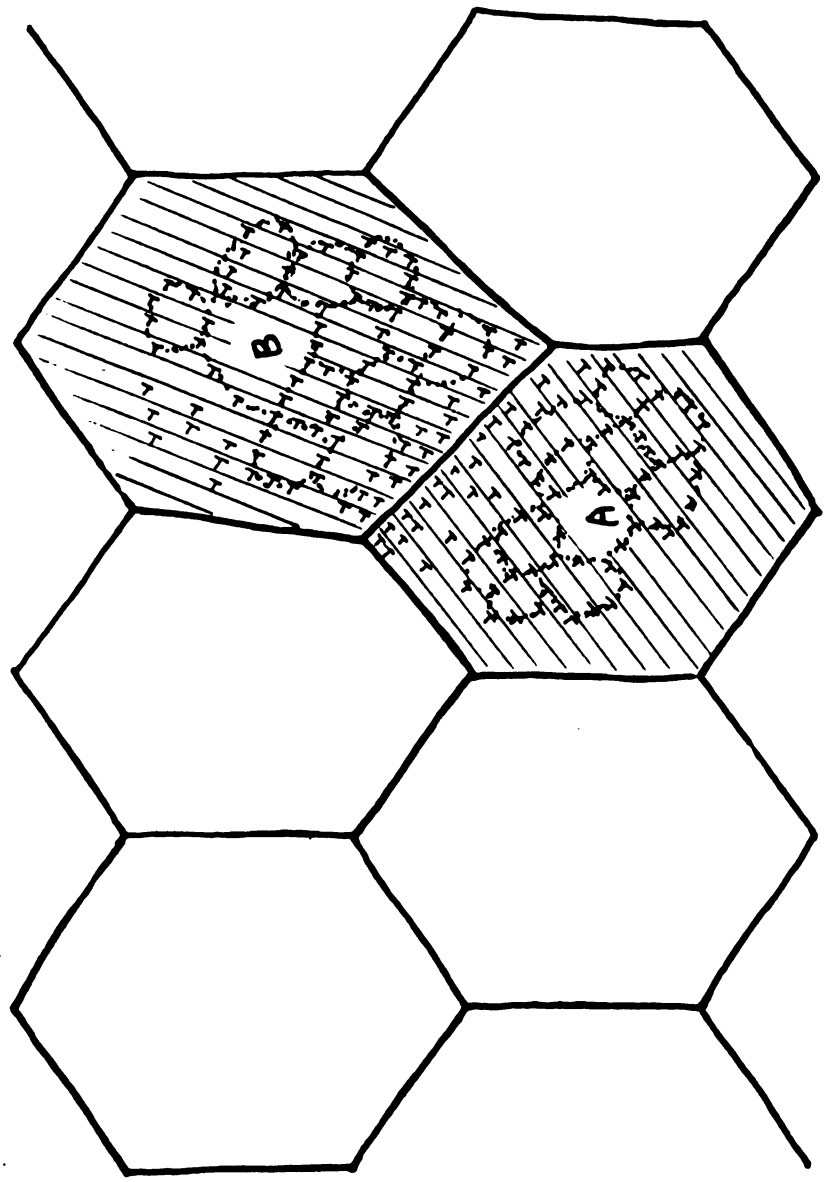

(c)

advance the crack between cavities, but the plastic zone size will be limited to the dimension of the distance between adjacent cavities. The SEM micrograph of the fracture surface, clearly reveals the occurrence of plastic deformation between cavities (Fig. 5-4). The relation of recrystallized grain size to the spacing of major cavities can be seen in Fig. 5-5. A small grain formed between these two large cavities but remains attached to the preexisting grain boundary. In terms of deformation mechanisms, dislocations will be produced and emitted along the glide plane with the highest resolved shear stress (Fig. 5-6). These dislocations provide the driving force for nucleation of a viable recrystallization nucleus which can grow to the size of the plastic zone. It is also worthy to note that the nucleation of grains is not symmetric, i.e., grains do not appear equally on both sides of the boundary. This can be understood from the plastic anisotropy owing to the difference of orientation on both sides of the boundary. One grain will usually have a slip system oriented most favorably, i.e. will experience the largest resolved shear stress and thus, carry the plastic deformation. This grain will be most liable to recrystallization, as indeed was observed.

With regard to structural applications, the main question to be answered is whether and how the occurrence of dynamic recrystallization affects the crack propagation, that is the toughness of the material.

In this regard there are three cases which should be distinguished: (a) Dynamic recrystallization is slow compared to crack growth. Then the newly formed grain will only form behind the crack tip and thus, will have no effect on crack propagation (Fig. 5-7(a)).

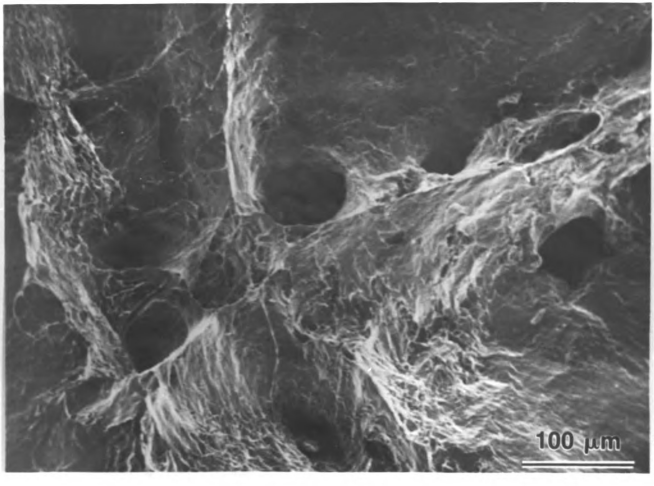

Fig. 5-4. SEM micrograph of the fracture surface of a Ni fatigued at 600°C with 0.5% total strain amplitude.

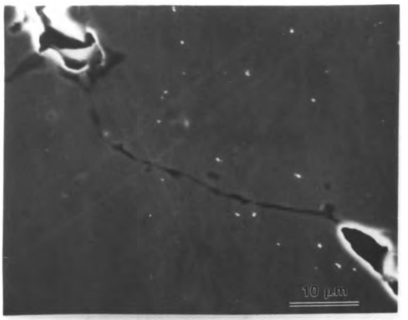

(a)

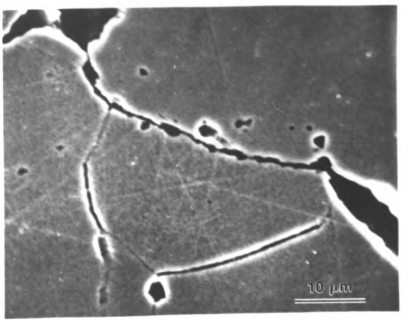

(b)

Fig. 5-5. SEM micrograph of a Ni fatigued at 600°C with 0.5% total strain amplitude. (a) after polishing; (b) after etching.

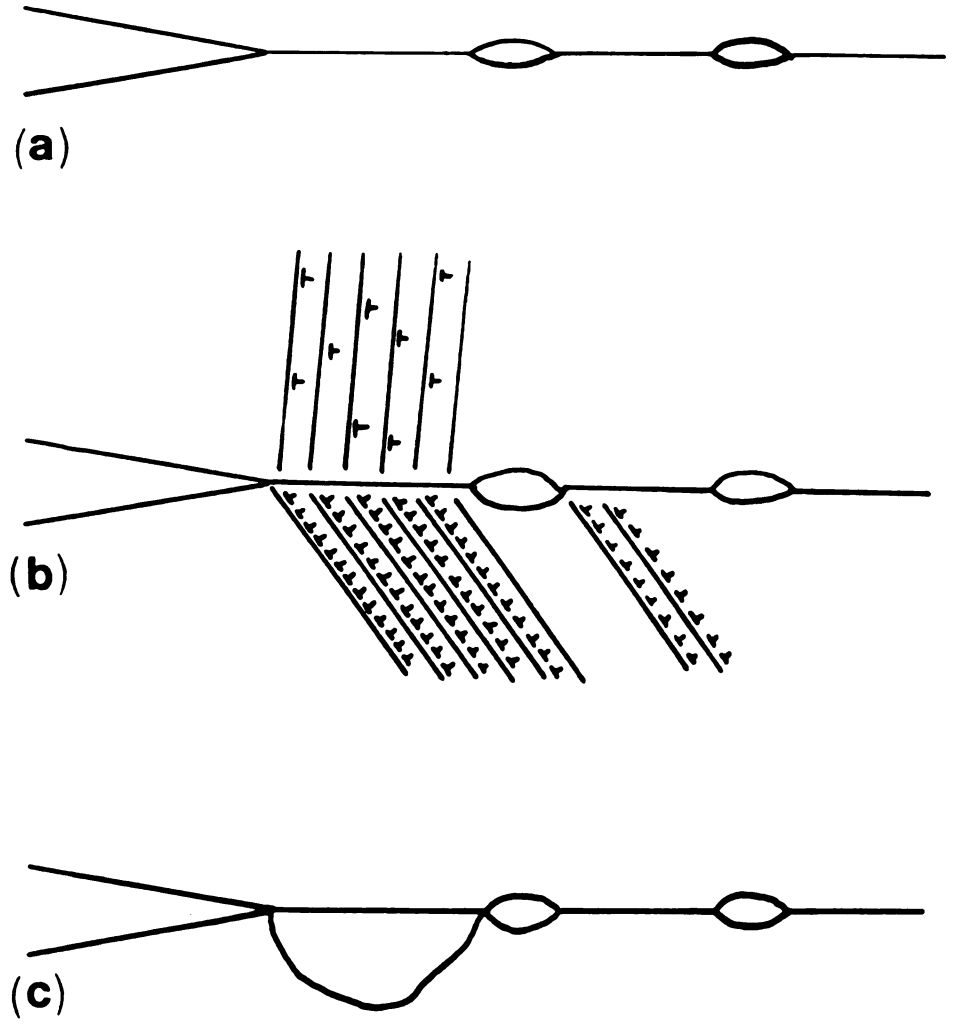

Fig. 5-6. Schematic sketch showing DRX due to plastic deformation associated with the crack propagation.

(b) Dynamic recrystallization is fast compared to crack growth. Then the newly formed grain will form ahead of the crack, although most likely leave unchanged the original boundary orientation (Fig. 5-7(b)), along which the crack advances. However, the new grain changes the orientation relationship across the boundary and therefore, its structure. This may change the grain boundary energy and thus, the crack extension force. No major influence on crack propagation would be expected in this case, because

(1) The grain boundary energy is substantially changed only for very few special orientations.

(2) The new grain boundary will not change the density of cavities already present in the previous boundary. This however constitutes the major effect on grain boundary strength.

(c) Dynamic recrystallization not associated with crack growth but with the imposed cyclic deformation, changes the overall microstructure (Fig. 5-7(c)). This unzips the grain boundaries from their cavities which are left in the new grain interior. This would blunt the crack tip and temporarily impede crack propagation until new cavities are produced in the recrystallized grain boundaries.

For small strain amplitude tests (<1%), it has almost always observed case (a), in some instance it is difficult to discriminate between case (a) and (b). From the discussions about cases (a) and (b), the DRX will not affect the toughness of the materials. However, occasionally imposing high strain amplitude (≃5%) test has shown a large scale or even overall microstructural changes as revealed in Figs. 4-41 and 4-47. The crack tips have been fully blunted as can be seen in

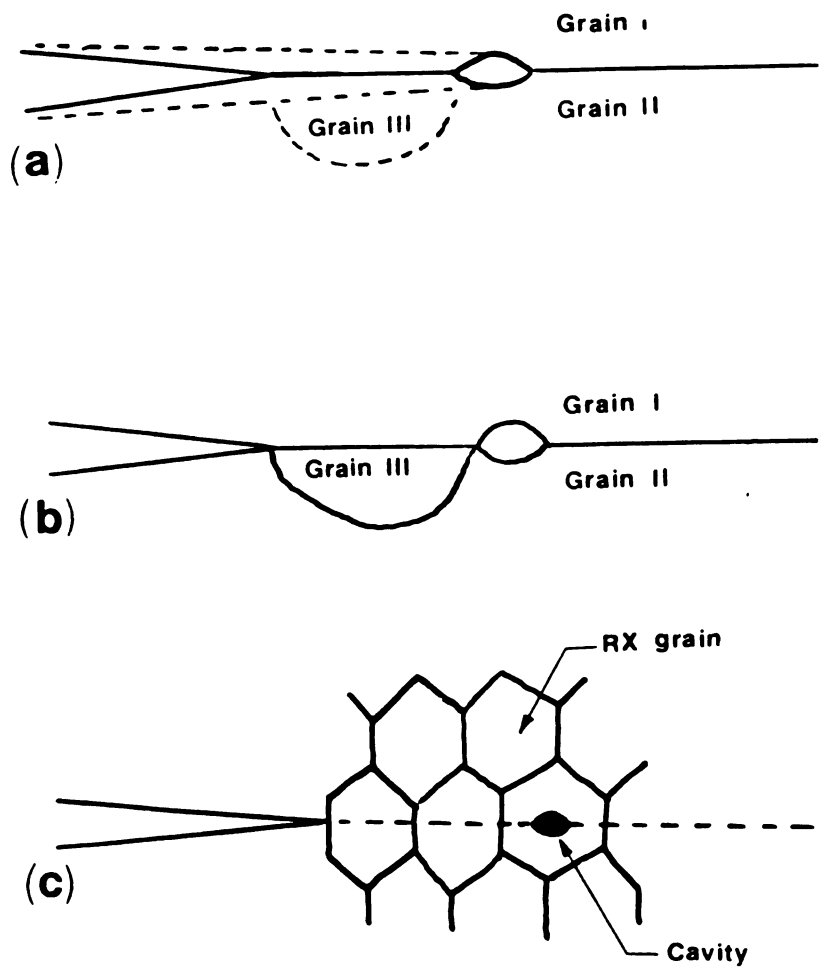

Fig. 5-7. Schematic sketch showing three possible cases related to the effect of DRX on crack propagation.

Figs. 4-42 and 4-43. One may suspect that these newly formed grains are soft, then the stress field ahead of the blunted crack tip is still enough to 'tear' the grains apart and accelerate the crack propagation. From the pure tensile test of a notched specimen, it was found that the crack tips were rounded which would not be if tearing mode occurred.

Direct comparison of fatigue life, however, shows the opposite result. The load - cumulative displacement curves of Test Nos. CRK6081 and CRK6091 were plotted and shown in Fig. 5-8. The test with occasional high compression strain amplitude failed at half of the number of cycles which the specimen without over-straining could withstand. However, when predicting or evaluating the material fatigue life, one should not neglect the statistical characteristics of fatigue and in particular flaws on the surface or within the specimen. For both tests, the final fracture surface is along the prenotched plane which is expected. But the sample fatigued without occasional over-straining whose surface along gauge length revealed numerous cracks as can be seen in Fig. 4-55. This indicates that the notch artificially introduced to this specimen is not as critical to the specimen as the one with occasional over-straining which in return higher fatigue life was obtained. Also, the over-straining was applied in the compression direction did not give rise to an overall DRX instead more damage was accumulated from this compression strain which partially contributed to the early fracture.

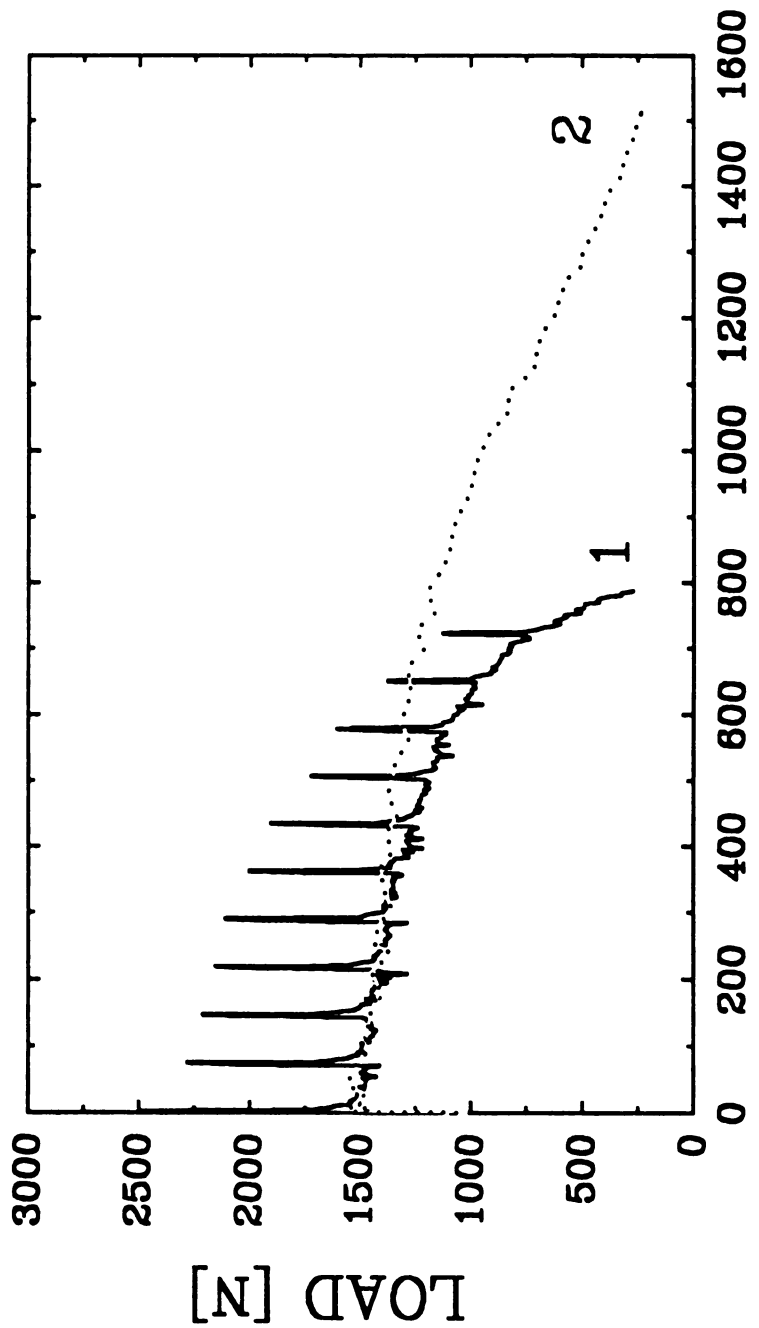

Fig. 5-8. Flow curves of Ni having double edge notches fatigued at 600°C with (curve 1) and without (curve 2) occasional over-straining.

For a quantitative comparison, more knowledge about the crack tip stress and strain field is necessary in order to select optimal test condition.

IV CONCLUSIONS

The present investigations yield the following results:

(1). Under cyclic deformation the flow stress amplitude as function of the cumulative strain shows a maximum after a large number of cycles, and subsequently the stress decreases continuously. The cumulative strain at the maximum increases with decreasing total strain amplitude. These results indicate that a strong softening mechanism that occurs at large cumulative strains.

(2). Most grain boundaries show extensive migration. The migration rate decreases as the number of cycles increases. The grain boundaries move such as to align under 45° with respect to the stress axis. The driving force for grain boundary migration can be explained as the unequal amounts of dislocations produced on opposite sides of boundaries which causes strain induced boundary migration.

(3). Under cyclic deformation, even at a total strain amplitude as small as 0.375%, there is evidence that Ni also undergoes dynamic recrystallization, although very locally and progressing very slowly. Dynamic recrystallization appears to be the major softening mechanism at large cumulative strains during low cycle fatigue of Ni at high temperature. With high strain amplitudes ($\simeq$3-5%), dynamic recrystallization occurs in a large scale and induces the overall microstructural change. The microstructural investigations suggest that the nucleation of dynamic recrystallization during low cycle fatigue can be attributed to grain boundary bulging and recrystallization twinning.

(4). The current results support the hypothesis that the initiation of DRX is controlled by nucleation rather than growth of recrystallized grains.

(5). With progressing cyclic deformation a cell structure develops; the cell boundaries become increasingly condensed and the cell interior become free of dislocations. Dislocation structures near grain boundaries indicate that the migration of grain boundaries destroys the previously established cell structure and that a new cell structure is generated through all development stages involved. Grain boundary motion during cyclic deformation leads to a gradient in dislocation density and arrangement on a path away from the boundary. This gradient seems to provide potential nucleation sites for DRX during HTLCF.

(6). Strain path changes do not lead to sequential destruction and rebuilding of the cell structure. Rather the new cell structure is continuously superimposed to the former structure until a homogeneous structure is attained.

(7). Cu single crystals reveal that only recovery occurred during HTLCF as well as during annealing of specimens fatigued at ambient temperature. No indication of recrystallization was found for strain amplitudes less than 2%, irrespective of the cumulative strain. Therefore DRX during HTLCF is a grain boundary effect and thus, occurs only in polycrystals.

(8). Transgranular crack propagation was found in room temperature fatigue test, but invariably intergranular crack propagation was observed in high temperature low cycle fatigue test.

(9). Dynamic recrystallization was observed to occur along the crack surface during high temperature low cycle fatigue with prenotched specimens. The plastic zone associated with crack propagation at elevated temperature is much smaller than during transgranular crack growth at room temperature.

(10). The recrystallization phenomena associated with crack growth during high temperature low cycle fatigue can be described by cavity formation at the grain boundaries and the development of localized plastic zones between cavities.

(11). Dynamic recrystallization was in no case found detrimental to fatigue resistance. Under occasionally over-straining fatigue tests, DRX was found to occur on a large scale, and crack blunting was observed.

Directions For Future Research:

The current study has demonstrated the occurrence of dynamic recrystallization during high temperature low cycle fatigue with a small strain amplitude. Since dynamic recrystallization occurs locally and slowly, also due to concurrent deformation, it is difficult to identify the dynamically recrystallized grains as well as to prepare specimens containing DRX grains for TEM observations. The nucleation mechanism remains unresolved. It is proposed to run tests using large grain specimens with hour-glass shape in the gauge length for various numbers of cycles such that the microstructural evolution can be observed. The initiation of DRX and nucleation mechanisms shall be understood.

The mechanical testing system available in this laboratory is capable of performing a wide range and precise tests, by changing the strain rate, test temperature and strain amplitude, it is possible to derive a constitutive equation for dynamic recrystallization under high temperature low cycle fatigue.

The diamond structure forms after large number of cyclic deformation. Most grain boundaries align under 45° with respect to the stress axis. It will be interesting to develop a computer code to model this phenomenon by considering a two dimensional hexagonal contiguous grain subjected to a macroscopic strain that is partially accommodated by grain boundary sliding. The grain boundary will migrate under the

driving of unbalanced energy stored on the opposite sides of boundary as shown in Fig. 5-3.

The theoretical understanding about the stress and strain field around crack tips becomes necessary in order to select an optimal condition for the investigation of the interaction between DRX and crack propagation without introducing excessive damage to the specimen which will affect the quantitative evaluation of the fatigue life.

The high temperature grips design is an important issue in the current testing system. It is also an intriguing topic to pursue. The problem due to bonding between tungsten pins and TZM pull rod may be possible to solve by coating with ceramics onto pins as a diffusion barrier. The nature and magnitude of the stress experienced by the pins should be evaluated in order to simulate the test condition.

VII REFERENCES

[1] H.J. McQueen and J.J. Jonas, in "Recovery and Recrystallization during High Temperature Deformation" in Treatise on Materials Science and Technology, **6**, 393 (1975).

[2] G. Gottstein, Met. Sci. **17**, 497 1983.

[3] P. Karduck, G. Gottstein and H. Mecking, Acta Metall. **31**, 1525 (1983).

[4] R. Bromley and C.M. Sellars, in "The Microstructure and Design of Alloys (ICSMA 3)", **2**, Institute of Metals, London, 380 (1973).

[5] B.J. Sunter and N.M. Burman, J. Australian Inst. Metals **17**, 91 (1972).

[6] P.J.I. Stuitjie and G. Gottstein, Z. Metallk. **71**, 279 (1980).

[7] G. Gottstein and U.F. Kocks, Acta Metall. **31**, 175 (1983).

[8] M.J. Luton and C.M. Sellars, Acta Metall. **17**, 1033 (1969).

[9] A.A. Guimaraes and J.J. Jonas, Metall. Trans. **12A**, 1655 (1981).

[10] D.R. Barraclough and C.M. Sellars, Met. Sci. **13**, 257 (1979).

[11] L.C. Lim and R. Raj, Acta Metall. **33**, 2205 (1985).

[12] V. Raman and T.C. Reiley, Scripta Metall. **20**, 1343 (1986).

[13] R.E. Cook, G. Gottstein and U.F. Kocks, J. Mat. Sci. **18**, 2650 (1983).

[14] S.P. Bhat and C. Laird, Int. J. Fatigue Engng. Mater. Struct., **1**, 59 (1979).

[15] S.P. Bhat and C. Laird, Int. J. Fatigue Engng. Mater. Struct., **1**, 79 (1979).

[16] H. Nahm, J. Moteff and D.R. Dierks, Acta Metall. **25**, 107 (1977).

[17] A.M. Ermi and J. Moteff, Metall. Trans. **13A**, 1577 (1982).

[18] A.M. Ermi and J. Moteff, J. Eng. Mat. Tech. **105**, 21 (1983).

[19] K.U. Snowden, Phil. Mag., **6**, 321 (1961)

[20] T.G. Langdon and R.C. Gifkins, Acta Metall. **31**, 927 (1983).

[21] T.G. Langdon, D. Simpson and R.C. Gifkins, Acta Metall. **31**, 939 (1983).

[22] P. Yavari and T.G. Langdon, Acta Metall. **31**, 1595 (1983).

[23] P. Yavari and T.G. Langdon, Acta Metall. **31**, 1605 (1983).

[24] E. Furubayashi and M. Nakamura, Proc. ICOTOM 6, Iron Steel Inst. Japan, Tokyo, 619 (1981).

[25] T. Ito, T. Taketani and Y. Nakayama, Scripta, Metall. **20**, 1329 (1986).

[26] J.R. Rice and R. Thomson, Phil. Mag. **29**, 73 (1974).

[27] V. Raman and T.G. Langdon, J. Mat. Sci. Lett. **2**, 180 (1983).

[28] H.S. Betrabet and V. Raman, Metall. Trans. **19A**, 1437 (1988).

[29] V. Raman and T.C. Reiley, Scripta Metall. **20**, 1343 (1986).

[30] V. Raman and T.G. Langdon, Acta Metall. **37**, 725 (1989).

[31] H. Abdel-Raouf, A. Plumtree and T.H. Topper, Metall. Trans., **5**, 267 (1974).

[32] H. Mecking and G. Gottstein, in "Recrystallization of Metallic Materials" (edited by F. Haessner), 2nd edn., pp. 195-222, Dr. Riederer Verlag, Stuttgart, 1978.

[33] G. Gottstein, D. Zabardjadi and H. Mecking, Metal Sci. **13**, 223 (1979)

[34] T. Hasegawa and U.F. Kocks, Acta Metall. **27**, 1705 (1979).

[35] I.L. Dillamore, P.K. Morris, C.J.E. Smith and W.B. Hutchinson, Proc. R. Soc. Lon. **A329**, 405 (1972).

[36] C. Rossard, Metaux **35**, pp. 102-115, 140-153, 190-205, (1960).

[37] T. Sakai and J.J. Jonas, Acta Metall. **32**, 189 (1984).

[38] J. Takada, N. Nishino and S. Kikuchi, J. Mat. Sci. **21**, 3420 (1986).

[39] G. Gottstein, Proc. 5-th Conf. Textures of Materials, **1**, Springer, Berlin, 73 (1978).

[40] W. Roberts and B. Ahlblom, Acta Metall. **26**, 801 (1978).

[41] L.F. Coffin Jr., J. Mat. Sci. **6**, 388 (1971).

[42] L.F. Coffin Jr., S.S. Manson, A.E. Carden, L.K. Serverud and W.L. Greenstreet in "The Dependent Fatigue of Structural Alloys, A General Assessment", 1975, ORNL-5073, Published Jan. 1977.

[43] S.S. Manson in "Fatigue at Elevated Temperature", ASTM STP 520, 744 (1973).

[44] D.R. Dierks in "Advances in Design for Elevated Temperature Environment", ASME, 29 (1975).

[45] H. Mughrabi in "Strength of Metals and Alloys", eds. P. Haasen, V. Gerold and G. Kostorz, Pergamon Press, 1615 (1980).

[46] L.M. Brown, Met. Sci. **11**, 315 (1977).

[47] S.J. Basinski, Z.S. Basinski and A.W. Howe, Phil. Mag. **19**, 899 (1969).

[48] V. Raman and T.C. Reiley, Metall. Trans. **19A**, 1533 (1988).

[49] T. Saegusa and J. R. Weertman, Scripta Metall. **12**, 187 (1978).

[50] V. Raman and T.G. Langdon, Acta. Metall. **37**, 725 (1989).

[51] D. Broek, "Elementary Engineering Fracture Mechanics", Noordhoff, Leyden, 1974.

[52] Y. Birol, J. Mat. Sci. Lett. **6**, 46 (1987)

[53] Y. Birol, Metallography **21**, 77 (1988).

[54] Y. Birol, J. Mat. Sci. **23**, 2079 (1988).

[55] Y. Birol, Scripta Metall. **22**, 405 (1988).

[56] G.E. Dieter "Mechanical Metallurgy", 2nd edn., McGraw-Hill Inc., 396 (1976).

[57] C. Laird, 'Cyclic Deformation of Metals and Alloys' in Treatise on Materials Science and Technology, **6**, Academic Press, 101, (1975).

[58] H. Mughrabi, Mater. Sci. & Engng. **33**, 207 (1978).

[59] C. Messager and O. Dimitrov, Cpt. Rd. Acad. Sc., **251**, 88 (1960).

[60] K. Lucke and H. P. Stuwe, Acta Metall. **9**, 1087 (1971).

[61] J. E. Pratt, Acta Metall. **15**, 319 (1967).

[62] G. I. Taylor, J. Inst. Met. **62**, (i) 307 (1938).

APPENDIX A :

PROGRAM SOURCE CODES

```
MTS.BAS                                                          1

COMMON user.name$, SPEC.NAME$, TEST.NAME$, CRYSTAL.TYPE, LAMBDA, KAPPA,
SLIP.MODE
COMMON STRAIN.RATE, GAUGE.LEN, CROSS.SEC, VOLUME, test.type, GRIP.SPEED,
TEST.TEMP, sum.no
COMMON SAMPLE.RATE.MM, FS.STROKE, FS.LOAD, FS.STRAIN, PAR.FILE$,
DATA.FILE$, CYCLE.FILE$
   DIM test.type$(5), CRYSTAL.TYPE$(2), SLIP.MODE$(3)
*************************************************************************
*                                                                       *
*                          - MTS -                                      *
*                                                                       *
*                         VERSION 1.0                                   *
*                         01-JAN-1988                                   *
*                    AUTHOR:  SHUHRONG CHEN                             *
*                                                                       *
*  This program handles the menu selection and test parameters input    *
*  used in the chaining programs for the 458.91 MicroProfiler           *
*                                                                       *
*                     Chaining programs :                               *
*                                                                       *
*   TENSION.EXE  - Performs the tensile test and data storage           *
*   COMPRESS.EXE - Performs the compression test and data storage       *
*   STRAINCF.EXE - Performs the low cycle fatigue test by strain        *
*                  amplitude control and stores data                    *
*   STRESSCF.EXE - Performs the low cycle fatigue test by stress        *
*                  amplitude control and stores data                    *
*   MTSEZ.EXE    - Performs the test which is defined by user and       *
*                  collects data for further process                    *
*                                                                       *
*                     Shelling programs :                               *
*                                                                       *
*   PRINTMTS.EXE - Prints out the test data  } AUTHOR : G. GOTTSTEIN    *
*   PLOTMTS.EXE  - Plots the test result     }                           *
*                                                                       *
*                                                                       *
*************************************************************************

 IF PAR.FILE$ <> "" THEN 530
 SCREEN 0, 1: KEY OFF: COLOR 1, 1: CLS : CLEAR
 CHDIR "\MTS": SHELL "DEL *.T": SHELL "DEL *.S"
          SHELL "DEL *.CYC": COLOR 15, 1: CLS
 SHELL "type memo"
90 a$ = INKEY$: IF a$ = "" THEN 90
'
 VERSION$ = "1.0"
'
 DASH$ = STRING$(79, 45)
 GOSUB 705: GOSUB 800
 PRINT "--------------- MAIN SPECIFICATION INPUT ---------------":
PRINT
 GOSUB 1000
'       general specification
 PRINT " USER PASSWORD .......?": LOCATE 3, 24: COLOR 1, 1: INPUT
password$: COLOR 15, 1
    IF (password$ = "csr") OR (password$ = "CSR") THEN
        user.name$ = "CHEN"
```

```
       ELSEIF (password$ = "a161") OR (password$ = "A161") THEN
        user.name$ = "YUNG"
       ELSEIF (password$ = "boss") OR (password$ = "BOSS") THEN
        user.name$ = "GG"
       ELSEIF password$ = "0202" THEN
        user.name$ = "LEE"
       ELSE CLS : LOCATE 10, 10: PRINT " Unauthorized user, please see
Shuhrong Chen for instructions": GOTO 600
    END IF
100 LOCATE 4, 1: INPUT " SPECIMEN NAME ......."; SPEC.NAME$
110 INPUT " TEST NAME ..........."; TEST.NAME$
    IF TEST.NAME$ = "" THEN PRINT : GOTO 110
'       test specification
120 LOCATE 8, 1: PRINT " INDICATE TYPE OF TEST :"
 PRINT
 PRINT " TENSION ................. 1 "
 PRINT " COMPRESSION ............. 2 "
 PRINT " STRESS CYCLE ............ 3 "
 PRINT " STRAIN CYCLE ............ 4 "
 PRINT " USER DEFINES ............ 5 "
 INPUT " TEST TYPE ...... "; test.type
IF test.type <= 0 OR test.type > 5 THEN 120
IF test.type = 1 THEN PRINT : PRINT " Please refer to the compression
test program to update this program ": END
IF test.type = 3 THEN PRINT : PRINT " Please refer to the strain cyclic
test program to update this program ": END
IF test.type = 5 THEN 520
    GOSUB 800
 PRINT : REM       specimen specification
130 PRINT " TYPE OF CRYSTAL : ": PRINT
 PRINT " POLYCRYSTAL ............. 1 "
 PRINT " SINGLE CRYSTAL .......... 2 "
 INPUT " CRYSTAL TYPE ...... "; CRYSTAL.TYPE
 IF CRYSTAL.TYPE = 1 THEN 140
 IF CRYSTAL.TYPE <> 2 THEN 130
PRINT
 PRINT " CRYSTAL ORIENTATION : "
 PRINT
 INPUT " LAMBDA = "; LAMBDA
 INPUT " KAPPA  = "; KAPPA
 PRINT
 PRINT " MODE OF SLIP "
 PRINT
PRINT " SINGLE SLIP ............. 1 "
PRINT " DOUBLE SLIP ............. 2 "
PRINT " MULTIPLE SLIP ........... 3 "
INPUT " SLIP MODE ...... "; SLIP.MODE
140 PRINT : PRINT
 INPUT " GAUGE LENGTH ............ [mm] "; GAUGE.LEN
 INPUT " GAUGE DIAMETER .......... [mm] "; GAUGE.DIAM
 IF GAUGE.LEN = 0 OR GAUGE.DIAM = 0 THEN 140
 PI = 4 * ATN(1): CROSS.SEC = PI * ((GAUGE.DIAM / 2) ^ 2)
 VOLUME = GAUGE.LEN * CROSS.SEC
 PRINT : PRINT : IF test.type = 3 THEN 160
150 INPUT " INITIAL STRAIN RATE ...(ex. 2E-4) [1/sec] "; STRAIN.RATE
 IF STRAIN.RATE = 0 THEN 150
```

```
    sum.no = INT(-4 * LOG(STRAIN.RATE))
 GRIP.SPEED = GAUGE.LEN * STRAIN.RATE
 IF test.type > 2 THEN PRINT : GOTO 160
 INPUT " SAMPLING RATE ..................... [um/set] "; SAMPLE.RATE
 IF SAMPLE.RATE = 0 THEN SAMPLE.RATE = 10
 SAMPLE.RATE.MM = SAMPLE.RATE / 1000: PRINT
160 INPUT " FULL SCALE STROKE ..... [mm]  "; FS.STROKE
    INPUT " FULL SCALE LOAD ..... [kN]  "; FS.LOAD
 INPUT " FULL SCALE STRAIN ..... [%]   "; FS.STRAIN: FS.STRAIN =
FS.STRAIN * .25
 INPUT " TEST TEMPERATURE ..... [C]   "; TEST.TEMP
 IF FS.LOAD = 0 OR FS.STRAIN = 0 THEN PRINT : GOTO 160
'         print out of input data
 PRINT
 GOSUB 800
 PRINT " CHECK YOUR INPUT DATA : "
 PRINT
 PRINT " USER LAST NAME .....  "; user.name$
 PRINT " SPECIMEN NAME .....  "; SPEC.NAME$
 PRINT " TEST NAME .....  "; TEST.NAME$
 PRINT " DATE .....  "; DATE$
 PRINT
 PRINT " TEST TYPE .....  "; test.type$(test.type)
 PRINT " CRYSTAL TYPE .....  ";
CRYSTAL.TYPE$(CRYSTAL.TYPE)
 IF CRYSTAL.TYPE = 1 THEN 500
 PRINT " LAMBDA ..... "; LAMBDA; " [Degrees]"
 PRINT " KAPPA ..... "; KAPPA; " [Degrees]"
 PRINT " SLIP MODE .....  "; SLIP.MODE$(SLIP.MODE)
500 PRINT
 PRINT " GAUGE LENGTH ..... "; GAUGE.LEN; " [mm]"
 PRINT " GAUGE DIAMETER ..... "; GAUGE.DIAM; " [mm]"
 PRINT " CROSS SECTION ..... "; CROSS.SEC; " [mm^2]"
 PRINT
 IF test.type = 3 THEN PRINT : GOTO 510
 PRINT " INITIAL STRAIN RATE ..... "; STRAIN.RATE; " [1/sec]"
 PRINT " CROSS HEAD SPEED ..... "; GRIP.SPEED * 60; "
[mm/min]"
 IF test.type > 2 THEN 510
 PRINT " SAMPLING RATE ..... "; SAMPLE.RATE; "
[um/set]"
510 PRINT " FULL SCALE STROKE ..... "; FS.STROKE; " [mm]"
     PRINT " FULL SCALE LOAD ..... "; FS.LOAD; " [kN]"
     PRINT " FULL SCALE STRAIN ..... "; FS.STRAIN; " [mm]"
     PRINT " TEST TEMPERATURE ..... "; TEST.TEMP; " [C]"
 PRINT
 INPUT " INPUT DATA OK ----------(Y/N) "; ANS$
 IF ANS$ <> "Y" AND ANS$ <> "y" THEN GOSUB 800: GOTO 100
 LPRINT TAB(11); CHR$(14); "M T S ": GOSUB 1100
 LPRINT "                    *** MAIN DATA INPUT ***       "
 LPRINT TAB(11); "-----------------------------------------------
---"
 LPRINT
 GOSUB 900
```

```
520 IF test.type = 1 THEN chn$ = "TENSION" ELSE IF test.type = 2 THEN
chn$ = "COMPRESS" ELSE IF test.type = 3 THEN chn$ = "STRESSCF" ELSE IF
test.type = 4 THEN chn$
     COLOR 1, 1: CLS
     temp$ = "TEMP"
     OPEN "o", #1, temp$
     PRINT #1, " ** user ID        :  "; user.name$
     PRINT #1, "    test start at  :  "; DATE$; "  "; TIME$
     CLOSE #1
     SHELL "attrib -r monitor.mts"
     SHELL "copy monitor.mts + temp monitor.mts"
     SHELL "attrib +r monitor.mts"
     KILL temp$: COLOR 15, 1: CLS
   IF user.name$ = "CHEN" AND test.type = 4 THEN 523 ELSE 525
523  LOCATE 10, 12: PRINT "1. STRAINCF ": PRINT TAB(12); "2. SCHEN    "
     PRINT : INPUT "            Your choice ... "; ttype
     IF ttype = 2 THEN chn$ = "SCHEN"
525   CHAIN chn$
530 CHDIR user.name$
     SHELL "COPY C:\MTS\*.T": IF test.type = 5 THEN 540
     SHELL "COPY C:\MTS\*.S": IF test.type < 3 THEN 540
     SHELL "COPY C:\MTS\*.CYC"
540 CLS : CHDIR ".."
     COLOR 1, 1: CLS
     temp$ = "TEMP"
     OPEN "o", #1, temp$
     PRINT #1, "    test finish at :  "; DATE$; "  "; TIME$
     PRINT #1, "                      "
     CLOSE #1
     SHELL "attrib -r monitor.mts"
     SHELL "copy monitor.mts + temp monitor.mts"
     SHELL "attrib +r monitor.mts"
     KILL temp$: COLOR 15, 1: CLS
    IF test.type = 5 THEN 570
     GOSUB 1100: LPRINT CHR$(12)
   LOCATE 8, 10: INPUT " Do you want to print the data .....(Y/N) "; C$
 IF C$ <> "Y" AND C$ <> "y" THEN 560
 SHELL "PRINTMTS"
 LOCATE 24, 15: PRINT "Wait until the printer finished printing"
 PRINT TAB(15); "Press any key to continue .... "
550 a$ = INKEY$: IF a$ = "" THEN 550
 CLS
560 LOCATE 14, 10: INPUT " Do you want to plot the result .... (Y/N) ";
D$
   IF D$ <> "Y" AND D$ <> "y" THEN 570
 SHELL "PLOTMTS"
570 CLS : LOCATE 9, 20: PRINT " *** Test Complete ***": PRINT : PRINT
   LOCATE 14, 14: PRINT " Run another test ?   Just type MTS ": PRINT :
PRINT
600 END
'     check condition of Micro's REMOTE and RUN ENABLE
700      OPEN "COM1:9600,e,7,,cs,ds,pe" FOR RANDOM AS #1
       PRINT #1, "M"
       GOSUB 1200: INPUT #1, status
       CLOSE #1
  IF status <> -1 THEN 720
```

```
705    CLS
   TTLE$ = " Check Machine Status "
   LOCATE 1, INT(40 - LEN(TTLE$) / 2)
     PRINT TTLE$;
     PRINT DASH$;
 LOCATE 5, 10
 PRINT " VERIFY THAT : "
 LOCATE 7, 15
 PRINT " MicroProfiler is in REMOTE and RUN ENABLE conditions "
 LOCATE 9, 15
 PRINT " The Error, Upper and Lower Limit are in ENABLE condition "
 LOCATE 23, 1: PRINT DASH$
 LOCATE 24, 1
 PRINT "                                          < Page Down > =
continue";
710 a$ = INKEY$: IF a$ = "" THEN 710
 IF LEN(a$) < 2 THEN 710
 ANS = ASC(RIGHT$(a$, 1))
 IF ANS <> 81 THEN 710
 GOTO 700
720  RETURN
800 CLS : LOCATE 25, 15
 PRINT " P R O G R A M     M T S                  version  "; VERSION$
 LOCATE 1, 1
 RETURN
900 LPRINT TAB(11); " TEST NAME ........................  "; CHR$(14);
TEST.NAME$
 LPRINT TAB(11); " SPECIMEN NAME ......................  "; SPEC.NAME$
 LPRINT
 LPRINT TAB(11); " TEST TYPE ..........................  ";
test.type$(test.type)
 LPRINT TAB(11); " CRYSTAL TYPE .......................  ";
CRYSTAL.TYPE$(CRYSTAL.TYPE)
 IF CRYSTAL.TYPE = 1 THEN 910
 LPRINT TAB(11); " LAMBDA ............................. "; LAMBDA; "
[Degrees]"
 LPRINT TAB(11); " KAPPA .............................. "; KAPPA; "
[Degrees]"
 LPRINT TAB(11); " SLIP MODE ..........................  ";
SLIP.MODE$(SLIP.MODE)
910 LPRINT
 LPRINT TAB(11); " GAUGE LENGTH ....................... "; GAUGE.LEN; "
[mm]"
 LPRINT TAB(11); " GAUGE DIAMETER ..................... "; GAUGE.DIAM; "
[mm]"
 LPRINT TAB(11); " CROSS SECTION ...................... "; CROSS.SEC; "
[mm^2]"
 LPRINT
 IF test.type = 3 THEN LPRINT : GOTO 930
 LPRINT
 LPRINT TAB(11); " INITIAL STRAIN RATE ................ "; STRAIN.RATE;
" [1/sec]"
 LPRINT TAB(11); " CROSS HEAD SPEED ................... "; GRIP.SPEED *
60; " [mm/min]"
 IF test.type > 2 THEN 920
```

```
 LPRINT TAB(11); " SAMPLING RATE ..... "; SAMPLE.RATE;
" [um/set]"
 LPRINT
920 LPRINT TAB(11); " FULL SCALE STROKE ..... "; FS.STROKE;
" [mm]"
930 LPRINT TAB(11); " FULL SCALE LOAD ..... "; FS.LOAD; "
[kN]"
     LPRINT TAB(11); " FULL SCALE STRAIN ..... ";
FS.STRAIN; " [mm]"
 LPRINT
 LPRINT TAB(11); " TEST TEMPERATURE ..... "; TEST.TEMP; "
[C]"
 RETURN
1000 test.type$(1) = "TENSION"
 test.type$(2) = "COMPRESSION"
 test.type$(3) = "STRESS CYCLING"
 test.type$(4) = "STRAIN CYCLING"
 CRYSTAL.TYPE$(1) = "POLYCRYSTAL"
 CRYSTAL.TYPE$(2) = "SINGLE CRYSTAL"
 SLIP.MODE$(1) = "SINGLE SLIP"
 SLIP.MODE$(2) = "DOUBLE SLIP"
 SLIP.MODE$(3) = "MULTIPLE SLIP"
 RETURN
1100 LPRINT : LPRINT
     LPRINT "          "; CHR$(14); DATE$; "          "; CHR$(14); TIME$
     LPRINT
   RETURN
1200 t1 = TIMER
1210 t2 = TIMER
     IF ABS(t2 - t1) < .1 THEN 1210
     RETURN
```

```
STRAINCF.BAS                                                    1

COMMON USER.NAME$, SPEC.NAME$, TEST.NAME$, CRYSTAL.TYPE, LAMBDA, KAPPA,
SLIP.MODE
COMMON STRAIN.RATE, gauge.len, CROSS.SEC, VOLUME, TEST.TYPE, grip.speed,
TEST.TEMP, sum.no
COMMON SAMPLE.RATE.MM, fs.stroke, fs.load, fs.strain, PAR.FILE$,
DATA.FILE$, CYCLE.FILE$
' $INCLUDE: 'pcldefs.bi'
'                              --- STRAINCF ---
'                                VERSION  2.0
'                                 27-MAR-1989
' ********************************************************************
 DIM analog.val%(10): DIM AX$(20): DIM stop.mode$(3): DIM
digit.val%(200)
 DIM digit(5): DIM a#(2, 3): DIM f(100, 2)
100 CLS : LOCATE 3, 10
    PRINT " Indicate the type of test "
    PRINT : PRINT TAB(10); " 1. Symmetry +/-  strain amplitude test "
    PRINT TAB(10); " 2. Asymmetry +/-  strain amplitude test "
    LOCATE 8, 11: INPUT " => Your choice is ..... "; amp.type
    IF amp.type <> 1 THEN IF amp.type <> 2 THEN 100
    LOCATE 10, 10: INPUT " Are you using the extensometer ? (Y/N) ";
etsm$
    IF etsm$ = "y" OR etsm$ = "Y" THEN etsm = 1 ELSE etsm = 2
    IF amp.type = 1 THEN 200 ELSE LOCATE 12, 10: GOTO 300
200 LOCATE 12, 10: INPUT " The strain amplitude is ... [%] "; strain.amp
    frequency = grip.speed * 100 / (4 * strain.amp * gauge.len)
    LPRINT TAB(11); " STRAIN AMPLITUDE ..................... ";
strain.amp; " [%]  OR "; strain.amp * gauge.len * 10; "um": GOTO 400
300 INPUT " The positive strain amplitude ...... [%] "; pos.strain
 LOCATE 13, 10: INPUT " The negative strain amplitude ...... [%] ";
neg.strain
    neg.strain = ABS(neg.strain)
    frequency = grip.speed * 100 / (2 * (pos.strain + neg.strain) *
gauge.len)
 LPRINT TAB(11); " POSITIVE STRAIN AMPLITUDE .......... "; pos.strain; "
[%]  OR "; pos.strain * gauge.len * 10; "um"
 LPRINT TAB(11); " NEGATIVE STRAIN AMPLITUDE .......... "; neg.strain; "
[%]  OR "; neg.strain * gauge.len * 10; "um"
400 LPRINT TAB(11); " CYCLE FREQUENCY ..................... "; frequency;
" [1/sec]"
    IF etsm = 1 THEN LPRINT TAB(11); " USING THE EXTENSOMETER
.............  YES"
    LPRINT
 period = (1.03 + pos.strain / (2 * (pos.strain + neg.strain))) /
frequency
410    LOCATE 15, 10: INPUT " Cycle plot interval ....................
"; plot.int
    LOCATE 17, 10: INPUT " Cycle store interval ................... ";
store.int
    LPRINT TAB(11); " CYCLE STORAGE INTERVAL ............. "; store.int
    LOCATE 19, 10: PRINT " Cylce print interval ( must be different"
    LOCATE 20, 10: INPUT "  from plot interval ) ................. ";
print.int
    LPRINT TAB(11); " CYCLE PRINT INTERVAL ............... "; print.int
    IF plot.int = 0 OR store.int = 0 THEN 410
    IF print.int = 0 THEN 410
```

```
  CLS
    LOCATE 7, 8: PRINT " Indicate the test terminated condition : "
    LOCATE 9, 8: PRINT " 1. After tested certain number of cycles "
    LOCATE 10, 8: PRINT " 2. After fully fractured "
    LOCATE 11, 8: PRINT " 3. After stress decreased to certain amount "
    LOCATE 13, 8: INPUT " =>  Your selection is ..... "; stop.mode
    LOCATE 15, 8
    IF stop.mode = 1 THEN INPUT " test terminated cycle .....";
end.cyc: ec$ = STR$(end.cyc)
    IF stop.mode = 3 THEN INPUT " percent of stress decreased .... [%]
"; stress.de: sd$ = STR$(stress.de) + "%"
  stop.mode$(1) = "AT CYCLE # " + ec$: stop.mode$(2) = "FULLY FRACTURE":
stop.mode$(3) = "AFTER STRESS DECREASED " + sd$
  LPRINT TAB(11); " STOP MODE .....  ";
stop.mode$(stop.mode)
   LOCATE 18, 8: PRINT " Input the scales for real-time plot "
   LOCATE 20, 8: INPUT " Maximum scale of X axis (true strain) ... [ % ]
"; xmax
   LOCATE 21, 8: INPUT " Maximum scale of Y axis (true stress) ... [MPa]
"; ymax
 LPRINT
 LPRINT "          ------------------------------------------------------
----"
 LPRINT CHR$(27); "H"
 LPRINT CHR$(27); "G"; "  CYCLE           SIG[MPa]            LOAD[N]
  EPSON[%]  PLASTIC STRAIN[%]"
 LPRINT "          <MAXIMUM>   <MINIMUM> "
 LPRINT : LPRINT CHR$(27); "H"
  CLS : IF etsm = 1 THEN fs.scale = fs.strain ELSE fs.scale = fs.stroke
    IF amp.type = 2 THEN 500
    command.high = strain.amp * gauge.len / fs.scale
    command.low = -command.high: GOTO 600
500 command.high = pos.strain * gauge.len / fs.scale
    command.low = -neg.strain * gauge.len / fs.scale
600 DEF fnfs (X, Y) = (X * 2 / 4096 - 1) * Y
    ERROR.WORD% = 0
     error.code% = INITIALIZE%
     error.code% = SET.ERROR.CONTROL.WORD%(ERROR.WORD%)
'               DI/O variables
PORT.OUT% = 1: PORT.IN% = 0: MASK.OUT% = 255: MASK.HIGH% = 2: PORT1% = 0
  PORT0% = 0: PORT1.RUN% = 2: PORT1.STOP% = 1: PORT1.OFF% = 0
'               A/D variables
TIMING.SOURCE% = 0:   START.CHAN% = 0:    end.chan% = etsm:    GAIN% = 1
'               Initialize Real Time Variables
test.load = 0: strain = 0: SEGMENT.NO = 2: cycle.no = 1: i = 0
: DATA.NO = 0
 area = 0: MAX.LOAD = -fs.load * 1000: MAX.STRAIN = -fs.scale
 MIN.LOAD = fs.load * 1000: MIN.STRAIN = fs.scale
'               Set up digital I/O
   error.code% = ENABLE.FOR.OUTPUT%(PORT.OUT%)
   error.code% = OUTPUT.DIGITAL.VALUE%(PORT.OUT%, MASK.OUT%, PORT1%)
   error.code% = ENABLE.FOR.INPUT%(PORT.IN%)
   error.code% = GET.ERROR.CODE%(error.code%)
 IF error.code% <> 0 THEN PRINT "DI/O Setup error "; error.code%: GOTO
3600
    DATA.FILE$ = TEST.NAME$ + ".T"
```

```
    CYCLE.FILE$ = TEST.NAME$ + ".CYC"
 OPEN "O", #1, DATA.FILE$
 OPEN "O", #2, CYCLE.FILE$
 OPEN "COM1:9600,E,7,,CS,DS,PE" FOR RANDOM AS #3
'
'          Set up the MicroProfiler
        PRINT #3, "10R"
        GOSUB 4000: INPUT #3, echo
        PRINT #3, "100S"
        GOSUB 4000: INPUT #3, echo
        PRINT #3, "1T"
        GOSUB 4000: INPUT #3, echo
        PRINT #3, "I"
        GOSUB 4000: INPUT #3, echo
     RATE = STRAIN.RATE * gauge.len / fs.scale * 100
        PRINT #3, RATE; "G"
        GOSUB 4000: INPUT #3, echo
        PRINT #3, command.high; "H"
        GOSUB 4000: INPUT #3, echo
        PRINT #3, "Q"
        GOSUB 4000: INPUT #3, echo
        PRINT #3, command.low; "H"
        GOSUB 4000: INPUT #3, echo
        PRINT #3, RATE; "G"
        GOSUB 4000: INPUT #3, echo
        PRINT #3, command.high; "H"
        GOSUB 4000: INPUT #3, echo
        PRINT #3, "Q"
        GOSUB 4000: INPUT #3, echo
        PRINT #3, command.low; "H"
        GOSUB 4000: INPUT #3, echo
'               Set up clock and A/D
   TICKS.AD% = 500
   error.code% = SET.CLOCK.DIVIDER%(TICKS.AD%)
   error.code% = GET.ERROR.CODE%(error.code%)
 IF error.code% <> 0 THEN PRINT " Clock setup error "; error.code%: GOTO
3600
   error.code% = SETUP.ADC%(TIMING.SOURCE%, START.CHAN%, end.chan%,
GAIN%)
   error.code% = GET.ERROR.CODE%(error.code%)
   IF error.code% <> 0 THEN PRINT "A/D Setup error "; error.code%: GOTO
3600
      number.of.val% = 200: number.data% = 15: last.val% = (1 + etsm) *
(sum.no + 3)
'               Prompt user for start
 CLS
     LOCATE 6, 19: PRINT " Strain Fatigue Test Execution "
 LOCATE 9, 12: PRINT "------------- Execution Control ----------------
"
 LOCATE 11, 12: PRINT "  TO START, RESTART OR END ..... PRESS   +"
 LOCATE 13, 12: PRINT "  TO INTERRUPT ................. PRESS   -"
 LOCATE 15, 12: PRINT "  TO CHANGE AMPLITUDE DURING TEST ... PRESS   *"
 LOCATE 17, 12: PRINT "-----------------------------------------------
-"
 LOCATE 20, 12: PRINT "Please remember these function keys ...."
700 LOCATE 21, 10: a$ = INKEY$
```

```
     IF a$ <> "+" THEN 700
  GOSUB 4500
'                Toggle run to on
   error.code% = OUTPUT.DIGITAL.VALUE%(PORT.OUT%, MASK.OUT%,
PORT1.RUN%): GOSUB 4000
   error.code% = OUTPUT.DIGITAL.VALUE%(PORT.OUT%, MASK.OUT%, PORT1.OFF%)
   error.code% = GET.ERROR.CODE%(error.code%)
 IF error.code% <> 0 THEN PRINT " Execution error "; error.code%: GOTO
3600
'           Start the MicroProfiler
    GOSUB 5500
    strain.ini = fnfs(analog.val%(etsm), fs.scale)
    DD = 1: ti = TIMER
    GOSUB 4000:   PRINT #3, "J"
    GOSUB 4000: INPUT #3, echo
   GOTO 2150
'               Data collection ( max + min for each cycle )
1000 MAX.VAL2% = 0: MIN.VAL2% = 4096: max.val0% = 0: min.val0% = 4096
      SEGMENT.NO = SEGMENT.NO + 1
      cycle.no = INT(SEGMENT.NO / 2)
       LOCATE 1, 73: PRINT "->"; USING "#####"; cycle.no
   IF cycle.no = plot.int * INT(cycle.no / plot.int) THEN 2000
   IF cycle.no = store.int * INT(cycle.no / store.int) THEN 2000
1100  GOSUB 5500
     IF SEGMENT.NO = 2 * INT(SEGMENT.NO / 2) THEN 1300
IF analog.val%(end.chan%) > MAX.VAL2% THEN MAX.VAL2% =
analog.val%(end.chan%): max.val0% = analog.val%(0)
     IF MAX.VAL2% - analog.val%(end.chan%) < 12 / etsm THEN 1500
     IF analog.val%(0) > (max.val0% + 8192) / 5 THEN 1500
       load.max = fnfs(max.val0%, fs.load) * 1000
       strain.max = fnfs(MAX.VAL2%, fs.scale) - strain.ini
       area = VOLUME / (gauge.len + strain.max)
       IF area < 0 THEN 1200
       SIGMA.MAX = load.max / area
       EPSON.MAX = LOG(1 + strain.max / gauge.len) * 100
   IF load.max > MAX.LOAD THEN MAX.LOAD = load.max: ma.strain =
strain.max
   IF strain.max > MAX.STRAIN THEN MAX.STRAIN = strain.max
1200   DATA.NO = DATA.NO + 1
       PRINT #1, DATA.NO; load.max; strain.max; SIGMA.MAX; EPSON.MAX
'             Failure check
      IF SEGMENT.NO = 2 * end.cyc + 1 THEN a$ = "+": GOTO 3000
      IF ABS(load.max) < fs.load * 20 THEN a$ = "+": GOTO 3000
      IF stop.mode = 3 THEN IF load.max < (1 - .01 * stress.de) *
MAX.LOAD THEN a$ = "+": GOTO 3000
     IF cycle.no > 2 THEN GOSUB 5600
   IF cycle.no <> print.int * INT(cycle.no / print.int) AND cycle.no >
10 THEN 1000
LPRINT TAB(12); SIGMA.MAX; TAB(37); load.max; TAB(52); EPSON.MAX;
TAB(67); plastic.strain
     GOTO 1000
1300 IF analog.val%(end.chan%) < MIN.VAL2% THEN MIN.VAL2% =
analog.val%(end.chan%): min.val0% = analog.val%(0)
     IF ABS(MIN.VAL2% - analog.val%(end.chan%)) < 12 / etsm THEN 1500
     IF analog.val%(0) < (min.val0% + 8192) / 5 THEN 1500
     load.min = fnfs(min.val0%, fs.load) * 1000
```

```
       strain.min = fnfs(MIN.VAL2%, fs.scale) - strain.ini
       area = VOLUME / (gauge.len + strain.min)
       IF area < 0 THEN 1400
       SIGMA.MIN = load.min / area
       EPSON.MIN = LOG(1 + strain.min / gauge.len) * 100
   IF load.min < MIN.LOAD THEN MIN.LOAD = load.min: mi.strain =
strain.min
   IF strain.min < MIN.STRAIN THEN MIN.STRAIN = strain.min
1400   DATA.NO = DATA.NO + 1
       PRINT #1, DATA.NO; load.min; strain.min; SIGMA.MIN; EPSON.MIN
       IF cycle.no > 2 THEN GOSUB 5600
   IF cycle.no <> print.int * INT(cycle.no / print.int) AND cycle.no >
10 THEN 1000
LPRINT TAB(3); cycle.no; TAB(24); SIGMA.MIN; TAB(37); load.min; TAB(52);
EPSON.MIN; TAB(67); plastic.strain
      GOTO 1000
1500 a$ = INKEY$: IF a$ <> "" THEN 3000 ELSE 1100
'            Plot detail curve and store data
2000 DD = 1
     period = 1.01 / frequency
     ti = TIMER
      i = i + 1: IF i > 17 THEN i = 1
      LOCATE 1, 4 * i: PRINT USING "####"; cycle.no: GOTO 2150
2100   GOSUB 5500
2150    test.load = fnfs(analog.val%(0), fs.load) * 1000
     strain = fnfs(analog.val%(end.chan%), fs.scale) - strain.ini
     area = VOLUME / (gauge.len + strain)
     IF area < 0 THEN 2100
     TRUE.STRESS = test.load / area
     TRUE.STRAIN = LOG(1 + strain / gauge.len) * 100
    XX = 346 + TRUE.STRAIN * UX: IF XX > 632 OR XX < 60 THEN 2200
    YY = 166 - TRUE.STRESS * UY: IF YY > 304 OR YY < 28 THEN 2200
      IF DD = 1 THEN PSET (XX, YY), 14: XX0 = XX: YY0 = YY: DD = 0: GOTO
2200
      LINE (XX0, YY0)-(XX, YY), 14: XX0 = XX: YY0 = YY
2200 IF cycle.no <> 1 AND cycle.no <> store.int * INT(cycle.no /
store.int) THEN 2290
     PRINT #2, TRUE.STRAIN; TRUE.STRESS; plastic.strain; cycle.no
2290 t1 = TIMER
2300 t2 = TIMER
     a$ = INKEY$: IF a$ = "+" THEN 3000
     IF ABS(t2 - t1) < 1 / (75 * frequency) THEN 2300
     tf = TIMER
     IF tf < ti THEN tf = tf + 86400
     IF tf - ti < period THEN 2100
2310    IF SEGMENT.NO = 2 * end.cyc THEN a$ = "+": GOTO 3000
     SEGMENT.NO = SEGMENT.NO + 1
     GOTO 1000
'                  Stop or Interrupt test
3000 IF a$ = "+" THEN 3100
     IF a$ = "-" THEN 3200
     IF a$ = "*" THEN 5000 ELSE 1100
3100 GOSUB 5500
       IF ABS(analog.val%(0) - 2048) > 20 THEN 3100
3200     GOSUB 4000:       PRINT #3, "C"
         GOSUB 4000:       INPUT #3, echo
```

```
       IF a$ = "+" THEN 3400
3300 a$ = INKEY$: IF a$ <> "+" THEN 3300
         GOSUB 4000:        PRINT #3, "D"
         GOSUB 4000:        INPUT #3, echo
     IF b$ <> "" THEN b$ = "": GOTO 5620
     GOTO 1100
3400 CLOSE
'                       Toggle stop
    error.code% = OUTPUT.DIGITAL.VALUE%(PORT.OUT%, MASK.OUT%,
PORT1.STOP%): GOSUB 4000
    error.code% = OUTPUT.DIGITAL.VALUE%(PORT.OUT%, MASK.OUT%,
PORT1.OFF%):
    error.code% = GET.ERROR.CODE%(error.code%)
     IF error.code% <> 0 THEN PRINT " DI/O Error "; error.code%: GOTO
3600
     t1 = TIMER
3500 t2 = TIMER
     kk$ = INKEY$: IF kk$ <> "" THEN 3510
     IF t2 - t1 < 30 THEN BEEP: GOTO 3500
3510 SCREEN 0: COLOR 15, 1: CLS : GOSUB 3700
3600 error.code% = TERMINATE%
     CHAIN "MTS"
  END
'                  Store test parameters
3700 PAR.FILE$ = TEST.NAME$ + ".S"
     OPEN "O", #2, PAR.FILE$
     MAX.ENG.STRAIN = MAX.STRAIN / gauge.len
     MIN.ENG.STRAIN = MIN.STRAIN / gauge.len
       MAX.TRUE.STRAIN = LOG(1 + MAX.STRAIN / gauge.len)
       MIN.TRUE.STRAIN = LOG(1 + MIN.STRAIN / gauge.len)
     MAX.ENG.STRESS = MAX.LOAD / CROSS.SEC
     MIN.ENG.STRESS = MIN.LOAD / CROSS.SEC
       MAX.TRUE.STRESS = MAX.ENG.STRESS * (1 + ma.strain / gauge.len)
       MIN.TRUE.STRESS = MIN.ENG.STRESS * (1 + mi.strain / gauge.len)
WRITE #2, SPEC.NAME$, TEST.NAME$, DATE$, CRYSTAL.TYPE, LAMBDA, KAPPA,
SLIP.MODE
WRITE #2, gauge.len, CROSS.SEC, TEST.TYPE, grip.speed, SAMPLE.RATE,
fs.load, TEST.TEMP
WRITE #2, DATA.NO, MAX.STRAIN, MAX.LOAD, MAX.ENG.STRAIN, MAX.ENG.STRESS,
MAX.TRUE.STRAIN, MAX.TRUE.STRESS
    CLOSE
'                    Test overview
PRINT : PRINT : LOCATE 3, 15: PRINT "*** TEST OVERVIEW ***"
PRINT "-----------------------------------------------------"
PRINT
PRINT " SPECIMEN NAME ....................  "; SPEC.NAME$
PRINT " TEST NAME ........................  "; TEST.NAME$
PRINT " DATE .............................  "; DATE$
PRINT " NUMBER OF CYCLE ..................  "; cycle.no
PRINT " MAXIMUM STRAIN ...................  "; MAX.STRAIN; " [mm]"
PRINT " MINIMUM STRAIN ...................  "; MIN.STRAIN; " [mm]"
PRINT " MAXIMUM LOAD .....................  "; MAX.LOAD; " [N]"
PRINT " MINIMUM LOAD .....................  "; MIN.LOAD; " [N]"
PRINT " MAXIMUM ENGINEERING STRAIN .......  "; MAX.ENG.STRAIN * 100; "
[%]"
```

```
PRINT " MINIMUM ENGINEERING STRAIN ..... "; MIN.ENG.STRAIN * 100; "
[%]"
PRINT " MAXIMUM ENGINEERING STRESS ..... "; MAX.ENG.STRESS; "
[MPa]"
PRINT " MINIMUM ENGINEERING STRESS ..... "; MIN.ENG.STRESS; "
[MPa]"
PRINT " MAXIMUM TRUE STRAIN ..... "; MAX.TRUE.STRAIN * 100;
" [%]"
PRINT " MINIMUM TRUE STRAIN ..... "; MIN.TRUE.STRAIN * 100;
" [%]"
PRINT " MAXIMUM TRUE STRESS ..... "; MAX.TRUE.STRESS; "
[MPa]"
PRINT " MINIMUM TRUE STRESS ..... "; MIN.TRUE.STRESS; "
[MPa]"
PRINT
PRINT "-------------------------------------------------------"
LPRINT : LPRINT : LPRINT TAB(23); "*** TEST OVERVIEW ***"
LPRINT TAB(11); "-------------------------------------------------
--"
LPRINT
LPRINT TAB(11); " NUMBER OF CYCLE ..... "; cycle.no
LPRINT TAB(11); " MAXIMUM STRAIN ..... "; MAX.STRAIN; "
[mm]"
LPRINT TAB(11); " MINIMUM STRAIN ..... "; MIN.STRAIN; "
[mm]"
LPRINT TAB(11); " MAXIMUM LOAD ..... "; MAX.LOAD; "
[N]"
LPRINT TAB(11); " MINIMUM LOAD ..... "; MIN.LOAD; "
[N]"
LPRINT TAB(11); " MAXIMUM ENGINEERING STRAIN ..... "; MAX.ENG.STRAIN
* 100; " [%]"
LPRINT TAB(11); " MINIMUM ENGINEERING STRAIN ..... "; MIN.ENG.STRAIN
* 100; " [%]"
LPRINT TAB(11); " MAXIMUM ENGINEERING STRESS ..... ";
MAX.ENG.STRESS; " [MPa]"
LPRINT TAB(11); " MINIMUM ENGINEERING STRESS ..... ";
MIN.ENG.STRESS; " [MPa]"
LPRINT TAB(11); " MAXIMUM TRUE STRAIN ..... ";
MAX.TRUE.STRAIN * 100; " [%]"
LPRINT TAB(11); " MINIMUM TRUE STRAIN ..... ";
MIN.TRUE.STRAIN * 100; " [%]"
LPRINT TAB(11); " MAXIMUM TRUE STRESS ..... ";
MAX.TRUE.STRESS; " [MPa]"
LPRINT TAB(11); " MINIMUM TRUE STRESS ..... ";
MIN.TRUE.STRESS; " [MPa]"
LPRINT
LPRINT TAB(11); "-------------------------------------------------
--"
     t1 = TIMER
3800 t2 = TIMER
     IF ABS(t2 - t1) < 3 THEN 3800
     CLS
     RETURN
'              Time relay
4000 t7 = TIMER
4010 t8 = TIMER
```

```
     IF ABS(t8 - t7) < .001 THEN 4010
     RETURN
'               Set up screen
4500 CLS
     UX = 286 / xmax
     UY = 138 / ymax
     ymax$ = STR$(ymax): xmax$ = STR$(xmax)
     SCREEN 9: COLOR 12, 7: CLS
      LINE (60, 28)-(632, 304), 1, BF
      LINE (60, 28)-(632, 304), 14, B: LINE (61, 29)-(631, 303), 14, B
      LINE (60, 166)-(632, 166), 3: LINE (346, 304)-(346, 28), 3
      LINE (60, 97)-(66, 97), 14: LINE (626, 97)-(632, 97), 14
      LINE (60, 235)-(66, 235), 14: LINE (626, 235)-(632, 235), 14
      LINE (203, 28)-(203, 33), 14: LINE (203, 299)-(203, 304), 14
      LINE (489, 28)-(489, 33), 14: LINE (489, 299)-(489, 304), 14
  LOCATE 1, 1: PRINT "N = "
  LOCATE 23, 8: PRINT -xmax: LOCATE 23, 44: PRINT "0": LOCATE 23, 54
       PRINT "TRUE STRAIN [%]": LOCATE 23, 80 - LEN(xmax$): PRINT xmax
  LOCATE 13, 6: PRINT "0": LOCATE 7, 6: PRINT "+": LOCATE 18, 6: PRINT
"-"
  LOCATE 3, 7 - LEN(ymax$): PRINT ymax: LOCATE 22, 7 - LEN(ymax$): PRINT
ymax
  LOCATE 2, 39: PRINT "TEST : "; TEST.NAME$
     RESTORE
    FOR AA = 1 TO 15
     READ AX$(AA)
    NEXT AA
     DATA T,R,U,E,,S,T,R,E,S,S,,M,P,A
    FOR BB = 1 TO 15
     LOCATE BB + 4, 3: PRINT AX$(BB)
    NEXT BB
  RETURN
'           Change strain amplitude while holding the test
5000                    GOSUB 4000: PRINT #3, "C"
                                              GOSUB 4000: INPUT #3,
echo
     blank$ = STRING$(80, 32)
     LOCATE 1, 1: PRINT blank$: LOCATE 1, 1
     IF amp.type = 2 THEN 5100
     INPUT " Input the strain amplitude ..... [%] "; strain.amp
     IF strain.amp = 0 THEN 5200
LPRINT
LPRINT TAB(2); "* The strain amplitude has been changed to"; strain.amp;
"% since cycle #"; cycle.no + 1
LPRINT
     command.high1 = strain.amp * gauge.len / fs.scale
     command.low1 = -command.high1
     frequency = grip.speed * 100 / (4 * strain.amp * gauge.len): GOTO
5200
5100 INPUT " Input the positive strain amplitude ..... [%] "; pos.strain
     LOCATE 1, 1: PRINT blank$: LOCATE 1, 1
     INPUT " Input the negative strain amplitude ..... [%] "; neg.strain
     IF pos.strain = 0 AND neg.strain = 0 THEN 5200
LPRINT
LPRINT TAB(2); "* The positive strain amplitude has been changed to";
pos.strain; "% since cycle #"; cycle.no + 1
```

```
LPRINT TAB(2); "* The negative strain amplitude has been changed to";
neg.strain; "%"
LPRINT
     command.high1 = pos.strain * gauge.len / fs.scale
     command.low1 = -ABS(neg.strain) * gauge.len / fs.scale
     frequency = grip.speed * 100 / (2 * (pos.strain + ABS(neg.strain))
* gauge.len)
5200 LOCATE 1, 1: PRINT blank$: LOCATE 1, 1
  INPUT " Do you want to start new screen with different scales ? (Y/N)
"; a$
    IF a$ <> "Y" AND a$ <> "y" THEN 5300
    CLS : LOCATE 10, 8: PRINT " Input the scales for real-time plot : "
5210  LOCATE 12, 8: INPUT " Maximum scale for X axis (true strain) .....
[%] "; xmax
  LOCATE 14, 8: INPUT " Maximum scale for Y axis (true stress) ... [MPa]
"; ymax
  LOCATE 17, 8: INPUT " Cycle plot interval ..... [ Default 20 ]
"; plot.int
  LOCATE 19, 8: INPUT " Cycle stroe interval ..... [ Default 100 ]
"; store.int
  LOCATE 21, 8: INPUT " Cycle print interval .....  [ Default 17 ]
"; print.int
  IF plot.int = 0 THEN plot.int = 20
  IF store.int = 0 THEN store.int = 100
  IF print.int = 0 THEN print.int = 17
  IF xmax = 0 OR ymax = 0 THEN 5210
     GOSUB 4500
5300 IF command.high1 = 0 AND command.low1 = 0 THEN 5400
     IF command.high1 = command.high AND command.low1 = command.low THEN
5400
       PRINT #3, "V"
       GOSUB 4000:        INPUT #3, echo
    IF command.high1 = command.high THEN command.high1 = command.high1 *
1.005
       PRINT #3, command.high1; "H"
       GOSUB 4000: INPUT #3, echo
       PRINT #3, "Q"
       GOSUB 4000: INPUT #3, echo
    IF command.low1 = command.low THEN command.low1 = command.low1 *
1.005
       PRINT #3, command.low1; "H"
       GOSUB 4000: INPUT #3, echo
      command.high = command.high1: command.low = command.low1
5400  LOCATE 1, 1: PRINT blank$: LOCATE 1, 1: PRINT "N = ": i = 0
      LOCATE 1, 75: PRINT cycle.no
      GOSUB 4000:        PRINT #3, "D"
      GOSUB 4000:        INPUT #3, echo
      IF b$ <> "" THEN b$ = "": GOTO 5620
      GOTO 1100
'      Data acquisition routine
5500  error.code% = BEGIN.ADC.DMA(number.of.val%, digit.val%(0))
      error.code% = WAIT.ADC.DMA(digit.val%(last.val%))
      error.code% = STOP.ADC.DMA
      FOR abc = 0 TO sum.no - 1
     digit(0) = digit(0) + digit.val%(abc * (1 + etsm))
     digit(etsm) = digit(etsm) + digit.val%(abc * (1 + etsm) + etsm)
```

```
      NEXT abc
analog.val%(0) = INT(digit(0) / sum.no): analog.val%(etsm) =
INT(digit(etsm) / sum.no)
digit(0) = 0: digit(etsm) = 0
  RETURN
'      Plastic strain amplitude control
5600  LOCATE 2, 1: PRINT "                                    "
    cde = 0
    FOR mm = 1 TO 2
    FOR mmm = 1 TO 3
    a#(mm, mmm) = 0
    NEXT mmm
    NEXT mm
    f(0, 1) = 0: f(0, 2) = 0
5610  GOSUB 5500
      cde = cde + 1
      f(cde, 1) = fnfs(analog.val%(0), fs.load) * 1000
      f(cde, 2) = fnfs(analog.val%(etsm), fs.scale) - strain.ini
      t8 = TIMER
      a$ = INKEY$
      IF a$ = "+" THEN 3100
      IF a$ = "-" THEN b$ = a$: GOTO 3200
      IF a$ = "*" THEN b$ = a$: GOTO 5000
5620  t9 = TIMER
     IF ABS(t9 - t8) < .0004 / grip.speed THEN 5620
     IF f(cde, 1) < load.max / 5 AND f(cde, 1) > load.min / 5 THEN 5610
5630 FOR fg = 1 TO cde
     a#(1, 1) = a#(1, 1) + f(fg, 2) ^ 2
     a#(1, 2) = a#(1, 2) + f(fg, 2)
     a#(1, 3) = a#(1, 3) + f(fg, 1) * f(fg, 2)
     a#(2, 3) = a#(2, 3) + f(fg, 1)
     NEXT fg
IF -cde * a#(1, 1) + a#(1, 2) ^ 2 = 0 OR a#(1, 1) = 0 THEN
plastic.strain = -plastic.strain: GOTO 5640
b = (a#(1, 3) * a#(1, 2) - a#(2, 3) * a#(1, 1)) / (-cde * a#(1, 1) +
a#(1, 2) ^ 2)
a = (a#(1, 3) - b * a#(1, 2)) / a#(1, 1)
IF a = 0 THEN 5640
ba = 1 - b / (a * gauge.len): IF ba < 0 THEN 5640
plastic.strain = INT(LOG(ba) * 100000) / 1000
5640 LOCATE 2, 1: PRINT "  Ep = "; plastic.strain; "% "; cde
RETURN
```